EXPLORING MICRORNA INTERACTION NETWORKS TO EXPLAIN THE RELATIONSHIP BETWEEN CALORIC RESTRICTION AND BREAST CANCER IN MICE

by
Atakan Ayden

Submitted to Graduate School of Natural and Applied Sciences
in Partial Fulfillment of the Requirements
for the Degree of Master of Science in
Biotechnology

Yeditepe University
2022

EXPLORING MICRORNA INTERACTION NETWORKS TO EXPLAIN THE RELATIONSHIP BETWEEN CALORIC RESTRICTION AND BREAST CANCER IN MICE

APPROVED BY:

Prof. Dr. Soner Dogan ……
(Thesis Supervisor)
(Yeditepe University)

Assist. Prof. Dr. Andres Aravena ……
(Thesis Co-supervisor)
(Istanbul University)

Assoc. Prof. Dr. Bilge Guvenc Tuna ……
(Yeditepe University)

Assist. Prof. Dr. Emrah Nikerel ……
(Yeditepe University)

Assist. Prof. Dr. Alper Yılmaz ……
(Yıldız Technical University)

DATE OF APPROVAL: …./…./20...

I hereby declare that this thesis is my own work and that all information in this thesis has been obtained and presented in accordance with academic rules and ethical conduct. I have fully cited and referenced all material and results as required by these rules and conduct, and this thesis study does not contain any plagiarism. If any material used in the thesis requires copyright, the necessary permissions have been obtained. No material from this thesis has been used for the award of another degree.

I accept all kinds of legal liability that may arise in case contrary to these situations.

Atakan Ayden

Signature …..…….……..

ACKNOWLEDGEMENTS

I am grateful to my supervisor, Dr. Andres Aravena, for his patience, guidance, and continuous support. He prevented me from losing my motivation and carried me like Atlas during the entire work. I also would like to thank Prof. Dr. Soner Doğan and Dr. Bilge Tuna for their guidance throughout this project.

I am extremely thankful to my lifelong friends and colleagues with whom I share the same laboratory, Elif Öztemiz and Elif Yılmaz, for their invaluable support.

Finally, I want to give my deepest gratitude to my parents for their constant support and encouragement throughout my years of study, as well as during the research and writing of this thesis. Without them, this accomplishment would not have been possible.

ABSTRACT

EXPLORING MICRORNA INTERACTION NETWORKS TO EXPLAIN THE RELATIONSHIP BETWEEN CALORIC RESTRICTION AND BREAST CANCER IN MICE

Caloric restriction (CR) —limiting average calorie intake without regressing in physical and mental activities— is known to enhance longevity and overall health and reduce aging-related disorders. The epigenetic fluctuation caused by CR in conjunction with microRNA (miRNA) expression has only been studied in the context of basic differentially expressed miRNAs and has not been used to characterize miRNA regulatory networks in a tissue- and diet-specific way. It is known that miRNAs act synergistically. However, little is known about the remodeling of miRNA interactions under different dietary restrictions and different tissues. Here we provide a novel approach to analyze miRNA-miRNA interactions and reveal different effects of dietary restriction in both blood and mammary fat pad (MFP). We analyzed miRNA expression from female C57BL/6 mice fed with three different diets: ad libitum (AL), chronic caloric restriction (CCR) with 15% CR, and intermittent caloric restriction (ICR) with three weeks of AL followed by one week 60% CR in a cyclic manner. We infer co-expression networks for each dietary group using a joint graphical model, then map the targets of the connected components of co-expression networks. To evaluate the influence on the pathways we used a network-based centrality approach to prioritize miRNAs and KEGG pathways. The miRNA miR-1a-3p is common to all conditions with high centrality, while miR-129-5p is specific to the MFP, and miR-505-5p is specific to only blood in the CCR group. In our analysis using the ranking according to the eigenvector centrality in the co-expression networks for the influence on pathways, we revealed that the KEGG pathways such as “Breast cancer” and “mTOR signaling pathway” increased their importance by CCR diet in blood. In addition to that, we revealed the KEGG pathways “p53 signaling pathway” and “Fatty acid degradation” increased their importance by CCR in MFP. These pathways are well-known regulators of both aging and cancer. mTOR and MAPK signaling pathway has crosstalk with many other cancer-related pathways, and these pathways may be the key to the anti-cancer mechanism of the CCR diet.

ÖZET

FARELERDE KALORİK KISITLAMA İLE MEME KANSERİ ARASINDAKİ İLİŞKİYİ AÇIKLAMAK İÇİN MİKRORNA ETKİLEŞİM AĞLARININ ARAŞTIRILMASI

Kalori kısıtlaması (KK), fiziksel ve zihinsel aktivitelerde gerileme olmaksızın ortalama kalori alımını sınırlamaya denir ve ömrü uzattığı ve yaşlanmayla ilgili bozuklukları azalttığı bilinmektedir. CR'nin mikroRNA (miRNA) ekspresyonu ile bağlantılı olarak neden olduğu epigenetik değişim, yalnızca temel diferansiyel olarak eksprese edilen miRNA'lar bağlamında incelenmiştir ve miRNA etkileşim ağları, doku ve diyete özgü bir şekilde karakterize etmek için kullanılmamıştır. MiRNA'ların sinerjistik olarak hareket ettiği bilinmektedir. Bununla birlikte, farklı diyet kısıtlamaları ve farklı dokular altında miRNA etkileşimlerinin yeniden şekillenmesi hakkında çok az şey bilinmektedir. Bu çalışmada, miRNA-miRNA etkileşimlerini analiz etmek ve hem kan hemde meme yağ bezinde (MYB) diyet kısıtlamalarının farklı etkilerini ortaya çıkarmak için yeni bir yaklaşım sunuyoruz. Üç farklı diyetle beslenen dişi C57BL/6 farelerinden miRNA ekspresyonunu analiz ettik: ad libitum (AL), yüzde 15 CR ile kronik kalori kısıtlaması (KKK) ve aylık döngüler halinde üç haftalık AL ve ardından bir hafta yüzde 40 KK ile aralıklı kalori kısıtlaması (AKK). Birleşik grafik LASSO (JGL) metodunu kullanarak her diyet grubu için koekspresyon ağlarını çıkarsadık ve yolaklar üzerindeki etkiyi değerlendirmek için yani önemli miRNA'lara ve KEGG yollarına öncelik vermek için ağ tabanlı bir merkezilik yaklaşımı kullandık. MiRNA miR-1a-3p yüksek merkeziliğe sahiptir ve tüm diyet gruplarında ortaktır, miR-129-5p MFP'ye özeldir ve miR-505-5p sadece CCR grubundaki kana özgüdür. Yolaklar üzerindeki etki için koekspresyon ağlarındaki merkeziliğine göre sıralamayı kullanan analizimizde, "Meme kanseri" ve "mTOR sinyal yolu" gibi KEGG yollarının kandaki CCR diyeti ile önemini artırdığını ortaya koyduk. Buna ek olarak, MFP'de CCR ile KEGG yollarının "p53 sinyal yolu" ve "Yağ asidi bozulmasının" önemini artırdığını ortaya koyduk. Bu yollar, hem yaşlanmanın hem de kanserin iyi bilinen düzenleyicileridir. mTOR ve MAPK sinyal yolu, kanserle ilgili diğer birçok yolla çapraz etkileşime sahiptir ve bu yollar CCR diyetinin kanser karşıtı mekanizmasının anahtarı olabilir.

TABLE OF CONTENTS

LIST OF FIGURES

LIST OF TABLES

LIST OF SYMBOLS/ABBREVIATIONS

AIC	Akaike information criterion
AL	*Ad libitum*
ANND	Average nearest neighbor degree
CCR	Chronic caloric restriction
EMT	Epithelial-to-mesenchymal transition
FC	Fold change
GGM	Gaussian graphical model
GO	Gene ontology
HDACs	Histone deacetylase
ICR	Intermittent caloric restriction
KEGG	Kyoto Encyclopedia of Genes and Genomes
MAPK	Mitogen-activated protein kinase
MFP	Mammary fat pad
miRISC	MicroRNA-induced silencing complex
miRNA	Micro ribonucleic acid
MMTV-TGFα	Mouse mammary tumor virus-transforming growth factor alpha
mTOR	Mammalian target of rapamycin
PCA	Principal component analysis
TGF	Tumor growth factor
UTR	Untranslated region

1. INTRODUCTION

This thesis deals with the relationship between CR and miRNA expression. In particular, we look for the molecular mechanisms that connect caloric restriction with lower incidence of breast cancer, using *Mus musculus* as a model organism.

As the human population gets older due to the advancements in the quality of life after the second millennia, diseases such as heart and cancer accumulate and become leading causes of death [1]. Inevitably, cellular and molecular mechanisms of aging are tried to be revealed. Healthy aging is defined as delaying the onset of molecular and cellular degeneration for the longest period of time possible [2]. There are genetic, pharmacological, and nutritional interventions that have proven to prevent age-related deterioration and increase life expectancy [3]. At this point, defining actions that promote healthy aging in humans remains an active area of research.

One of these interventions is CR, whose effectiveness has been known for a long time, which is defined as slowing the development by limiting the average caloric intake without regressing in physical and mental activities [4,5]. The restriction can be applied at various percentages, at various time intervals, or with various macronutrient ratios. Caloric restriction has been shown to enhance longevity by up to 50% while enhancing overall health and reducing aging-related disorders [6]. It slows the progression of a variety of diseases. Still, the exact molecular mechanisms that can explain how caloric restriction works are not completely understood. One line of investigation is to explore the role played by some RNA molecules.

Noncoding RNA (ncRNA) molecules are a relatively new RNA subclass and play a gene regulatory role by synthesizing from intra- and intergenic regions of the large genome [7]. MicroRNA (miRNA) molecules are short ncRNAs that regulate the post-transcriptional activity of the genes by recognizing base pairs in the 3'-untranslated region (UTR) of the target gene [8]. In the past several years, thousands of miRNAs have been discovered in a wide range of organisms, and it is now known that they engage in a wide range of biological functions by regulating genes involved in several cellular processes [9,10].

Both experimental and computational methods have been developed to reveal miRNA functions. The majority of the research has focused on miRNAs and their targets [11]. Understanding the regulation mechanism of miRNAs in the gene regulatory network, on the other hand, is critical to finding the roles of miRNA in complex biological systems [12]. The interaction between miRNAs and their target genes is complex in general. A single target gene may be regulated by many miRNAs, and vice versa, a single miRNA may have multiple target genes [13].

The measurement of epigenetic fluctuation caused by CR in conjunction with miRNA expression has only been studied in the context of basic differentially expressed miRNAs and their hypothetical targets and has not been used to characterize miRNA regulatory networks in a manner that is specific to tissue and diet. Through the comparison of dietary groups, we develop a strategy to investigate the diet–, age– and tissue–specific miRNA regulatory modules that connect between microRNAs and CR. These modules may help explain how dietary interventions affect the aging process and the development of cancer.

1.1. CALORIC RESTRICTION EXPANDS LIFE

CR is defined as the reduction of calorie intake, up to 60% of *ad libitum*, that does not result in malnutrition. Currently, CR is the only non-genetic intervention that has been demonstrated to reliably increase both mean and maximal lifespan across a wide range of animals [14]. Through a variety of methods, including enhanced glucose homeostasis and mitochondrial health, as well as through suppressing all of the molecular hallmarks of aging, CR increases healthspan and lifespan. Furthermore, it has been demonstrated to protect against age-related disorders, including atherosclerosis [15], cancer [16], diabetes [17], and neurological diseases [18].

Regarding limitation of food intake, the most common CR strategies are chronic calorie restriction (CCR) and intermittent calorie restriction (ICR) [19]. CCR is the constant regulation of food and energy intake, whereas ICR is the regulation of food and energy consumption in a specific period followed by ad libitum food intake.

Interest in the potential of CR to extend life first arose in the late 1970s and early 1980s, and has continued since then. However, despite the fact that the effect of CR on people is a

complex process to study, research has shown that a reduced energy expenditure has beneficial impacts on human aging and age-related disorders in general [14]. People who consumed less calories than they would have had on a normal diet had decreased incidences of cancer and other chronic diseases when compared to people who ate a typical diet. Long-term CR has been shown to reverse gene expression changes linked with aging-related inflammation and altered stress responses [20], as well as DNA replication/cell cycle abnormalities [21], oxidative stress [22] and macromolecular damage [23].

1.1.1. Pathways That Change with Caloric Restriction

The expression of genes belonging to some of the major pathways is altered by the caloric restriction [24]. A major feature of aging is metabolic dysfunction, and current transcriptome evidence indicates that all restricted dietary interventions have an impact on pathways involved in glucose homeostasis and insulin signaling [25]. Many studies have found that these therapies are beneficial in terms of health because they decrease the activity of important insulin-related signaling pathways and their gene expression. In particular, [26] have shown that the activity of insulin signaling pathway and mTOR pathway decreases, while sirtuins and FOXO pathways increase with short- or long-term dietary interventions. All of these genes in metabolic pathways play important roles in energy sensing, growth, and metabolism [26].

Inflammation is a key component of aging, and it can affect the development and function of tissues and organisms. It is believed that dietary interventions can help decrease inflammatory activation. Interleukin-6, TNF-α, and interleukin-1β are three of the most important inflammatory mediators implicated in these pathways [27].

Long-term CR or intermittent fasting may harm immune system pathways, although brief periods of fasting are being studied as promising immune system repair and maintenance therapies [28]. There is evidence that the majority of healthy aging therapies have some effect on immunological responses, primarily by modifying NF-Kβ, a transcription factor involved in immune response and cytokine production [27]. Some evidence suggests that CR decreases the expression of additional immune-related transcripts, such as CXCR4 in T cells [29].

The majority of evidence suggests that caloric restriction inhibits oxidative phosphorylation gene expression, hence reducing the generation of reactive oxygen species (ROS) which is a huge contributor of age-related diseases [30]. Increased expression of mitochondrial biogenesis and turnover pathways as a result of good dietary treatments may also contribute to improved mitochondrial efficiency [22]. The sirtuins [31], AMPK [32], and PPARs [33] are key genes linked with these pathways.

1.1.2. Caloric Restriction Prevents Diseases

Dysregulation in metabolic parameters and cancer progression have been known to be tightly bound [34]. Cancer cells whose metabolism differs from normal cells are sensitive to the balance of food intake. One of the first observations which relates nutrition and cancer metabolism is the Warburg effect [35]. In the 1950s it was observed that unlike normal cells, cancer cells can do glycolysis. Systemic alterations of metabolism can also lead to cancer. Excessive accumulation of fatty lipids in the body increases the risk of cancer [36]. In a way that supports previous claims, the risk of developing cancerous diseases decreases with low fat and low sugar consumption [37].

Several studies show that CR that limits food intake can also reduce the risk of cancer [38]. CR proves protective effects as follows: it is able to delay onset of cancer, reduce incidence of tumors and increase overall survival. There are several targets of CR which also overlap with the molecular mechanism of cancer. According to multiple studies IGF1 expression decreases with the application of CR. In many tissues as well as cancer tissue IGF1 controls growth signaling pathways such as PI3K/Akt/mTOR pathway [39]. Thus, it can be suggested that application of CR retard the growth of the tumor via regulating IGF1 levels.

Cancer progression is also largely affected by chronic inflammation. Chronic inflammation is described as immune markers, such as circulating fatty acids, cytokines, and chemokines, that attract immune cells that stay in the tissue for a long period of time [40]. In most tumors an inflammatory response is triggered, and NF-Kβ is a crucial transcription factor responsible for inducing gene expression related to apoptosis, inflammation and metastasis. CR lowers the number of macrophages that enclose tumor, circulating and tissue cytokine levels, and NF-Kβ signaling [27]. Prostaglandin-endoperoxide synthase 2 (PTGS2, also known as COX2) is an enzyme that produces prostaglandins, chemicals that promote

inflammation [41]. Increased expression of PTGS2 in tumors is associated with poor prognosis in various cancer types. In a number of studies, caloric restriction reduces PTSG2 expression, and also reduces inflammation in colon, gastric, esophageal, and breast cancer. [27].

1.2. CALORIC RESTRICTION ALTERS THE EPIGENETIC LANDSCAPE

CR is considered to slow the aging process by causing epigenetic alterations. Cancer rates rise with age; yet CR both delays the consequences of aging and prevents the development of cancer [42]. Therefore, we assume that CR shows its beneficial effect by affecting the epigenetic factors that play a role in the development of cancer. The three main categories of epigenetic marks, DNA methylation [42], post-translational histone modifications [43] and small non-coding RNAs [44] are considered as central regulators of the aging process and diseases such as cancer.

There are numerous instances of how CR modifies epigenetic mechanisms. DNA methylation is a complex epigenetic process that is intimately linked to gene expression regulation. DNA methylation has been connected to the regulation of gene expression throughout development. The methylation pattern of some genes important in biological processes such as metabolism, oxidative stress, senescence, and aging has been reported to be altered by CR [45]. By modifying the epigenome during early developmental stages, CR procedures that compensate for malnutrition can help prevent the development of chronic diseases [46]. In one study, CR-induced weight loss resulted in a significant decrease in DNA methylation of the inflammatory cytokine tumor necrosis factor (TNF), as well as a difference in markers for weight loss prediction [47]. Additionally, identical TNF and leptin methylation patterns were identified in obese women on a short-term low-calorie diet, reducing the inflammatory load of obese patients [48].

The chromatin structure controls how the chromosome is packaged, hence determining the genome’s availability. Chromatin alterations are primarily a result of covalent modifications to histone proteins, which alter the capacity of genes for expression. Histone acetylation is one such alteration that occurs posttranscriptionally and is assisted by histone acetyltransferases and eliminated by histone deacetylases (HDACs). Changes in the nutrients and its sensors will have an effect on nuclear gene transcription, which is mediated

by protein, specifically histone modifiers that are vulnerable to CR [49]. It is well established that CR has an effect on sirtuins, a family of nutrient sensing HDACs. The PI3K/Akt/mTOR axis is a critical aging mechanism that is regulated by sirtuins, highlighting the tremendous therapeutic potential of CR and sirtuins [50].

MiRNAs are short noncoding RNA molecules that regulate gene post transcriptional stability. When miRNAs attach to a target gene, the multiprotein complex RNA-induced silencing complex (RISC) is recruited, which cleaves the target gene. This complex process is in charge of mRNA post transcriptional stability in the cytoplasm. As a result, environmental factors that affect a certain group of miRNAs will influence the gene expression pattern. Given their flexibility to many changes in the environment, miRNAs could be employed as a prognostic biomarker. The processes through which CR promotes health advantages are hypothesized to be mediated by changes in miRNA patterns in various tissues.

1.2.1. Non-coding RNAs are one of the Epigenetic Mechanisms

Protein-coding genes make up only a small percentage of the human genome. The proteins encoded by these genes regulate vital activities by undertaking various functions. However, the transcripts most abundant in the cell do not code for proteins. When addressing epigenetic control of genes, it is important to review the complex nature of noncoding RNAs and their regulatory properties [51]. Non-coding RNAs (ncRNAs) have recently been shown to have regulatory functions in a variety of biological processes other than coding for proteins.

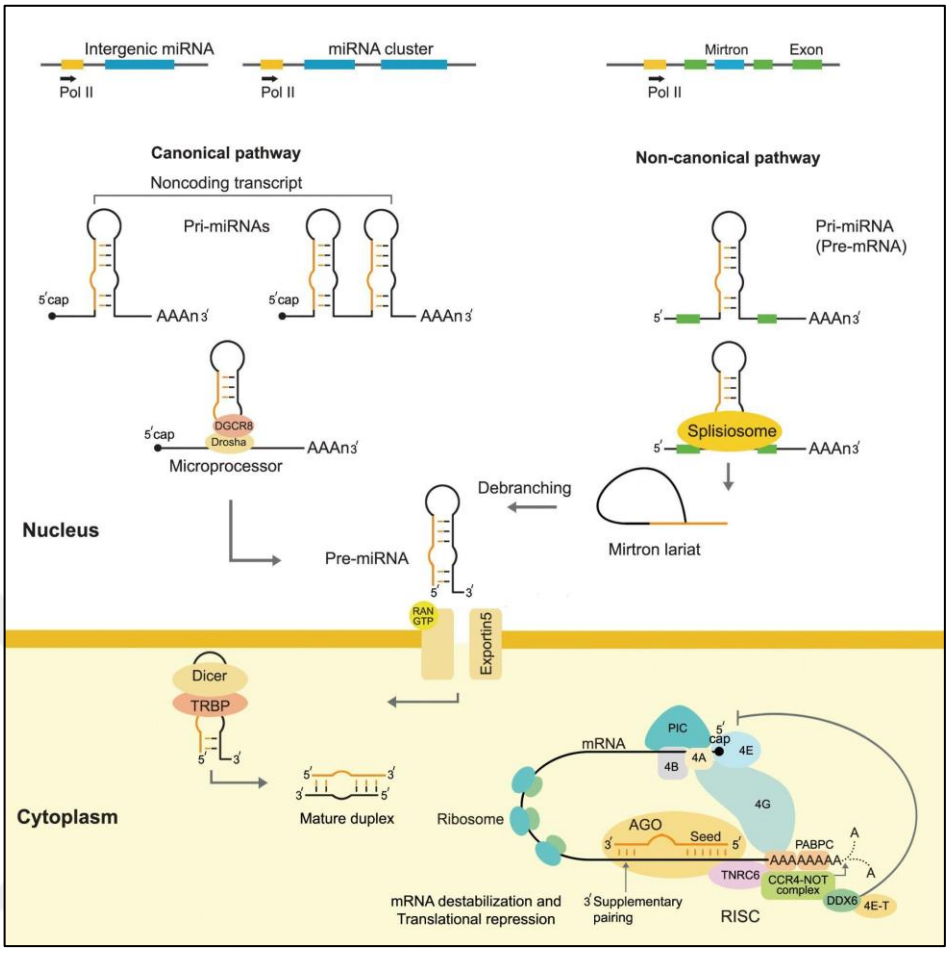

Figure 1.1. An overview of the biogenesis of miRNAs

Generally, ncRNAs are classified into two types, depending on whether the transcript is greater than 200 nucleotides (nt) in length: short ncRNAs and long ncRNAs. miRNAs are basically small non-coding RNA molecules that have a complementary sequence to the 3' UTR region of the mRNA and partially inhibit protein synthesis by binding to this region. Expression and maturation processes of miRNA molecule is summarized in Figure 1.1.

They are typically 22 nucleotides in length. MiRNAs are integrated into the effector complex in eukaryotic cells, where they bind to an Argonaute (AGO) protein and guide it to cleave complementary mRNA or delay translation [52]. This complex mechanism is required for the posttranscriptional operation of mRNAs [53].

The mature miRNA associates with an AGO protein, which is a single polypeptide chain consisting of four distinct domains: the amino-terminal (N) domain, the Piwi-Argonaute-Zwille (PAZ) domain, the middle (MID) domain, and the P element induced wimpy testes

(PIWI) domain [54]. Four AGO proteins are encoded by the mammalian genome. While certain human miRNAs preferentially connect with particular AGO proteins, the majority associate with all AGO proteins.

Target sites of miRNAs are often found in the 3' UTR of mRNAs; they exhibit a high degree of complementarity with the seed region, which is the primary criteria for target-site prediction. Canonical (seed-matching) target sites with the highest affinity are those that complement miRNA nucleotides 2–8 [55]. Complementarity with miRNA nucleotides 2–7 or 3–8 is much weaker, but still considered canonical.

DICER1 collaborates with an Argonaute protein to produce the miRNA-associated multiprotein RNA-induced silencing complex (miRISC). When miRISC binds to the 3' UTR, it silences genes via translation repression and mRNA degradation [56]. The first regulatory activity is that it prevents translation from initiating by interfering with the function of the eukaryotic initiation factor. Although different mechanisms have been proposed, it appears that miRISC promotes eIF4F cleavage from target mRNAs and inhibits ribosome scanning and eIF4F translation initiation complex assembly [57]. AGO recruits a member of the GW182 protein family during mRNA degradation. By engaging the poly(A) nuclease, GW182 interacts with polyadenylate-binding protein, causing mRNA deadenylation [58]. Deadenylation stimulates decapping, allowing the mRNA to be rapidly degraded by 5'3' exoribonuclease.

Because of the nature of miRNAs, research in this field can give significant information in the study of the causes of human diseases. Given their flexibility to many environmental conditions, miRNAs might be used as a prognostic biomarker for various tissues. Researchers think that changing miRNA patterns in various tissues will influence the processes via which CR promotes health advantages [59].

1.2.2. Epigenetic Basis of Small Non-coding RNA and Relation to CR

CR is one of the few non-genetic interventions that has been shown to increase lifespan. The processes through which CR promotes beneficial properties are considered to be mediated by changes in miRNA profiles in various tissues and organisms. Some CR studies conducted in vertebrate and invertebrate organisms reveal the principles of epigenetic mechanisms [59].

The flexible functioning of the miRNAs implies its importance in the explanation of diseases [53,60].

It has been shown in some studies with *C. elegans* that the CR changed the miRNA profile. Twelve hours of starvation in the model organism in which the first functional miRNA was discovered, results in significant alterations in miRNAs whose target genes are involved in metabolism, development, and oogenesis processes. Additionally, two-day food restriction resulted in whole body miRNA alterations associated with lifespan, and these changes were dependent on the drsh-1 [61]. Furthermore, 12 hours of food deprivation results in modifications similar to more developed organisms, such as decreased fat storage, decreased and extended life. There is limited evidence that CR regulates miRNAs in *D. melanogaster*, implying metabolic benefits and increased lifespan. When high- and low-nutrient diets were compared, CR-applied flies showed changed expression of miR-184, let-7, miR-125, and miR-100 [62]. Taken together, CR in non-vertebrates demonstrates the critical role of nutrient-sensing mechanisms in determining longevity and health span.

Various tissue types and restriction methods in rodents have revealed the efficacy of CR in regulating miRNA synthesis. In one study, with the CR applied for 27 months, a group of miRNAs in the blood of long-lived mice is shown to be related to the aging process and age-related diseases [63]. In long-lived Ames dwarf mice, several miRNAs appear to be genotype- and age-specific. Additionally, these miRNAs influence pathways involved in tumor suppression and inflammation [64]. Similarly, miRNAs frequently found in serum were increased in the liver of mice following a two-year increase in CR from 10% to 30%, and miR-125a-5p was identified as a direct contributor to age-related CR effects [65].

CR is effective in breast tissue to generate miRNA patterns related to lifespan and aging. One study indicated that numerous miRNAs were altered following CR therapy, with the most significant increases occurring in miR-29c, miR-203, miR-150, and miR-30 [66]. Co-transfection test indicated that miR-203 can inhibit CAV1 translation. CAV1 is a scaffolding protein that regulates signaling molecules that are active in tumor progression such as PKA, PKC, HRAS, and EGFR. Similarly, other miRNAs such as miR-10a, miR-10b, miR-21, miR-124, miR-125b, miR-126, miR-145, and miR-200a are related to mammary cancer [67]. Specifically, miR-200a expression levels increase during cancer progression in ad libitum rats and dramatically decrease in mammary tumors of CR rats. In light of miR-200a's role,

CR may help lower breast tumor burden by reducing miR-200a expression, which suppresses cellular proliferation.

1.3. THE INTERACTIONS ARE ORGANIZED AS BIOLOGICAL NETWORKS

Every subject analyzed in nature is somehow interconnected by various layers. Biology, in particular, effectively uses networks to describe organisms and their relationship to each other. On a large scale, the interactions of organisms that populate an ecosystem, such as the hunter - prey relationship or biodiversity, are difficult to model without networking. When we go down in size, the use of biological networks is inevitable in order to understand the relationship of the tissues that make up the organism, how the cells that make up the organs and the numerous biomolecules that make up the cells function together [68].

When it comes to gene expression control, a regulatory network is a complicated web of molecular components that interact with one another and with genes in order to regulate gene expression [69]. Transcriptional factors bind to regulatory regions in the gene regulatory network, and their interaction leads to the activation or repression of the gene. But, according to recent discoveries in molecular biology, not only proteins but also non-coding RNAs play a significant role in the regulation of gene expression [70]. An increasing number of studies have reported on the involvement of ncRNAs in various physiological processes over the last decade, and next generation sequencing technologies, combined with bioinformatics analyses, have revealed the widespread transcription of an unexpected variety of RNA molecules. MiRNAs are a type of noncoding RNA that has been proven to be involved in transcriptional control [71].

Many systems can naturally be depicted by networks and briefly describing them helps explain the theory. Protein–protein interaction (PPI) networks represent intermolecular interactions between proteins [72]. They are often shown using simple graphs. Gene expression regulation is modeled by transcriptional regulation networks [73]. Specific genes encode proteins that control the expression of other genes; this type of protein is known as a transcription factor. A transcriptional regulation network is a simplified description of this phenomena, in which gene 1 is linked to gene 2 if the protein product of gene 1 regulates gene 2 expression. This is an asymmetric relationship since gene 1 influences the expression of gene 2, whereas gene 2 has no influence on the expression of gene 1. Gene co-expression

networks refer to correlations in transcript levels [74]. if there is a significant correlation between two genes they are linked with an undirected edge. Several approaches for creating gene co-expression networks have been proposed, and they all consist of two fundamental steps:

1. calculating a co-expression measure, and
2. determining a significance threshold.

To understand biological networks, it is convenient to be familiar with the ideas and definitions of graph theory. A graph, or network, is a representation of a group of nodes and a group of edges corresponding to pairs of vertices and indicating vertices' interactions. Classifications can be made according to the relationship of each element in a network to each other. In other words, according to the attributes of the edges we can term different graphs.

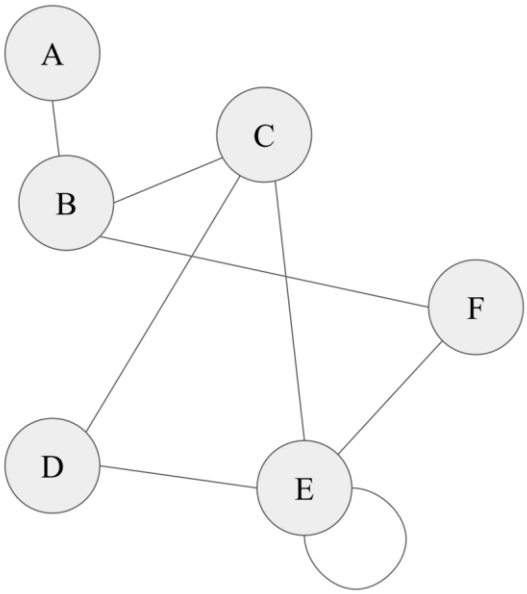

	A	B	C	D	E	F
A	0	1	0	0	0	0
B	1	0	1	0	0	1
C	0	1	0	1	1	0
D	0	0	1	0	1	0
E	0	0	1	1	1	1
F	0	1	0	0	1	0

Figure 1.2. An undirected graph with six nodes and eight edges. Adjacency matrix representation of undirected graph

An undirected graph is one in which the edges are an unordered pair of nodes with links between them. A simple graph is one that does not have a self-loop structure. A directed graph or digraph is a graph having an ordered pair of nodes and edges that are associated

with directions. A directed graph is a collection of nodes and edges in which each edge has a direction indicated by an arrow. Unlike an undirected graph, a directed edge has a tail that extends from the source node and a head that extends to the target node.

The degree of a node is equal to the number of edges that connect it. The neighborhood of a node is the collection of all edges that are adjacent to it. Consider the graph in Figure 1.2.: Node B has a degree of three. If the edges are directed, each node has an indegree (number of edges directed from neighbors to the node) and an outdegree (number edges directed from neighbors away from the node).

The adjacency matrix is the most often used data structure for representing graphs. A two-dimensional array or matrix termed an adjacency matrix is used to describe a graph sequentially using an array data structure. Given a graph such as the one shown in Figure 1.2., an adjacency matrix is a square matrix with a size equal to the square of the number of nodes. Each cell in the adjacency matrix represents a connection between two nodes.

1.3.1. Networks in Aging and Caloric Restriction

The great majority of aging studies have concentrated on individual genes/proteins, with little regard to the potential importance of interactions between them [2]. Given that aging related genes cooperate, it appears implausible to test the effect of unique gene combinations on aging experimentally [75]. As a result, a more efficient strategy is required to focus research on the effects of environmental factors and CR on aging and to determine the molecular links between aging and several diseases. One of the guiding concepts of such a strategy may be the concept of an interactome, or more precisely, a network. Collecting a significant amount of data and establishing comprehensive databases are the initial stages towards building interaction networks and adopting a global, integrative, strategy to research the molecular mechanisms of CR and aging [76].

Researchers have discovered new associations between aging and CR in yeast using network reconstruction. To infer gene regulatory networks in *S. cerevisiae*, they employed an integrated reverse-engineering technique called network identification by regression [77]. They used their method on a network made up of ten genes from the glucose responsive Snf1

pathway. They predicted and experimentally confirmed the role of Snf1, which is required for glucose-repressed gene expression during CR.

1.3.2. Networks in Cancer Research

Cancer is characterized by a high degree of heterogeneity; in contrast to the normal pattern, improperly expressed genes acquire complex activities. Depending on the stage of development of the cancer and the tissue from which it originates, different gene sets in the signaling pathways may inhibit or promote cancer development [78]. A network-based analysis, on the other hand, will clarify this perplexing outcome and point to the disease's causation. When a list of altered genes is projected onto biological pathways, a statistically unlikely group of normally unrelated genes is found to be in highly connective modules [79]. As a result, network-based research can reveal vital insights into the biology underpinning disease etiology.

Several studies have applied direct genetic variation data from primary tumors in biomarker research. In one study, researchers constructed a gene network using interactions that occur together or separately between gene mutations using just cancer gene mutation data [80]. The resulting network of cancer genes with co-occurring and anti-co-occurring mutations contained two complementary modules with unique activities and roles in carcinogenesis.

1.3.3. Non-coding RNA Networks

Due to the expanding significance of noncoding RNAs, the networks incorporating noncoding RNAs have also contributed massively to uncovering the unknown mechanisms of cancer [79]. The regulation patterns between microRNAs, genes transcription factors are represented by miRNA regulatory networks as shown in Figure 1.3. Using miRNA-mRNA regulation networks, researchers discovered that hsa-let-7i and its target genes play key roles in colorectal cancer metastasis [81]. Another study revealed miRNAs that regulate functional pathways in several types of cancer. They investigated data on gene expression levels in patient malignancies in order to identify functional miRNA-mRNA regulation networks that may have an effect on cell proliferation and/or patient survival [82]. The combinatorial regulatory network was built to identify essential regulators that contribute to hepatocellular

carcinoma metastasis. It includes interactions between miRNAs, genes and transcription factors.

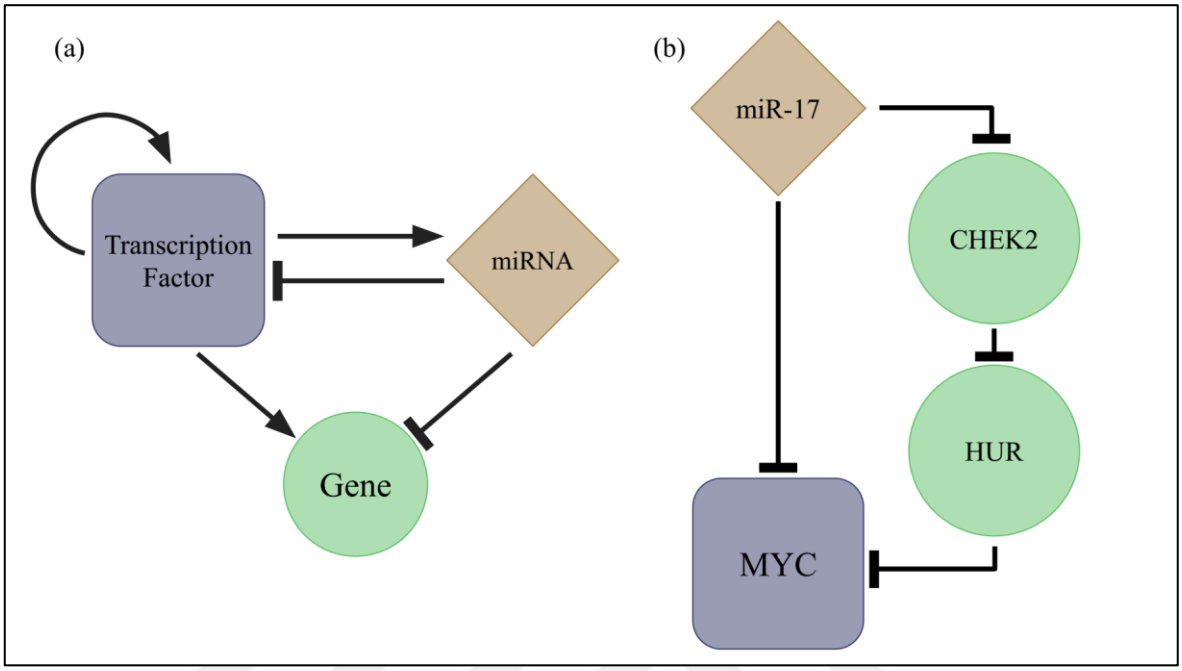

Figure 1.3. An example of a miRNA regulatory network (a) Interactions between transcription factors, miRNAs, and genes are depicted in the regulation network model (b) Example of negative regulation of MYC by genes CHEK2 and HUR and miR-17

1.4. BUILDING A BRIDGE OF NON-CODING RNAS BETWEEN CALORIC RESTRICTION AND CANCER

Coordinated variations in transcript abundance have been used to examine gene expression datasets by creating biological networks based on the expression profile among genes. Co-expression studies have been utilized to elucidate meaningful variation between experimental conditions, and tissue types [83]. Co-expression is the description of the change in the correlation relationships between genes. The argument underlying the idea is that functional links tend to be represented in co-expression relationships. Differential network methods are increasingly being utilized to highlight interdependence between genes by finding coordinated expressions that vary across conditions. More recently, differential network methods have been used to identify miRNA biomarkers in numerous diseases,

including cancer. The ideas mentioned inspired us to explore these ideas for miRNA interactions.

Recent breakthroughs in molecular biology have revealed that non-coding RNAs, as well as proteins, play a significant role in regulating gene expression. MiRNAs have been demonstrated to be involved in transcription regulation, chromatin remodeling, and post-transcriptional RNA modifications, hence it is obvious that miRNAs play an important part in gene regulatory networks.

In this thesis, the miRNA profiles of blood and MFP tissue samples were examined in mice subjected to various forms of CR. The primary goal of this study is to understand the impacts of different forms of CR on miRNA profiles in mice, as well as to assess the effects of CR by evaluating and comparing unique regulatory networks. Furthermore, comparing the miRNA profile in healthy tissues of mice with and without tumor development in order to assess the impact of tumor growth on specific tissues in mice will offer insight on how caloric restriction modifies the cancer epigenome.

The joint graphical lasso method was used to build a gene co-expression network. This model controls the sparsity across all condition-specific arrays and their differences. Because we are interested in network differences, combined estimates of various graphical models provide useful information into network similarities and differences. Graphical models consider co-expression information from additional genes, in contrast to Pearson correlation. In this way network inference was closer to real biological networks.

Once we inferred the miRNA co-expression networks, we evaluated in them two node centrality indices (degree and eigenvector centrality) to find miRNAs with higher topological significance. These miRNAs with high degree, relative to their neighbors, were called hubs, and were used for further analysis.

2. METHODS

2.1. STUDY DESIGN AND ANIMALS

When the mice were 10 weeks old, they were randomly assigned to one of three different CR diets. There are three types of CR: ad libitum (AL), chronic, and intermittent (CCR and ICR respectively). Water was freely available to all groups. Mean food consumption per mouse determined from AL mice food consumption in an age-dependent manner. However, in a monthly cycle, the CCR and ICR groups are subject to a 15% limit compared to AL. Mice in the AL group had free access to food. Compared to the AL group, 15% daily CR applied to mice in the CCR group, and these mice received 85% of the food consumed by the AL counterpart daily. Furthermore, in the ICR group, 60% CR was applied for one week, followed by three weeks of AL. This feeding regimen was used on mice until they were sacrificed at specific ages.

We separate the ICR group into two groups based on feeding schedule. ICR-refeeding mice were ICR group mice sacrificed after three weeks of AL interval (ICR-RF). ICR-restriction refers to mice sacrificed after one week of 60% CR in the ICR group (ICR-R). Animals were sacrificed after an overnight fast at the following ages: 10 (baseline), 49, 50, 81, and 82 weeks. Animal food consumption was tracked on a daily basis. The AL and ICR R groups were fed on the first day of each week, while the CCR and ICR-RF groups were fed on a daily basis.

2.2. SAMPLE COLLECTION AND RNA EXTRACTION

We used two different tissues (blood and MFP) to analyze miRNA expression using the microarray method. We isolated RNA from all samples with Direct-zol RNA Miniprep (Zymo Research), according to the manufacturer’s recommendation. Storing and homogenization of tissues vary only since mammary fat pad tissue has to be digested to extract RNA.

2.3. MICROARRAY DATA PROCESSING

The fragmented cDNA was hybridized using a GeneChip miRNA Array (Affymetrix) at 45°C for 16 h and a Hybridization Oven 640 (Affymetrix), and then was washed, stained in a GeneChip Fluidics Station 450 (Affymetrix), and scanned using an Affymetrix GeneChip Scanner. We analyzed the scanned chip images with Affymetrix GeneChip Command Console version 2.0 (AGCC) and processed using default settings.

2.3.1. Storage of Raw Data and Output Files

First, we prepared a master table with the information of all arrays (Table 2.1.) This table contains the following information: the identification number of each mouse, the scientific name of the organism, the diet administered, the sample collection period in weeks, the disease of the mouse, the type of sample collected, the microarray design applied, the microarray result file, and the folder containing the files during the analysis. A consistent analysis was made possible by this table. All analyzes were performed on the R platform if not stated otherwise. Inside the master folder, the *Data* folder contains all array results in *.CEL* format, and R data files in *.RData* format. The *.CEL* format stores intensity measurements from hybridized microarray pictures. The *Data/Blood* folder contains the microarray results from blood tissue. In the same way, the */Data/MFP* folder contains microarray results from mammary fat pad tissue. We have three replicates for each condition (n=3).

Table 2.1. Example of table with sample information

individual	organism	diet	age	disease	organism part
T095	Mus musculus	AL	49/50	FALSE	Blood
T096	Mus musculus	AL	49/50	FALSE	Blood
T207	Mus musculus	AL	49/50	FALSE	Blood
T106	Mus musculus	CCR	49/50	FALSE	Blood
T184	Mus musculus	CCR	49/50	FALSE	Blood
T185	Mus musculus	CCR	49/50	FALSE	Blood
T130	Mus musculus	ICRR	49/50	FALSE	Blood
T134	Mus musculus	ICRR	49/50	FALSE	Blood
T196	Mus musculus	ICRR	49/50	FALSE	Blood

2.3.2. Normalization and Filtering the Data

We imported the Affymetrix microarray outputs (CEL files) using the oligo [84] package (*read.celfiles*) to be able to analyze in the R interface for the presentation of the expression profiles. Before normalization of the arrays, we made some necessary filtering. Namely, we first filtered mice that developed tumors to only see differences in diet between tissues. Because the data contained probes from various species, including humans and rats, we preprocessed it to only include mouse probes. This will help us increase the power of the statistical test.

Affymetrix probe sets are composed of probes that measure either a perfect match (PM) or a paired mismatch (MM) signal independently. PM probes quantify effective gene expression, whereas MM probes quantify cross-hybridization and consequently background noise. The MAS5.0 algorithm developed by affymetrix calculates “Ideal Mismatch” value using MM values and corrects PM values with these “Ideal Mismatch” values. MAS5.0 then summarizes the data using a one-step Tukey Biweight procedure. The Robust Multi-array Average (RMA) [85] technique does not use MM values; instead, it estimates the background by convoluting the signal and noise distributions from the PM values. After background correction, RMA quantile normalizes the data and then utilizes the median

polish as a summarization procedure. Quantile normalization tries to homogenize the distribution of probe intensities across many arrays. Median polish algorithm iteratively subtracts the row medians and then the column medians. Following convergence, the row and column medians are set to zero, and the remainder of the matrix is subtracted from the original data matrix. We normalized microarrays using the RMA algorithm implemented in the *rma* package. Although there are alternative ways for correcting and normalizing the background, RMA is usually an acceptable default choice.

2.3.3. Principal Component Analysis

To get a "big picture" of the data, principal component analysis (PCA) is commonly performed initially. It captures variance in a dataset using main components. By lowering the dimensionality of the data, PCA can help identify sample outliers and analyze the source of variance. Because microarray data has more miRNAs (rows) than samples (columns), the expression matrix is transposed before being input into the function implemented in the R function *prcomp*.

2.3.4. Differential Expression Analysis

Next, we identified differentially expressed genes between dietary groups, and tissue types of blood and MFP. We merge two intermittent restrictions ICR-R and ICR-RF into the one factor ICR. This will allow us a less complicated hypothesis to compare diets. Limma [86] is a R package for analyzing gene expression microarray data, focusing particularly on the use of linear models for analyzing designed experiments and determining differential expression. Limma allows us to compare several RNA targets at the same time in arbitrarily complex constructed experiments. Output of limma is comparable to that of a t-test, but it has been stabilized against the effects of small sample sizes ($n<6$). Empirical Bayesian methods [87] are implemented to get reliable results even with a few arrays. To identify differentially expressed miRNAs, we compared the baseline of each group with CR-treated mouse tissues using a linear model, followed by a Benjamini-Hochberg correction.

To model the consequences of prolonged life under various dietary settings on mice, we used three well-established feeding patterns in conjunction with natural aging. Since we want to

find the differential expression between healthy-fed (CCR, ICR) or unhealthy (AL) old mice and mice with no effects, in principle it is these two variables, young controls and old mice, that we should consider. So we construct a design matrix with *formula(~ 0 + diet:age:tissue)* according to considered contrasts as seen in Table 2.2. The underlying principle for the design formula is that we assume constant noise variance across all experiments. If we evaluate each condition separately, we will not detect any DE miRNAs due to the low number of replicas. Using the homoscedasticity hypothesis, we can estimate the standard error using all of our replicates. We gain additional degrees of freedom. We set the cutoff criteria as adjusted *p*-value < 0.05 when analyzing differential expression. We constructed Upset plots to show commonly expressed miRNAs [88].

Table 2.2. First six contrasts we used in analysis

Contrast	**Condition**	**Reference**
d.AL.49.Blood	AL.49.Blood	BASELINE.10.Blood
d.CCR.49.Blood	CCR.49.Blood	BASELINE.10.Blood
d.ICR.49.Blood	ICR.49.Blood	BASELINE.10.Blood
d.AL.81.Blood	AL.81.Blood	BASELINE.10.Blood
d.CCR.81.Blood	CCR.81.Blood	BASELINE.10.Blood
d.ICR.81.Blood	ICR.81.Blood	BASELINE.10.Blood

2.4. PATHWAY FUNCTIONAL ENRICHMENT

The annotated DE miRNAs were then investigated for their related biological meaning using GO annotations and mapped to KEGG database biological pathway information. We used hypergeometric distribution statistical theory to calculate *p*-values for each route and GO term in the GO and KEGG pathway enrichment study. The simplest method for miRNA functional annotation is to do a functional enrichment analysis on enrichment of miRNA target genes. This method proposes that miRNAs perform similarly to their target genes, given the wealth of knowledge collected about genes over the last few decades. As a result, it is feasible to assign miRNAs functions that are strongly enriched for the targeted genes. This method involves three stages: determining which genes are targeted by selected

miRNAs, identifying target genes for their involvement in pathways and processes, and conducting statistical analysis to determine whether a biological process is overrepresented in the collection of targeted genes. However [89] demonstrated that most often used in technique for inferring miRNA-regulated pathways is not specific and results in the systematic discovery of strongly linked biological processes, such as cell cycle and cancer biology. The targets of miRNAs are compared to the pathways of protein-coding genes in this indirect approach. For the aforementioned reasons, we implemented the strategy suggested by [89]. They suggested the following steps:

1. convert pathways of protein-coding genes into miRNA lists targeting at least one of these genes,
2. directly compare the list of related miRNAs with lists of miRNAs previously associated with various pathways.

This technique assures that a miRNA is only represented once in a pathway, regardless of how many target genes it has in that pathway. A two-sided hypergeometric test to calculate the importance of each term was selected and Bonferroni were used for *p*-value correction.

$$P_j(N,n,K) = \sum_{k=i}^{(n,K)} \frac{\binom{K}{k}\binom{N-K}{n-k}}{\binom{N}{n}} \tag{2.1}$$

GO terms were retrieved from Mouse Genome Informatics Database (http://www.informatics.jax.org/downloads/reports/index.html#go).

2.5. INFERRING MIRNA REGULATORY NETWORK USING GRAPHICAL LASSO

Microarrays give genome-wide expression of miRNAs hence constructing a network from genome-wide expression provides extensive information about regulatory patterns. Instead of massive correlation matrices, networks are an effective technique to visualize the interactions between miRNAs. Probabilistic estimation of these interactions can be useful to depict the characteristics of the links between miRNAs. These interaction measurements can be simple covariances, correlations, or regression coefficients. Another feature seen in biological networks is that almost every variable is interconnected. In other words, inferring

networks using simple pairwise correlation coefficients produce spurious connections. Finding a sparse matrix can be useful because zeros in the inverse of the covariance matrix imply that two variables are independent.

If two genes correlate (there are lots of ways to measure association - correlation, weighted rank, distance covariance), it means they change together under a condition, so they are regulated together. It is critical to choose the gene connection method for co-expression network construction, since the approaches that can identify genes with accurate concordance frequently influence the types and quantity of knowledge we may gain from the analysis. Among many gene regulatory network analysis approaches, Gaussian Graphical Model (GGM) are favorable because of their straightforward interpretations and computing advantages [90]. Gene expression data is represented as a *n*p* matrix, with each row corresponding to a sample and each column to a gene. A GGM is based on the assumption that samples are drawn independently from a Gaussian distribution with mean μ and covariance matrix Σ, where the precision matrix $\Theta=\Sigma^{-1}$ represents a weighted undirected graph. Maximum likelihood is a natural method for estimating the precision matrix. If S represents the sample covariance matrix, the objective is to minimize the penalized log-likelihood function:

$$\hat{\theta}(\lambda_1) = argmin_{\theta>0}\{tr(S\Theta) - logdet(\Theta) + \lambda_1 \sum_{i \neq j} |\theta ij|\} \quad (2.2)$$

Penalized estimation has been created to regularize estimation and generate interpretable networks. Sample covariance matrix S is the measurement of individual relations between each pair of miRNAs, which describes the dependency between two random expressions.

Differential network analysis can uncover biologically significant differential co-expression modules that would be missed by conventional co-expression or differential expression analyses. Much interest has been directed toward estimating differential networks in biological studies, where recent findings suggest that the interactions between components of biological systems can change over time, particularly when the system responds to a perturbation or when the system is diseased. Joint estimate of various graphical models is a recent graphical modeling approach that attempts to account for shared edges in networks in order to better highlight their differences.

The purpose of joint estimation of various graphical models is to borrow knowledge from other conditions in order to improve network estimation in each condition. More precisely, let θ^1 and θ^2 be precision matrices with the same number of observations. Then, using joint estimation procedures, the estimations of θ^1 and θ^2 are encouraged to be similar:

$$min_{\theta^{(1)},\theta^{(2)}} \sum_g n_g \left(tr\left(S^{(g)}\Theta^{(g)}\right) - logdet\left(\Theta^{(g)}\right)\right) + \lambda_1\left(\sum_{i\neq j}|\theta^{(1)}ij|\right) + \sum_{i\neq j}|\theta^{(2)}ij|) + \lambda_2 \sum i,j|\theta^{(1)}ij - \theta^{(2)}ij| \quad (2.3)$$

In the first component of the formula, the sparse lasso penalty incentivizes the use of sparse precision matrices. The fused lasso penalty in the second component incentivizes the two condition-specific precision matrices to have similar edge values, allowing for the integration of information across conditions and the generation of a sparse estimate of the precision matrix difference. In this case, λ^1 and λ^2 are two non-negative tuning parameters. The first tuning parameter specifies the sparsity level of condition-specific precision matrices. The second tuning parameter determines the degree of similarity between condition-specific networks and the degree of sparsity between the networks.

Because the lambda parameter is responsible for network sparsity, finding the ideal lambda parameter to estimate the true network is very relevant. For microarray data, there is no conventional parameter method. The major difficulty here is to establish a balance between network sparsity and estimation accuracy in order to get closer to the genuine network. There are numerous methods for selecting models. One of the most common is cross-validation, which is based on the performance of the projected network on a test dataset. However, cross validation does not account for the complexity of the chosen network. We decided to minimize the Akaike information criterion (AIC) in order to locate sparse networks, hence the tuning parameters 1 and 2 in the JGL model were chosen using the AIC:

$$AIC(\lambda_1, \lambda_2) = \sum_g \{n_g tr(S_g \hat{\Theta}^{(\lambda_1,\lambda_2)}) - n_g logdet\hat{\Theta}^{(\lambda_1,\lambda_2)} + 2E^g \quad (2.4)$$

, where E^g is the number of non-zero elements in $\hat{\Theta}^{(\lambda_1,\lambda_2)}$. To build a miRNA - miRNA co-expression network we first filter most DE miRNAs among 1908 miRNAs as the number of observations (miRNAs) This step is important because when the number of observations passes the number of samples, the computational power spent to calculate the inverse of the covariance increases. At the end we have a matrix consisting of 98 most DE miRNAs and 54 arrays. We used the *FGL* package to implement joint graphical lasso to infer DCE miRNA networks among tissues [91]. To visualize the networks, we used the *igraph* package.

2.5.1. Topological Measurements

For a graph G, where V represents the nodes and E represents the edges defined as G = (V, E). The degree reflected the interactions of these nodes with other nodes by measuring how many edges were connected to these nodes. For example, if a node, v, had n edges connected to it, the degree of node v was defined as:

$$degree(V) = n \tag{2.5}$$

An approach that measures the distributive effect of nodes is called eigenvector centrality. Score of a node is increased more by connections coming from high-scoring nodes than by connections coming from nodes with low scores. A node that has a high eigenvector score is linked to numerous other nodes that also have high scores. Let A= ($a_{u,t}$) is the matrix representation of graph G. Eigenvector centrality can be calculated as:

$$x_v = \frac{1}{\lambda}\sum_{t\epsilon g} a_{v,t}x_t \tag{2.6}$$

In general, a non-zero eigenvector solution will exist for a wide range of various eigenvalues λ. The relative centrality score of node v in the network is therefore provided by the v^{th} component of the corresponding eigenvector.

2.6. CONSTRUCTING MIRNA INTERACTION NETWORKS

Edges give information about the direction and intensity of the node-to-node connection. Edges reflect positive or negative correlation/covariance between variables based on the strength between two nodes. The spectrum of positive and negative value connections may be depicted visually by using various colored lines to show the edges. However, we used only one color and one edge width for the visualization since these properties did not add more info in networks.

2.6.1. miRNA - Target Gene Interaction Network

MiRNAs generally bind to the 3’ UTR region of the gene transcript partially complementary base pairings. Several computational methods have been developed to find target genes of

the miRNAs based on binding sites. Common characteristics of prediction algorithms are seed match between nucleotides, free energy of miRNA-mRNA duplex, conservation of the sequence across species and site accessibility of the mRNA.

Table 2.3. All target prediction databases/algorithms used

Algorithm	**Source of data**	**Reference**
miRanda	http://www.microrna.org	[92]
PicTar	http://pictar.mdc-berlin.de/	[93]
TargetScan	http://www.targetscan.org/	[94]
DIANA-microT	http://diana.cslab.ece.ntua.gr/microT/	[95]
miRDB	http://mirdb.org/miRDB/	[96]

We combined validated miRNA targets from miRTarBase [97] with predicted targets. To predict the upstream genes of key differentially expressed miRNAs, we used *miRNAtap* package. Aggregation of commonly used prediction algorithms outputs in a way that improves on the performance of every single one of them on their own when compared against experimentally derived targets. Targets are aggregated from five most commonly cited prediction algorithms: DIANA, Miranda, PicTar, TargetScan, and miRDB (Table 2.3.). If the target gene was found in at least two of these databases, it was considered among the predicted genes. To test the significance of the targets, we applied the randomized decision rule. We selected 1000 random target genes from the target list of each miRNA and calculated the probability scores of the genes. We considered those scores with a *p*-value higher than 0.05 significant. Most targeted genes were visualized with the *circlize* package [98].

2.6.2. miRNA Influence on KEGG Pathways

Enrichment-based methods consider the relationship between miRNA and pathway by looking at the enrichment of targeted genes in a pathway rather than the topological significance of those genes. Enrichment-based methods also do not aim to evaluate changes in differential or rewired connections.

We implement the ideas from the study [99] that proposes a new network-based method for analyzing the degradation caused by rewired miRNA-target gene interactions at the pathway network level. This method contributes to a better understanding of miRNA regulation by describing how formation of a new connection affects genes in a pathway. For example, in some cases, a miRNA can regulate multiple genes in the same pathway, and one gene can be regulated by multiple miRNAs in a diet but not others. The importance of miRNA will change depending on the rewiring between different diets. If a miRNA in a network has connections with genes of high topological importance, miRNA itself has also high topological importance. By focusing solely on miRNA-mediated changes, we can define the relationship between a set of miRNAs and a set of pathways.

Since genes in the pathways are directed, we created new directed networks, which we achieved by making miRNA-miRNA connections mutually directed. Then, for each KEGG pathway, we integrated the miRNA network according to the target genes in a given network. We measure the importance of miRNAs with eigenvector centrality. As suggested in [99] we sum all scores of miRNAs in a rewiring network which gives total influence on a given pathway. We construct and analyze all networks with the *igraph* package (https://igraph.org/) and KEGG pathways acquired from the *graphite* package [100].

3. RESULTS

We analyzed miRNA expression profiles of calorie-restricted mice, then we integrated miRNA expression data to create tissue-specific networks and observed their response to the different dietary regimens, summarizing tissue-specific relationships between pathways.

We will present our findings in two separate sections. In the first part, we will explain how we process our data, namely the quality control of samples, sample selection, and normalization. As a result of this analysis, we will show the effect of diet on different tissues and compare between tissues. In the second part, we will show how we create networks and compare these networks. Figure 3.1. summarizes the data collection time points.

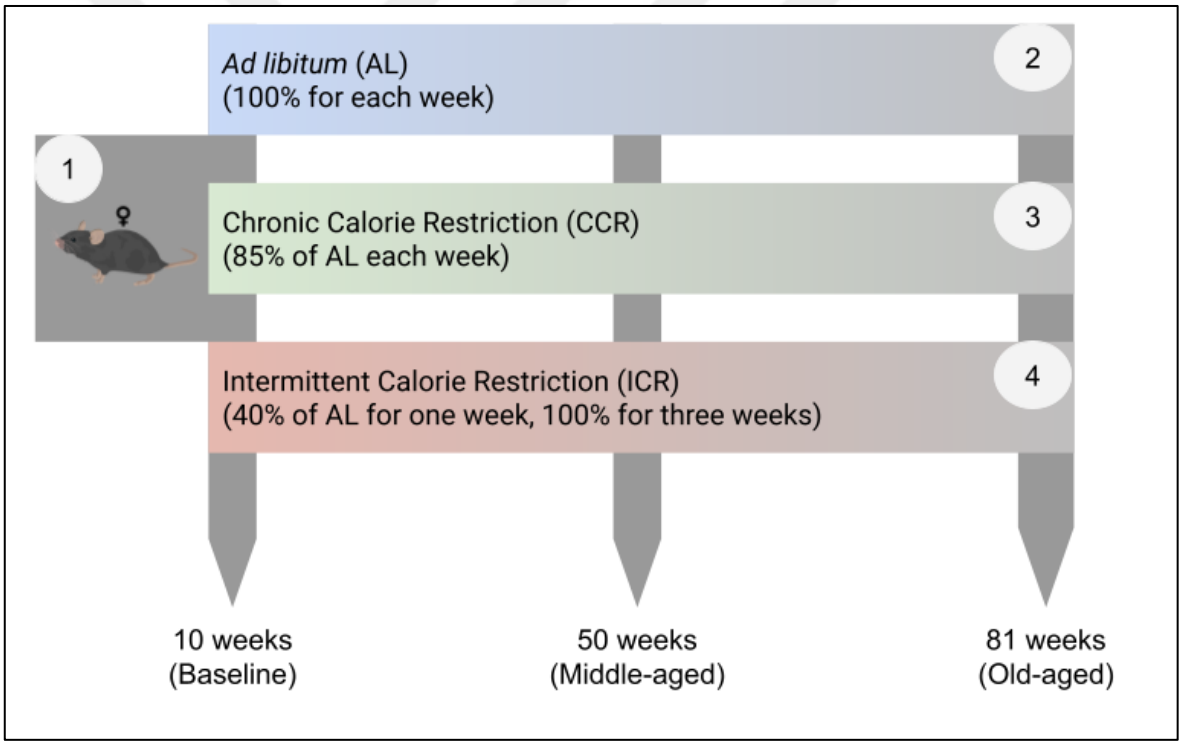

Figure 3.1. Schematic diagram of CR application with sacrifice intervals

3.1. DESCRIPTIVE ANALYSIS OF MIRNA MICROARRAYS IN MICE

This section shows how to use the method to find which miRNAs in mice respond to caloric restriction. Therefore, the goal is to find groups of miRNAs closely linked to the diet whose expression changes how tissues respond to systemic effects of CR.

There are n_0 = 1908 miRNA expression profiles of mammary, and blood tissues, with n = 3 biological replicates for each of them. As discussed in the previous chapters, there are three diets: ad libitum (AL), chronic caloric restriction (CCR), intermittent caloric restriction (ICR). Moreover, the condition before the dietary intervention is labeled BASELINE. We will use these abbreviations in the following figures and tables. The specific details of each diet are explained in Method section.

3.2. DATA PREPROCESSING

Following the initial data import, the next step is to perform quality control on the data. Here, we look for outliers and determine if the expression values are coherent with the experimental conditions.

We visualize the data using principal component analysis (PCA) over logarithmic-transformed raw data. Each point in the Figure 3.2. corresponds to a single sample, with the color denoting the type of tissue and the shape reflecting the diet. The figure shows that the samples naturally cluster according to the experimental conditions, even before normalization. This figure also shows that tissue type has a significant role in miRNA expression variation.

Each cluster shows how well the data is separated. For example, the distance between miRNA expression in blood and miRNA expression in the MFP is explained by the multitude of data variations between the conditions.

Although there are alternative ways to correct and normalize the background signal, RMA is usually an acceptable choice. RMA distributes data across arrays and uses the flexible quantile normalization approach to align the array intensity distributions.

Figure 3.3. shows the PCA of normalized data. Compared to the first PCA analysis before normalization, we see that now the first principal component separates between the tissue types. Indeed, all blood samples have PC1 over 30 and PC2 below zero, and all MFP samples have PC1 between -28 and 30, and PC2 above zero. Most samples from different tissues are separated, except for some cases of blood and MFP.

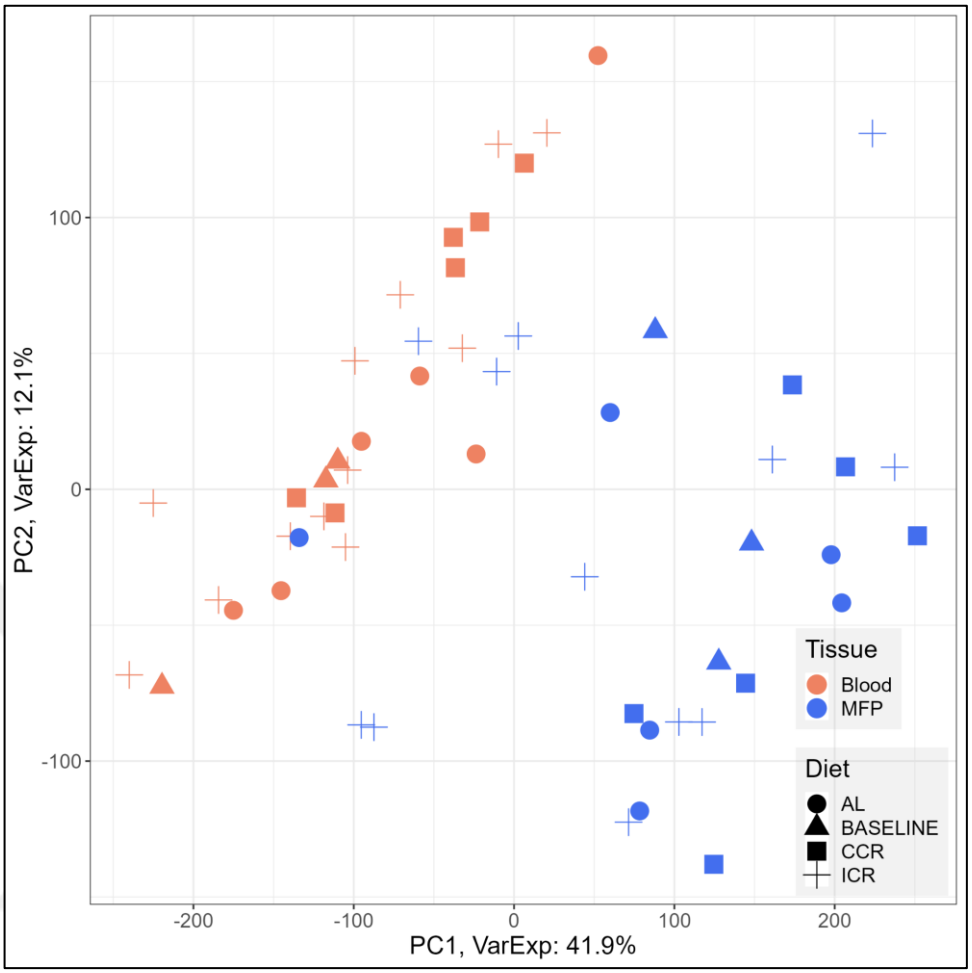

Figure 3.2. PCA plot of raw samples before normalization for each CR group

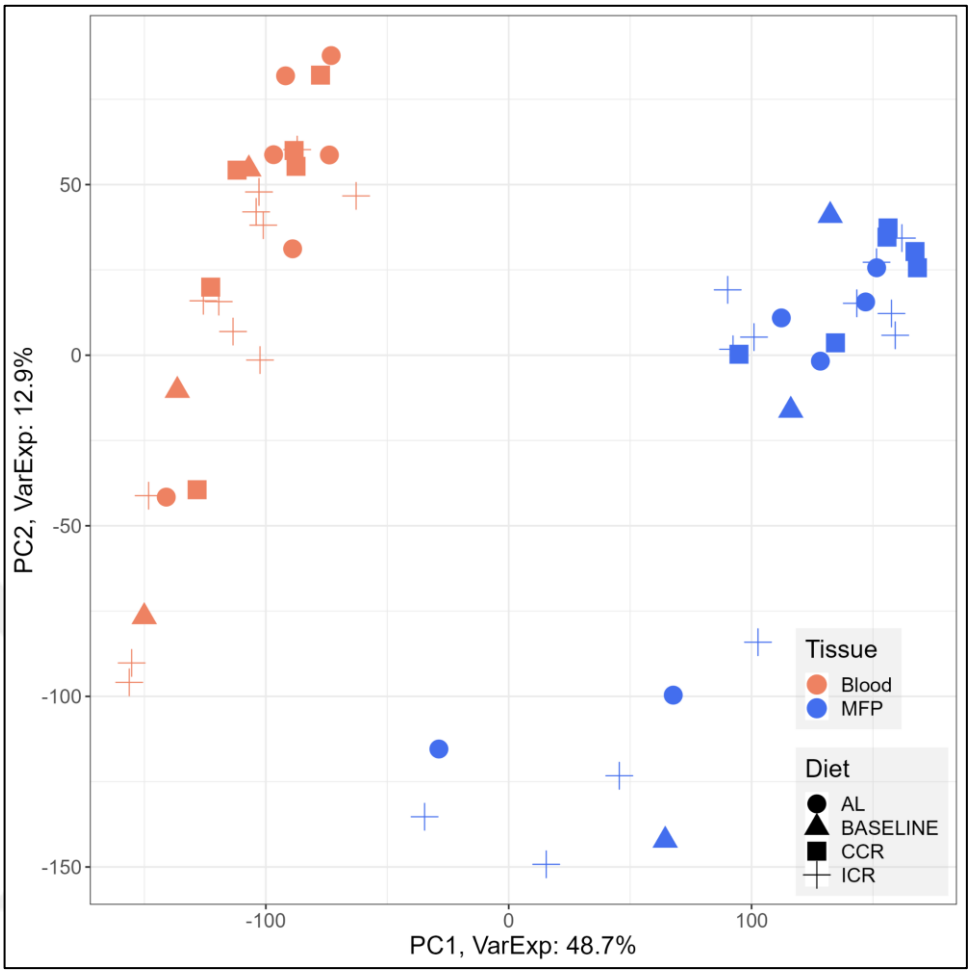

Figure 3.3. PCA of the normalized samples for each dietary group

3.3. CORRELATION OF EXPRESSIONS BETWEEN TISSUES

Correlation between miRNA expression in different tissues for the same animal is significant but not very high. Figure 3.4. shows the correlation between miRNA expression in blood and MFP for animal T95. Each of these variables has a distribution that can be described as a combination of normal distribution of low values and a long tail with high values.

To get a broad characterization of mouse miRNA expression, we performed a sample correlation of blood and MFP samples to determine which of the primary known causes of variation is responsible for the sample division.

Pearson correlation coefficients were calculated based only on mature miRNA probes. There are a few animals where we measured gene expression in different tissues. Animal T95 was

chosen to demonstrate variance across samples since it has samples from both tissues, as shown in Figure 3.4. Blood samples vary greatly among different animals and diets. In contrast, MFP samples preset lower variability among different animals. As shown in Figure 3.5. we select different animals but the same tissue to be consistent for comparing diets. For MFP tissue, the average pairwise correlation between animals T95, T106, and T116 is 0.97. For blood tissue, the average pairwise correlation between the same animals is 0.84. Based on both clustering and correlation of normalized miRNA expression values, we conclude that the main source of variation is the tissue. For this reason, the following analyses are performed on each tissue separately.

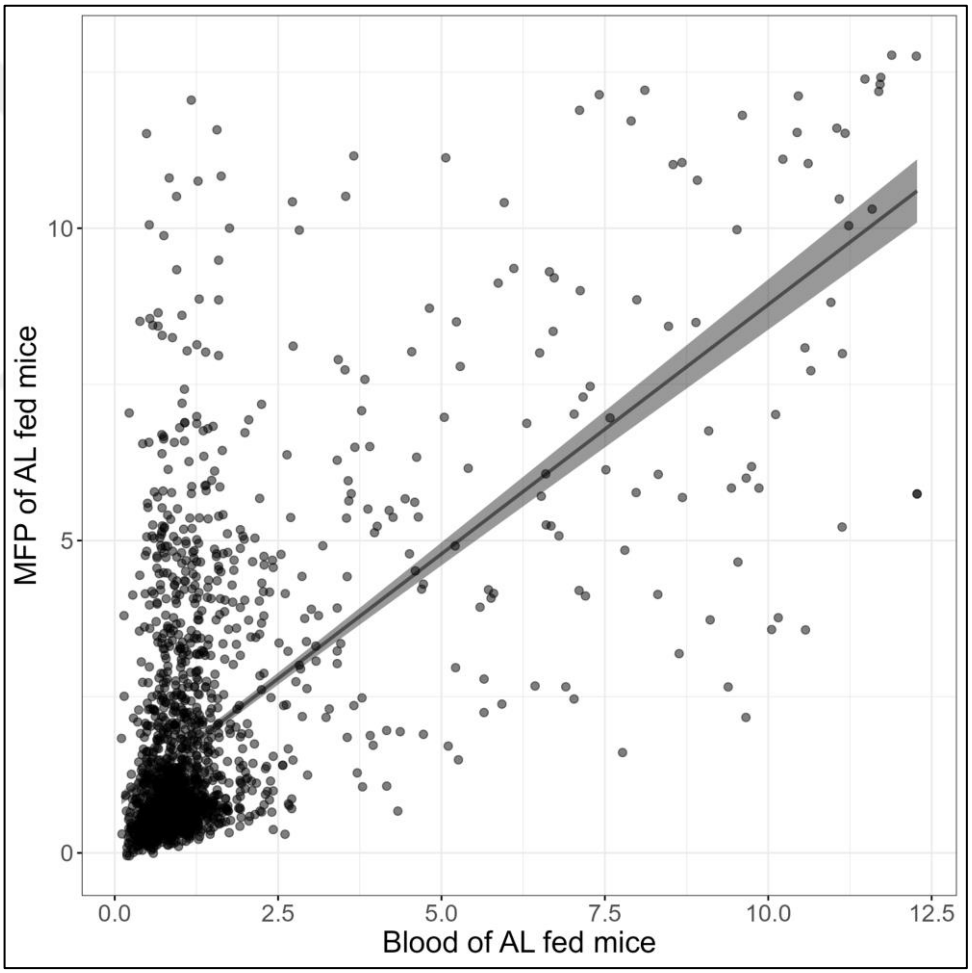

Figure 3.4. Scatter plot showing the correlation between miRNA expression in blood and in MFP samples taken from the same animal

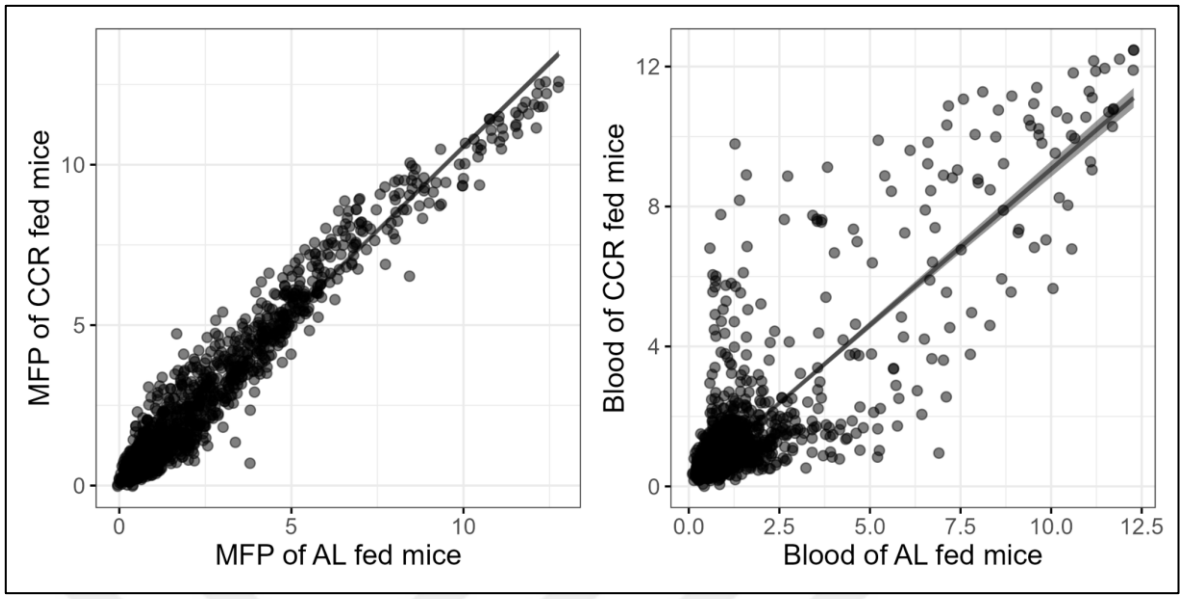

Figure 3.5. Scatter plot showing the correlation between miRNA expression of animals fed with different diets (AL vs CCR)

3.4. BASELINE-CORRECTED MIRNA EXPRESSION

To identify which miRNAs had the most significant expression, we measured miRNA expression in mice of different age groups and different diets and compared them against the baseline for the corresponding tissue. This change in expression with respect to the baseline corresponds to the miRNA expression. Significant expression corresponds to significant differential expression with respect to the baseline.

Across all conditions there are 98 significantly expressed miRNAs, with an adjusted p-value under 0.05. Their normalized expression is shown in Figure 3.6. Expression values of tissues were divided into two distinct clusters according to hierarchical clustering.

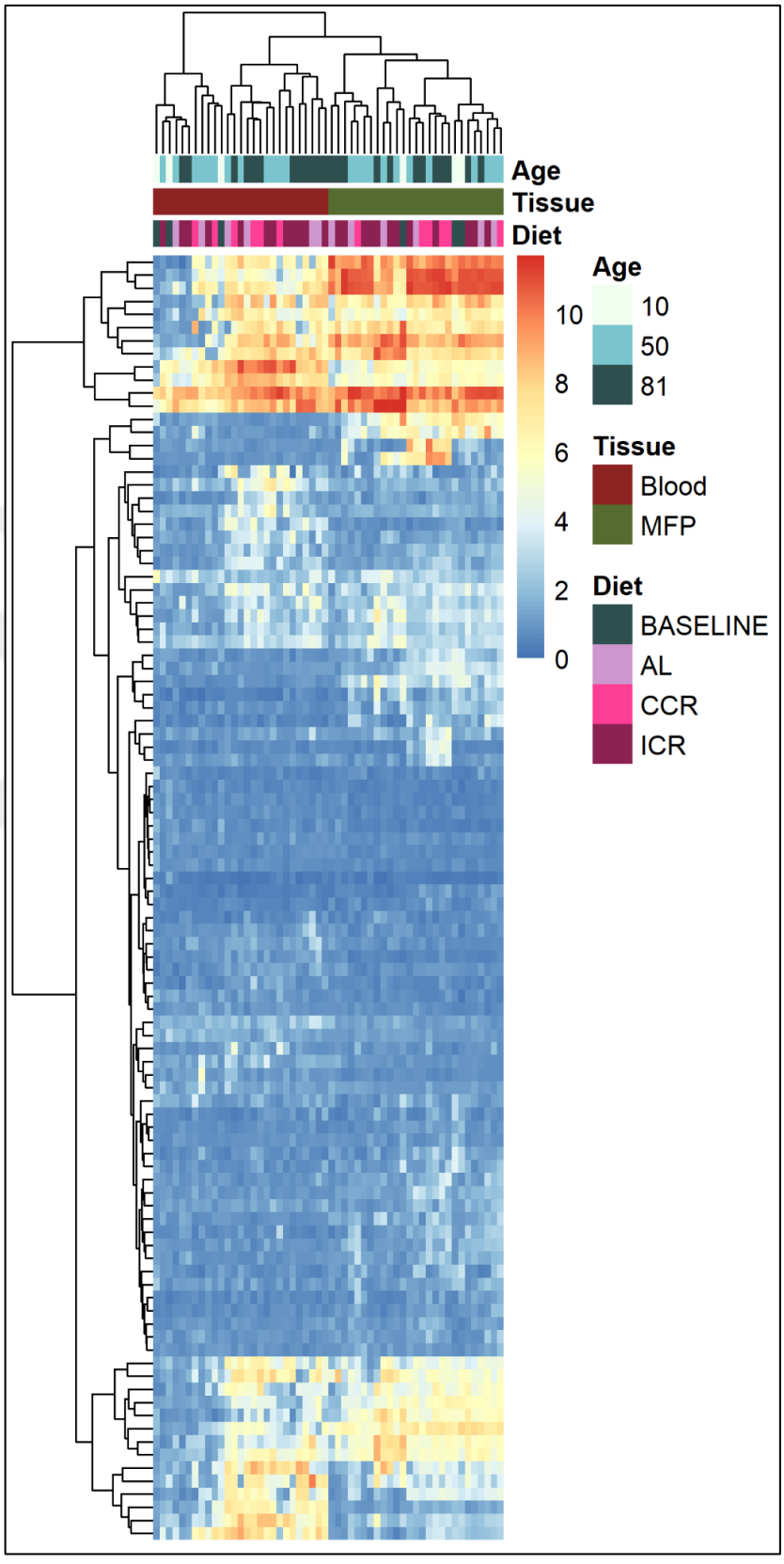

Figure 3.6. Heatmap of miRNAs significantly expressed for each dietary restriction group

3.5. MICRORNA EXPRESSION IN THE BLOOD

Each tissue has its own unique expression pattern. None of the miRNAs are significantly expressed in both tissues (see Appendix 5). Figure 3.7. shows the number of significantly expressed miRNAs under every separate diet and age, as well as in their combinations. There are 63 significantly expressed miRNAs, 51 of them upregulated, and the remaining 12 ones downregulated. The most significantly upregulated miRNA is miR-494-3p, and the most significantly downregulated one is miR-365-1-5p.

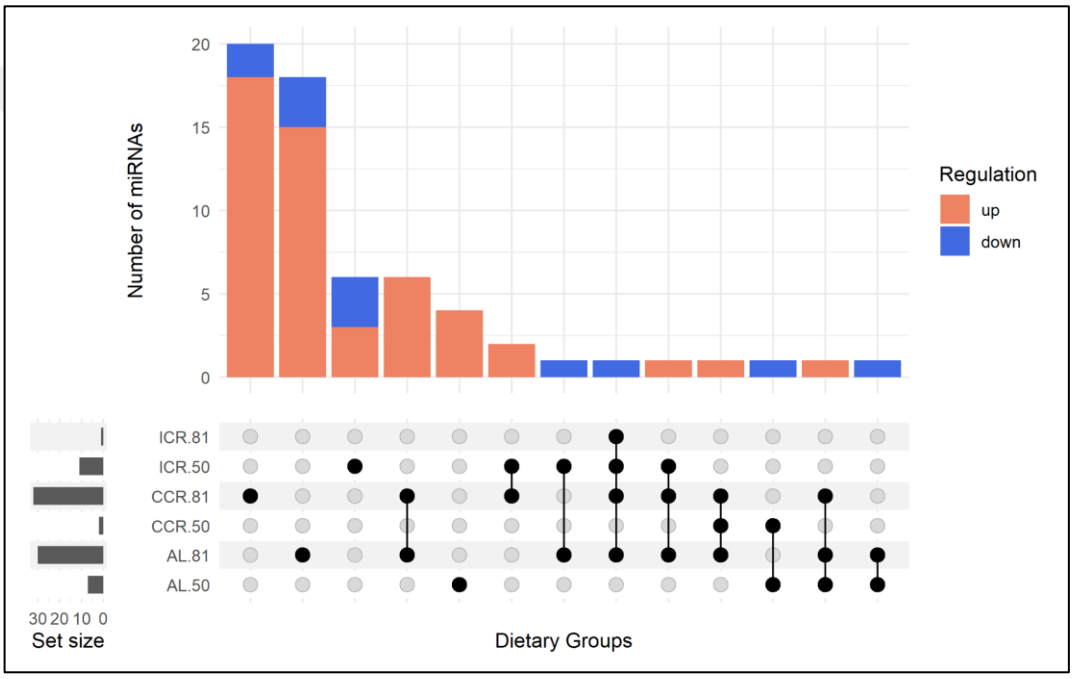

Figure 3.7. Upset plot of miRNAs significantly expressed in blood samples for each dietary group. Horizontal bars show the number of miRNAs for each condition. Vertical bars show the number of miRNAs of each intersection as described by the bullet points in the lower part

In the blood of middle-aged mice, seven miRNAs are significantly expressed in AL, two miRNAs are significantly expressed in CCR, and only one miRNA (miR-3073a-3p) is significantly expressed in both diets (Table 3.1.). Under ICR, the expression of 11 miRNAs is significant. None of the miRNAs significantly expressed in ICR are significantly expressed in the other diets. In other words, in the blood of middle-aged mice, ICR has an expression, unlike any other diet.

In the blood of old-aged mice, there are 30 miRNAs significantly expressed in mice fed with an *ad libitum* diet, and 32 miRNAs significantly expressed in mice fed with CCR diet. Ten of these miRNAs are significantly expressed in both diets. Only one miRNA (miR-742-5p) has a significant expression in mice fed with ICR, and it is also significantly expressed in the other diets.

Table 3.1. Numbers of miRNAs significantly up- and down-regulated in blood samples for each dietary group

Age	**Diet**	**Downregulated**	**Upregulated**	**Downregulated with logFC < -1**	**Upregulated with logFC > 1**
50	AL	2	5	0	4
50	CCR	1	1	0	1
50	ICR	5	6	1	6
81	AL	6	24	1	23
81	CCR	3	29	1	29
81	ICR	1	0	0	0

3.6. TARGETS OF SIGNIFICANTLY EXPRESSED MIRNAS IN THE BLOOD

Each miRNA can target several genes due to their ubiquitous nature. Moreover, target prediction algorithms can produce many false positives. To control the number of false positives, we used the permutation test described in method section.

There are 2175 genes predicted as targets of at least one significantly expressed miRNA. The gene targeted by the largest number of miRNAs is Tnrc6b, as seen in Figure 3.8. This gene is targeted by eight miRNAs. Two of these interactions are experimentally validated and the remainder interactions are predicted. The gene Lin28b is targeted by six miRNAs and Celf1 is targeted by five miRNAs.

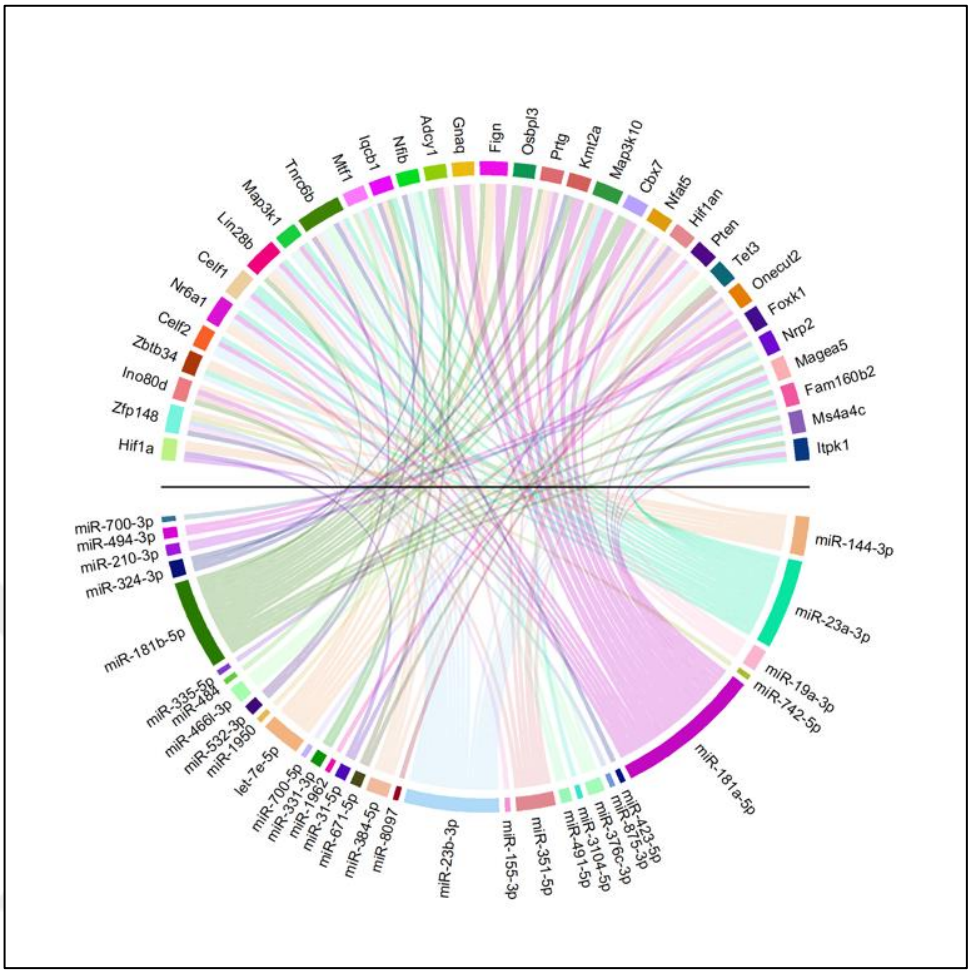

Figure 3.8. Chord diagram of frequently targeted genes of miRNAs significantly expressed in blood samples

3.7. TOPOLOGICAL PROPERTIES OF CO-EXPRESSION NETWORKS IN THE BLOOD

Since small graphs are easier to visualize and understand, we focus on the set of 98 miRNA that has significant expression in any of the examined conditions. The networks were generated jointly for each tissue and diet, as described in the methods section. A key condition we require is that the networks be *sparse*. That is, only a few of all pairs of nodes are connected. Looking at the topological properties of the constructed co-expression networks, we consider only connected nodes for each network. Table 3.2. shows the global network characteristics, such as the number of nodes, number of edges, density (ratio of existing versus possible edges), and average clustering coefficient.

Table 3.2. Global network properties of co-expression networks of miRNAs in blood samples for each dietary group. Columns nodes and edges show the number of nodes and edges in each network

Tissue	**Diet**	**Edges**	**Nodes**	**Clustering**	**Density**
Blood	AL	291	75	0.23	0.10
Blood	CCR	253	71	0.22	0.10
Blood	ICR	206	64	0.24	0.10

The relevant topological properties of each node are its degree, the average degree of its neighbors, and its eigenvector centrality. To illustrate this, Figure 3.9. depicts the distributions of all centrality measures in the networks based on blood data. The degree distributions of all networks follow a power law, indicating that these networks are indeed scale-free, as expected in biological networks. All co-expression networks have a density of around ten percent, which means that only a small proportion of all pairs of nodes are connected. In other words, the networks are sparse.

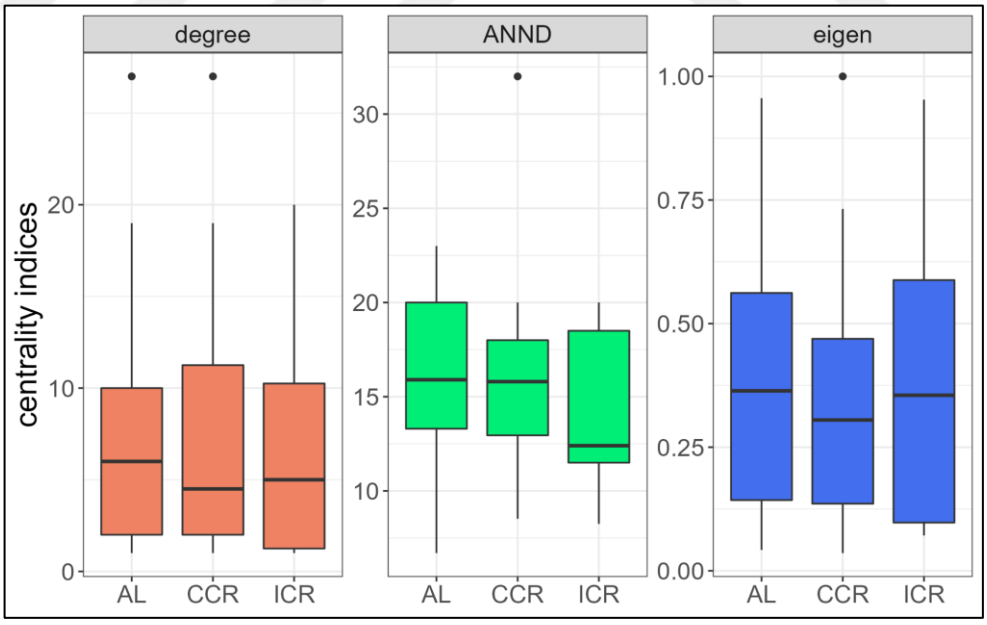

Figure 3.9. Boxplot of centrality indices of co-expression networks of miRNAs in blood samples for each dietary group. Degree, average nearest neighbor degree (ANND), and eigenvector centrality are visualized as boxplots

For blood, the co-expression network for AL has 75 nodes and 291 edges, for CCR it has 71 nodes and 253 edges, and for ICR, 64 nodes and 206 edges. That makes the AL co-expression network the largest size and ICR the smallest one. On the other hand, although the number of nodes and edges changes between co-expression networks, the average clustering and density do not show any significant difference.

3.7.1. Hub miRNAs in the Blood for the AL Group

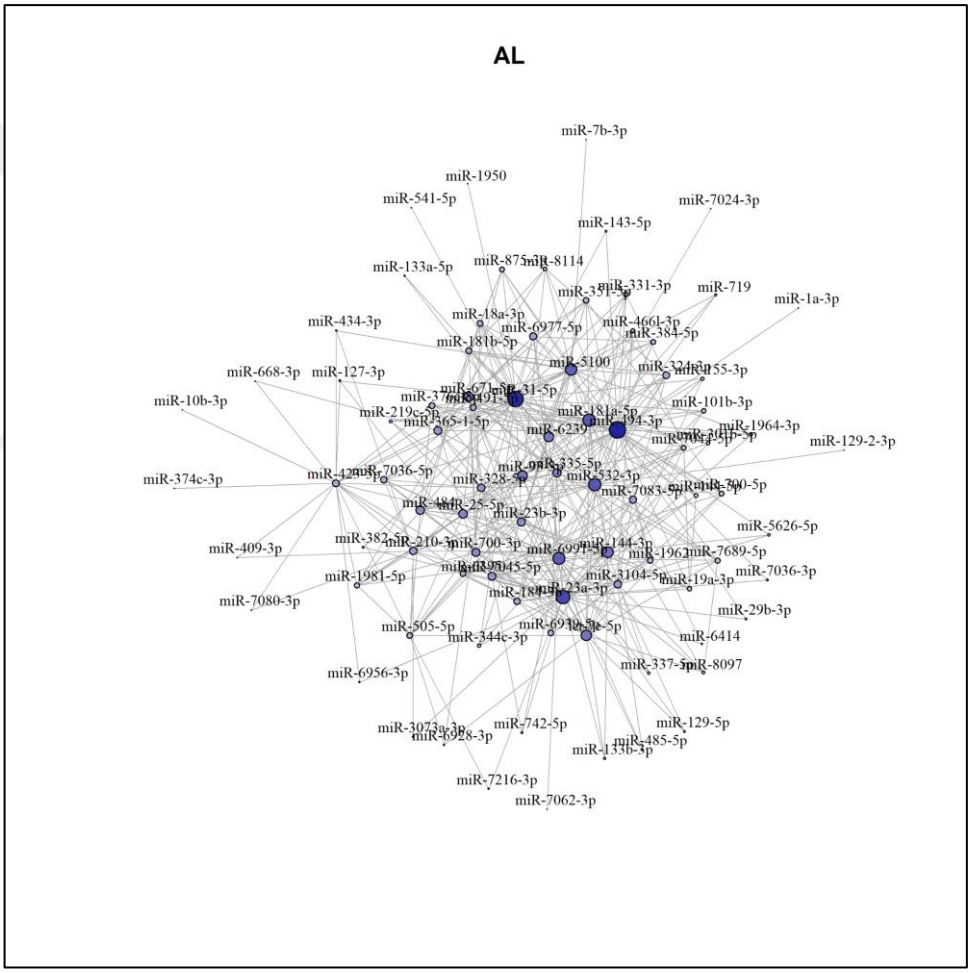

Figure 3.10. Co-expression network of miRNAs in blood samples for the AL group. The node size is proportional to its eigenvector centrality. Darker nodes have higher eigenvector centrality

Figure 3.10. shows the co-expression network of miRNAs in blood for mice fed with AL diet. The centrality measurements of each node of this network can be seen in Table 3.3.

We defined *hub nodes* as the ones having degree larger than the average degree of their neighbors. In other words, these are nodes that connect to more nodes than the nodes they connect. There are 14 miRNAs identified as hubs in this network. The highest degree and eigenvector centrality correspond to miR-494-3p. The miRNA miR-3104-5p is a hub specific to the AL co-expression in blood.

Table 3.3. Centrality indices of hubs of co-expression network of miRNAs in blood samples for the AL group. miRNAs highlighted with bold represent a hub only in the AL group

ranking	**miRNA**	**degree**	**eigenvector centrality**	**ANND**
1	miR-494-3p	27	1.00	7.70
1	miR-6991-5p	24	1.00	9.17
3	miR-31-5p	26	0.95	8.23
4	miR-6239	19	0.90	10.6
5	miR-5100	21	0.89	9.86
6	miR-181a-5p	19	0.87	10.4
7	let-7e-5p	17	0.83	11.4
8	miR-484	14	0.74	13.1
9	miR-532-3p	16	0.76	11.4
10	**miR-3104-5p**	**17**	**0.75**	**10.9**
11	miR-23a-3p	23	0.70	6.70
12	miR-210-3p	15	0.59	10.4
13	miR-505-5p	13	0.56	10.3
14	miR-423-5p	17	0.50	7.24

3.7.2. Hub miRNAs in the Blood for the CCR Group

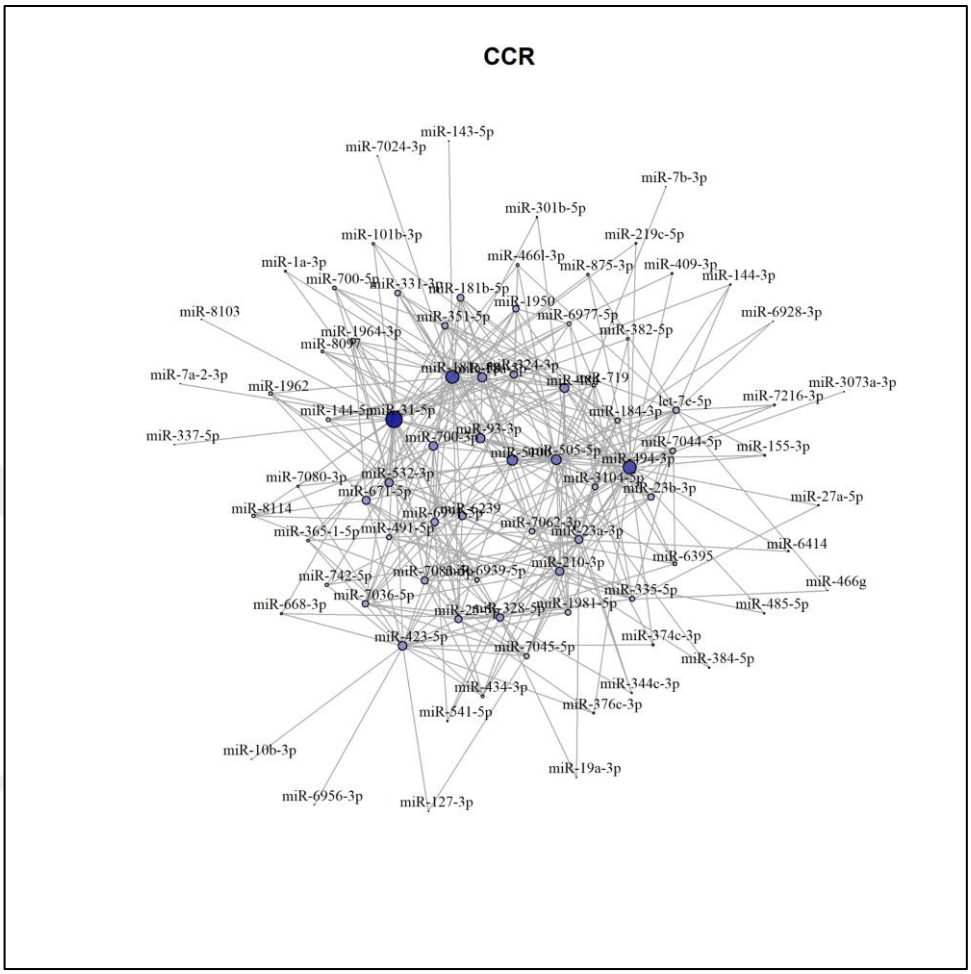

Figure 3.11. Co-expression network of miRNAs in blood samples for the CCR group. The node size is proportional to its eigenvector centrality. Darker nodes have higher eigenvector centrality

The co-expression network of the CCR in blood can be seen in Figure 3.11. Table 3.4. shows the centrality measurements of each node. There are 15 miRNAs identified as hubs in this network. The node with highest degree and eigenvector centrality corresponds to miR-31-5p. There are no hubs in the network for CCR co-expression in miRNA from blood.

Table 3.4. Centrality indices of hubs of co-expression network of miRNAs in blood samples for the CCR group. There is no hub specific to the CCR group

ranking	**miRNA**	**degree**	**eigenvector centrality**	**ANND**
1	miR-31-5p	32	1.00	7.09
2	miR-494-3p	27	0.94	8.11
3	miR-5100	18	0.73	9.89
3	miR-6239	15	0.73	12.9
5	miR-181a-5p	19	0.72	9.11
6	miR-505-5p	21	0.70	8.52
7	miR-210-3p	15	0.66	11.4
8	miR-93-3p	13	0.58	11.5
9	miR-23a-3p	15	0.57	9.53
9	miR-484	13	0.57	11.2
11	miR-532-3p	12	0.50	10.6
12	miR-328-5p	12	0.48	11.1
12	let-7e-5p	12	0.48	10.8
14	miR-6991-5p	11	0.46	10.6
15	miR-423-5p	15	0.40	7.13

3.7.3. Hub miRNAs in the Blood for the ICR Group

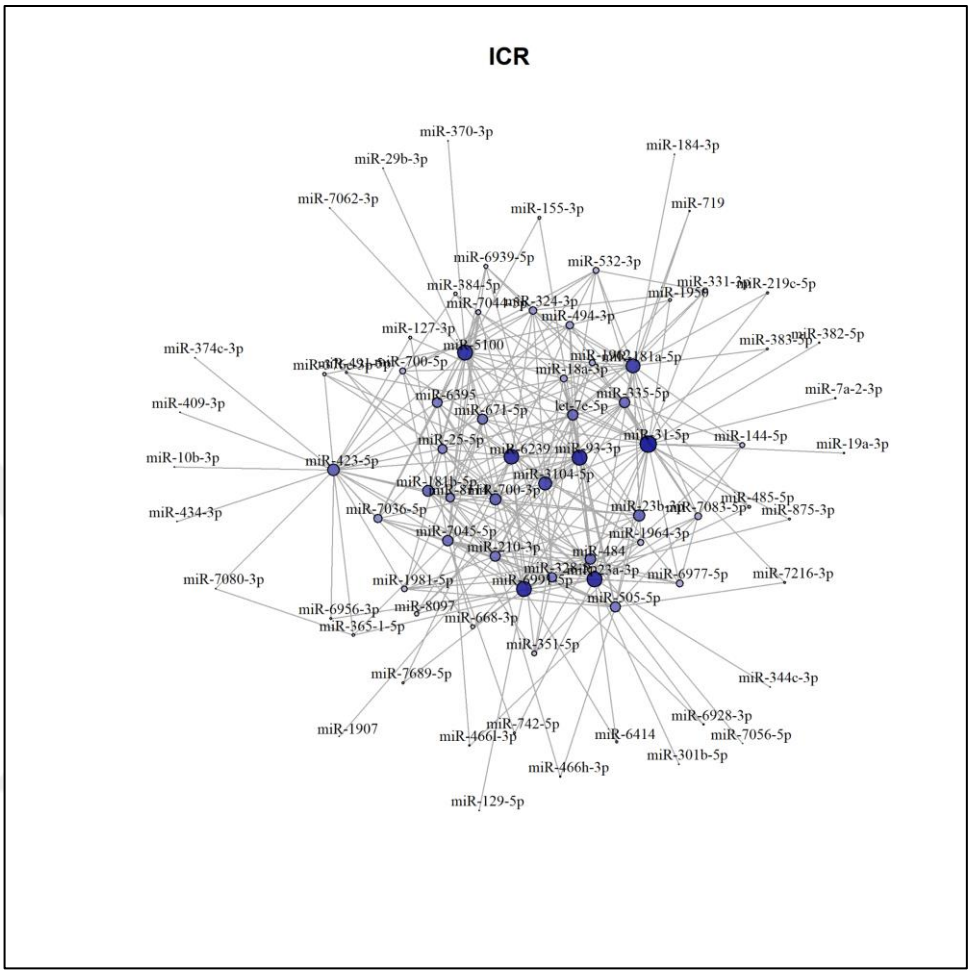

Figure 3.12. Co-expression network of miRNAs in blood samples for the ICR group. The node size is proportional to its eigenvector centrality. Darker nodes have higher eigenvector centrality

The co-expression network of ICR in blood is shown in Figure 3.12., and Table 3.5. shows the centrality measurements of each node. There are 16 miRNAs identified as hubs in this network. The highest degree and eigenvector centrality node is miR-31-5p. There is a hub miRNA, miR-6395, that is specific to the ICR co-expression in blood.

Table 3.5. Centrality indices of hubs of co-expression network of miRNAs in blood samples for the ICR group. miRNAs highlighted with bold represent a hub only in the ICR group

ranking	**miRNA**	**degree**	**eigenvector centrality**	**ANND**
1	miR-181a-5p	20	1.00	8.25
2	miR-31-5p	20	0.98	8.25
3	miR-5100	18	0.95	9.28
4	miR-6239	15	0.91	11.3
5	let-7e-5p	16	0.88	9.31
6	miR-6991-5p	17	0.87	8.24
7	miR-23a-3p	15	0.81	9.47
8	**miR-6395**	**12**	**0.77**	**11.7**
9	miR-93-3p	14	0.73	8.29
9	miR-423-5p	20	0.73	6.05
11	miR-210-3p	12	0.69	10.8
12	miR-484	11	0.65	10.4
13	miR-328-5p	11	0.59	8.82
14	miR-505-5p	11	0.56	9.82

3.7.4. GO Terms Enriched by Hub miRNAs in the Blood

In blood samples from mice with different types of CR, we investigated which GO terms are enriched by the targets of the hubs of the co-expression network of miRNAs. Figure 3.13. shows the top ten enriched GO terms for hubs in co-expression networks in blood samples for each dietary group. We consider GO terms to be statistically significant when their adjusted p-value is under 0.01. To avoid redundant and uninformative results, we only consider terms involving at least eight genes.

There are 49 significantly enriched GO terms in the AL co-expression network, 40 in the CCR co-expression network, and 16 in the ICR co-expression network. Specifically, seven,

five and two terms are related to the immune system in AL, CCR, ICR groups respectively. For instance, “cytokine-mediated signaling pathway”, “leukocyte tethering or rolling” and “negative regulation of immune response” are GO terms related to the immune system and they are enriched in the three dietary groups (Figure 3.13.). In contrast, the GO term “Type I interferon signaling pathway”, also related to the immune system, is enriched only in the AL co-expression network. Moreover, seven, four and one term are related to apoptosis AL, CCR, ICR groups respectively.

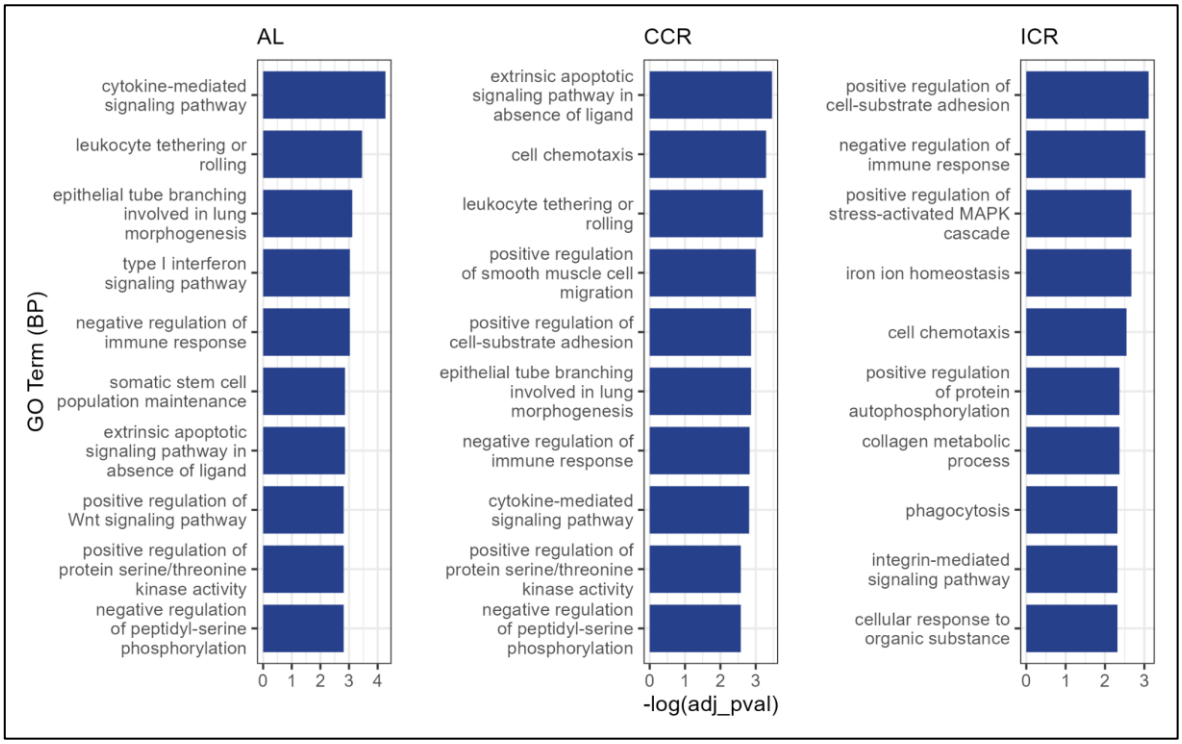

Figure 3.13. Top ten GO terms enriched by the target of hubs in blood samples for each dietary group. Top ten enriched terms are arranged by the log of the adjusted p-value

3.8. CHANGE OF MIRNA RANKING IN THE BLOOD

Different diets change the miRNA expression, resulting in different co-expression networks. The centrality of each miRNA can change when they take a more important role in a given diet. If a miRNA has a higher ranking in CCR than in AL network, then its relevance is higher in CCR than in AL. Here we evaluate the ranking using the eigenvector centrality index.

Minor changes of ranking are common, but major changes are unusual and also relevant. Here we focus on these ones. As a general criterion, we evaluate the mean and standard deviation of the change of rank, and we calculate a z-score. The underlying statistical distribution for the z-score is hard to calculate and it is beyond the scope of this thesis. For this work we use the operational definition of *significant change of ranking* when the z-score has an absolute value greater than or equal to one.

3.8.1. Comparison of miRNA Ranking Between CCR and AL in the Blood

Table 3.6. shows the miRNAs with major change in ranking (either positive or negative) between CCR and AL co-expression networks from blood samples. The largest increase of ranking (from AL to CCR) corresponds to miR-374c-3p, while the largest decrease of ranking corresponds to miR-144-3p (Table 3.6.).

Table 3.6. Top miRNAs that changed ranking between the CCR and the AL groups in blood samples. The table is sorted according to the change of ranking. A positive change of ranking means the importance of miRNA increases with CCR. A negative change of ranking means the importance of miRNA decreases with CCR

miRNA	**rank under AL**	**rank under CCR**	**change of ranking**	**z-score of rank**
miR-374c-3p	75	49	26	1.90
miR-181b-5p	47	22	25	1.82
miR-6414	71	53	18	1.29
miR-742-5p	57	40	17	1.22
miR-719	62	45	17	1.22
miR-324-3p	36	20	16	1.14
miR-7216-3p	64	48	16	1.14
miR-505-5p	21	6	15	1.06
miR-184-3p	40	25	15	1.06

miRNA	rank under AL	rank under CCR	change of ranking	z-score of rank
miR-1964-3p	49	34	15	1.06
miR-6928-3p	72	57	15	1.06
miR-6991-5p	2	19	-17	-1.36
miR-3104-5p	10	27	-17	-1.36
miR-23b-3p	15	32	-17	-1.36
miR-700-5p	34	51	-17	-1.36
miR-376c-3p	37	55	-18	-1.44
miR-6977-5p	17	38	-21	-1.67
miR-365-1-5p	16	59	-43	-3.34
miR-144-3p	14	58	-44	-3.42

3.8.2. Comparison of miRNA Ranking Between ICR and AL in the Blood

Table 3.7. shows the miRNAs with major change in ranking (positive or negative) between ICR and AL co-expression networks from blood samples. The largest increase of ranking (from AL to CCR) corresponds to miRNA miR-668-3p. The largest decrease of ranking corresponds to miR-365-1-5p and miR-6939-5p.

Table 3.7. Top miRNAs that changed ranking between the ICR and the AL groups in blood samples. The table is sorted according to the change of ranking. A positive change of ranking means the importance of miRNA increases with ICR. A negative change of ranking means the importance of miRNA decreases with ICR

miRNA	rank under AL	rank under ICR	change of ranking	z-score of rank
miR-668-3p	74	44	30	2.24
miR-181b-5p	47	22	25	1.84
miR-6395	32	8	24	1.75

miRNA	rank under AL	rank under ICR	change of ranking	z-score of rank
miR-1964-3p	49	26	23	1.67
miR-6956-3p	65	42	23	1.67
miR-8114	43	23	20	1.43
miR-719	62	45	17	1.18
miR-423-5p	26	10	16	1.10
miR-331-3p	46	30	16	1.10
miR-155-3p	56	40	16	1.10
miR-671-5p	22	32	-10	-1.01
miR-19a-3p	41	51	-10	-1.01
miR-384-5p	48	60	-12	-1.17
miR-344c-3p	44	57	-13	-1.25
miR-1981-5p	25	39	-14	-1.33
miR-3104-5p	10	25	-15	-1.41
miR-494-3p	1	20	-19	-1.74
miR-365-1-5p	16	41	-25	-2.23
miR-6939-5p	30	55	-25	-2.23

3.8.3. GO Terms Enriched by miRNAs with Major Change of Ranking Between Dietary groups in the Blood

The GO terms most enriched with targets of miRNAs that change their relevance between AL and CCR co-expression networks are “positive regulation of JUN kinase activity”, “negative regulation of intrinsic apoptotic signaling pathway”, and “protein kinase B signaling” (Figure 3.14.).

The GO terms most enriched with targets of miRNAs that change their relevance between AL and ICR are “positive regulation of protein-containing complex assembly” and “ubiquitin-dependent ERAD pathway”.

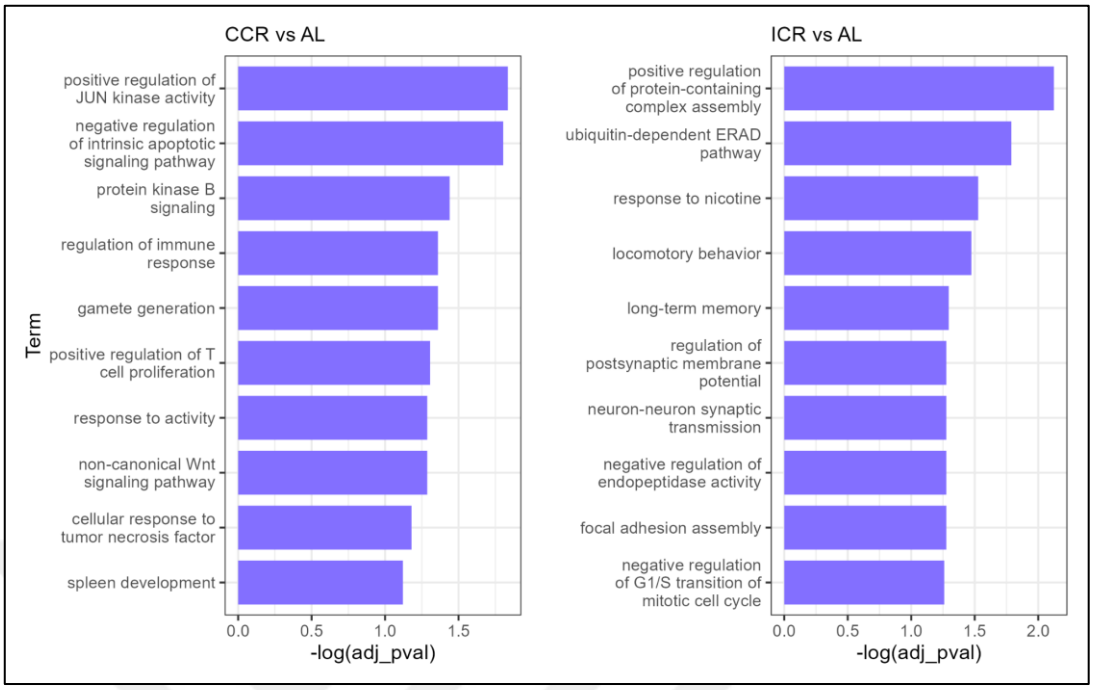

Figure 3.14. Top ten GO terms enriched by targets of miRNAs that changed ranking between dietary groups in blood samples. Enriched GO terms are arranged by adjusted p-value. The length of the bar represents the significance of the term

3.9. PATHWAY INFLUENCE OF CO-EXPRESSION NETWORKS

The enrichment analysis of each set of significantly expressed miRNAs, described in the methods section, did not find any significantly enriched pathway in the KEGG database. The full results are described in the Appendix.

If the target genes of a miRNA have a high topological relevance in a given pathway, then this miRNA has a high influence on the pathway. To evaluate the topological relevance of every target gene we need to consider the diet-dependent miRNA co-expression network.

To find the impact of the diet-specific co-expression network, we evaluated the sum of the eigenvector centrality of all the target genes in every pathway. The eigenvector centrality of the targets depends on the co-expression network (that is, on the diet) and on the metabolic pathway.

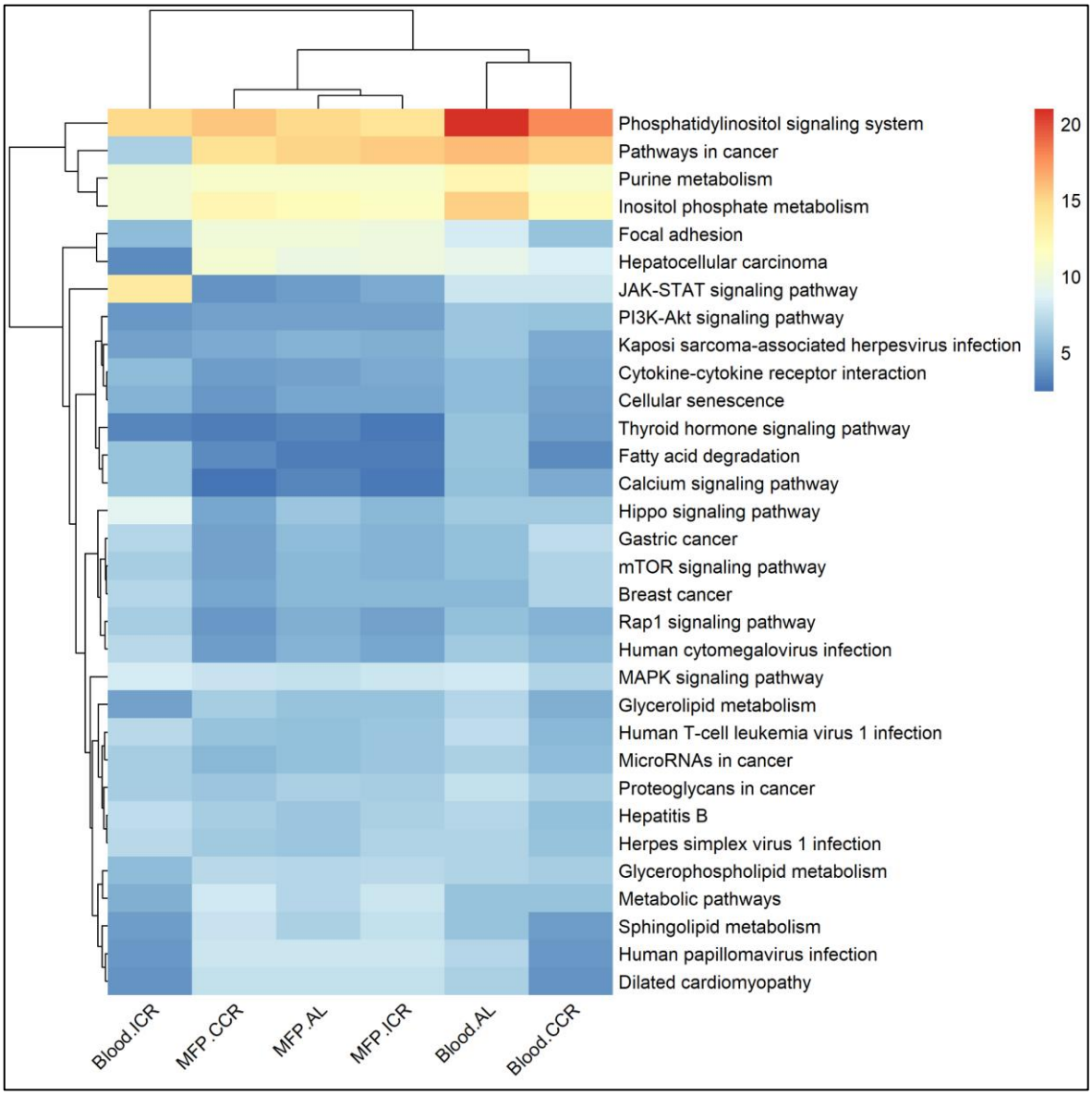

Figure 3.15. Heatmap of influence scores for KEGG pathways affected by miRNA interaction networks for each dietary restriction group

3.9.1. Conserved Pathways for Each Dietary Group

To see which pathways gained or lost importance under different dietary groups, we compared their ranks when sorting by their influence score. This analysis is similar to the previous one done with the ranking according to differential eigenvector centrality of miRNAs. We assume that some of the connections between miRNAs are rewired when diet changes. That is, some edges are different in the co-expression networks of different diets.

Despite the differences between diet-specific co-expression networks, there are pathways that are equally important in all diets (Figure 3.15.). The shared influenced pathways in both blood and MFP are

- "Pathways in cancer", with an average influence score of 11.71 in blood and 14.99 in MFP,
- "Phosphatidylinositol signaling system" with an influence score of 17.78 in blood and 14.97 in MFP,
- "Inositol phosphate metabolism" with an influence score of 12.51 in blood and 11.96 in MFP,
- "Purine metabolism" with an influence score of 11.33 in blood and 11.14 in MFP,
- "Focal adhesion" with an influence score of 6.50 in blood and 10.25 in MFP, and
- "MAPK signaling pathway" with an influence score of 7.33 in blood and 7.70 in MFP.

3.10. CHANGE OF PATHWAY INFLUENCE RANKING IN THE BLOOD

When diet changes, the miRNA network changes. Therefore, the influence of the miRNA network in every KEGG pathway changes. That changes the ranking of each KEGG pathway when the diet changes. Table 3.8. and Table 3.9. shows the KEGG pathways that have a different ranking under AL and CCR diets.

The pathway that most changed ranking between AL and CCR diet is "Fluid shear stress and atherosclerosis", followed by the "Glucagon signaling pathway". Several cancer-related pathways, such as "breast cancer" and "gastric cancer" are more influenced by the miRNA co-expression network in the CCR diet than in the AL diet.

The "One carbon pool by folate" pathway is the lowest differential ranked pathway with CCR with respect to AL followed by "Tyrosine metabolism". Several cancer-related pathways such as "Central carbon metabolism in cancer", "PD-1 checkpoint pathway in cancer", "Choline metabolism in cancer" and "Small cell lung cancer" are less influenced by the miRNA rewiring due to the CCR diet in mice blood.

Table 3.8. Top 20 pathways that increased ranking of influence between the CCR and the AL groups in blood samples. A positive z score means the importance of pathways increased with the CCR diet, with respect to the AL diet

KEGG pathway	**rank AL**	**rank CCR**	**z score**
Fluid shear stress and atherosclerosis	136	36	5.78
Glucagon signaling pathway	95	18	4.45
Alcoholism	142	75	3.87
Alanine. aspartate and glutamate metabolism	162	100	3.58
Pyruvate metabolism	200	138	3.58
Coronavirus disease - COVID-19	96	37	3.41
Pyrimidine metabolism	103	74	1.68
Leukocyte transendothelial migration	146	118	1.62
Ras signaling pathway	71	47	1.39
Breast cancer	32	10	1.27
mTOR signaling pathway	29	8	1.21
Neutrophil extracellular trap formation	198	177	1.21
Olfactory transduction	244	223	1.21
Galactose metabolism	284	263	1.21
Retinol metabolism	93	73	1.16
Pentose phosphate pathway	117	97	1.16
Huntington disease	144	124	1.16
Carbohydrate digestion and absorption	236	216	1.16
Gastric cancer	26	7	1.10

Table 3.9. Top 20 pathways that decreased ranking of influence between the CCR and the AL groups in blood samples. A negative z score means the importance of pathways decreased with the CCR diet. with respect to the AL diet

KEGG pathway	**rank AL**	**rank CCR**	**z score**
One carbon pool by folate	210	304	-5.43
Tyrosine metabolism	237	300	-3.64
Central carbon metabolism in cancer	64	116	-3.01
Mitophagy - animal	122	166	-2.54
Tight junction	139	180	-2.37
PPAR signaling pathway	169	209	-2.31
Glycine. serine and threonine metabolism	153	191	-2.20
PD-1 checkpoint pathway in cancer	40	77	-2.14
Choline metabolism in cancer	79	112	-1.91
Fatty acid degradation	23	55	-1.85
beta-Alanine metabolism	105	137	-1.85
Fatty acid metabolism	194	225	-1.79
Dilated cardiomyopathy	16	43	-1.56
Small cell lung cancer	54	80	-1.50
Renal cell carcinoma	67	92	-1.44
Human papillomavirus infection	11	35	-1.39
Notch signaling pathway	163	187	-1.39
Regulation of lipolysis in adipocytes	187	211	-1.39
Porphyrin and chlorophyll metabolism	264	287	-1.33

Table 3.10. and Table 3.11. shows the top regulated KEGG pathways by rewired miRNA-target gene connections with the ICR diet in blood. The “Propanoate, pyruvate metabolism” pathway is the highest differential ranked pathway with ICR with respect to AL followed by the “Olfactory transduction”. Other highly differential pathways are similar to metabolic processes such as “Tryptophan, Tyrosine, Butanoate, and Galactose metabolism”.

The “Ascorbate and aldarate metabolism” pathway is the lowest differential ranked pathway with ICR in respect to AL followed by “Pentose and glucuronate interconversions.” Several cancer-related pathways such as “Choline metabolism in cancer”, and “PD-1 checkpoint pathway in cancer” are less influenced by the miRNA rewiring due to the ICR diet in mice blood same as in CCR diet.

Table 3.10. Top 20 pathways that increased ranking of influence between the ICR and the AL groups in blood samples. A Positive z score means the importance of pathways increased with the ICR diet, with respect to the AL diet

KEGG pathway	**rank AL**	**rank ICR**	**z score**
Propanoate metabolism	213	85	4.28
Pyruvate metabolism	200	91	3.64
Olfactory transduction	244	137	3.57
Tryptophan metabolism	206	117	2.97
Tyrosine metabolism	237	149	2.94
Aldosterone synthesis and secretion	115	30	2.84
Butanoate metabolism	227	147	2.67
Galactose metabolism	284	214	2.34
Glucagon signaling pathway	95	41	1.80
Long-term depression	148	108	1.34
Morphine addiction	160	122	1.27
Amino sugar and nucleotide sugar metabolism	265	227	1.27
African trypanosomiasis	170	134	1.20
Serotonergic synapse	152	118	1.14
Platinum drug resistance	164	130	1.14
Pancreatic secretion	145	113	1.07
GnRH secretion	172	140	1.07
Circadian entrainment	107	76	1.04

Natural killer cell mediated cytotoxicity	112	81	1.04

Table 3.11. Top 20 pathways that decreased ranking of influence between the ICR and the AL groups in blood samples. A negative z score means the importance of pathways decreased with the ICR diet, with respect to the AL diet

KEGG pathway	**rank AL**	**rank ICR**	**z score**
Pentose and glucuronate interconversions	191	296	-3.51
Ascorbate and aldarate metabolism	192	297	-3.51
Central carbon metabolism in cancer	64	164	-3.34
beta-Alanine metabolism	105	202	-3.24
Mitophagy - animal	122	217	-3.17
One carbon pool by folate	210	304	-3.14
Choline metabolism in cancer	79	161	-2.74
Steroid hormone biosynthesis	168	250	-2.74
PD-1 checkpoint pathway in cancer	40	112	-2.40
Salmonella infection	55	126	-2.37
Hepatocellular carcinoma	5	70	-2.17
Nicotinate and nicotinamide metabolism	51	116	-2.17
Renal cell carcinoma	67	129	-2.07
Ether lipid metabolism	84	143	-1.97
Pentose phosphate pathway	117	174	-1.90
Alzheimer disease	135	192	-1.90
Thyroid hormone signaling pathway	24	80	-1.87
HIF-1 signaling pathway	37	92	-1.84
Autophagy - animal	33	87	-1.80

3.11. MICRORNA EXPRESSION IN THE MFP

In the previous section we examined the expression levels of miRNAs in blood. In this section we present the results of miRNA expression in breast tissue. The mouse model used in this study has a predisposition to develop breast cancer. The analysis shown here was performed using only samples from mice that did not develop breast cancer.

Figure 3.16. shows the number of significantly expressed miRNAs under every separate diet and age, as well as in their combinations. There are 35 significantly expressed miRNAs, 20 of them upregulated, and 15 miRNAs downregulated. The most significantly upregulated and downregulated miRNAs were miR-133b-3p and miR-127-3p, respectively. Two miRNAs miR-409-3p and miR-540-3p are downregulated in all age and diet.

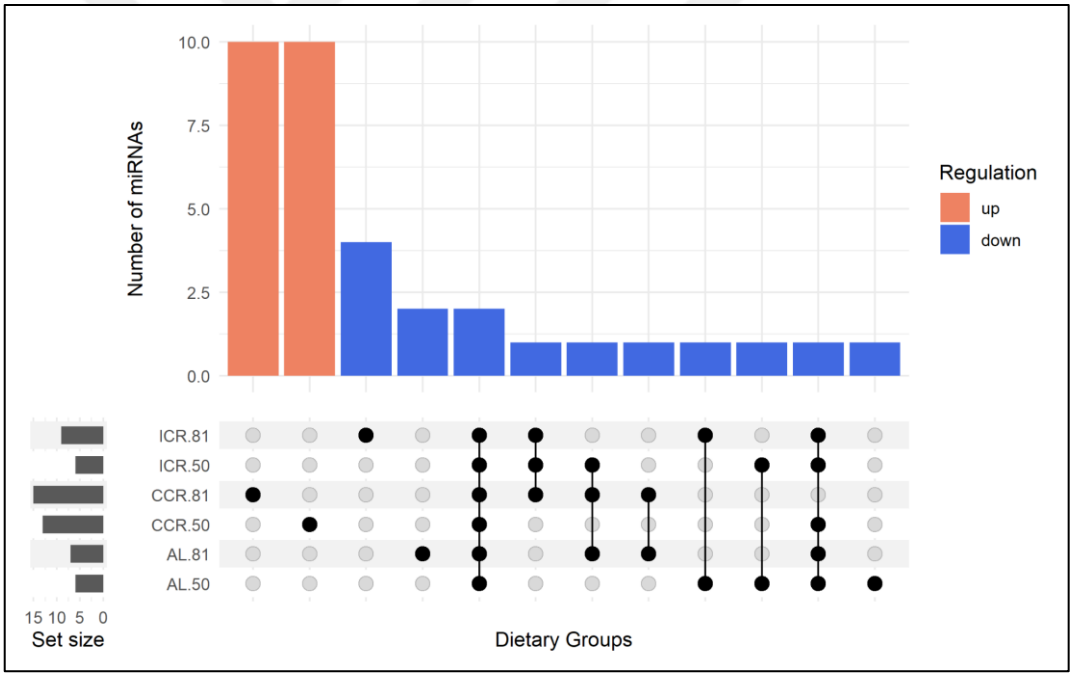

Figure 3.16. Upset plot of miRNAs significantly expressed in MFP samples for each dietary group. Horizontal bars show the number of miRNAs for each condition. Vertical bars show the number of miRNAs of each intersection as described by the bullet points in the lower part

Table 3.12. lists the number of miRNAs that were upregulated and downregulated in each comparison. In middle-aged MFP tissue, six miRNAs are significantly expressed in the AL diet, 13 miRNAs are significantly expressed in CCR and six miRNAs are significantly

expressed in the ICR diet. While one miRNA (miR-337-5p) is expressed in both AL and ICR diets at the same time, three miRNAs are expressed in all diets. In the old-aged MFP tissue, seven miRNAs are significantly expressed with the AL diet, 15 miRNAs are differentially expressed in the CCR diet, and nine miRNAs are significantly expressed in the ICR diet.

Table 3.12. Numbers of miRNAs significantly up- and down-regulated in MFP samples for each dietary group

Age	**Diet**	**Downregulated**	**Upregulated**	**Downregulated with logFC < -1**	**Upregulated with logFC > 1**
50	AL	6	0	6	0
50	CCR	3	10	3	7
50	ICR	6	0	5	0
81	AL	7	0	7	0
81	CCR	5	10	4	8
81	ICR	9	0	8	0

3.12. TARGETS OF SIGNIFICANTLY EXPRESSED MICRORNAS IN THE MFP

Each miRNA can target several genes due to their ubiquitous nature. Moreover, target prediction algorithms can produce many false positives. To control the number of false positives, we used the permutation test described in method section.

There are 1393 genes predicted as targets of at least one significantly expressed miRNA. The gene targeted by the largest number of miRNAs is Cadm2, as seen in Figure 3.17. This gene is targeted by six miRNAs. Two of these interactions are experimentally validated and the remainder interactions are predicted. The genes Dnmt3a and Tnrc6b are targeted by five miRNAs, thus they both are targeted by the second largest number of miRNAs.

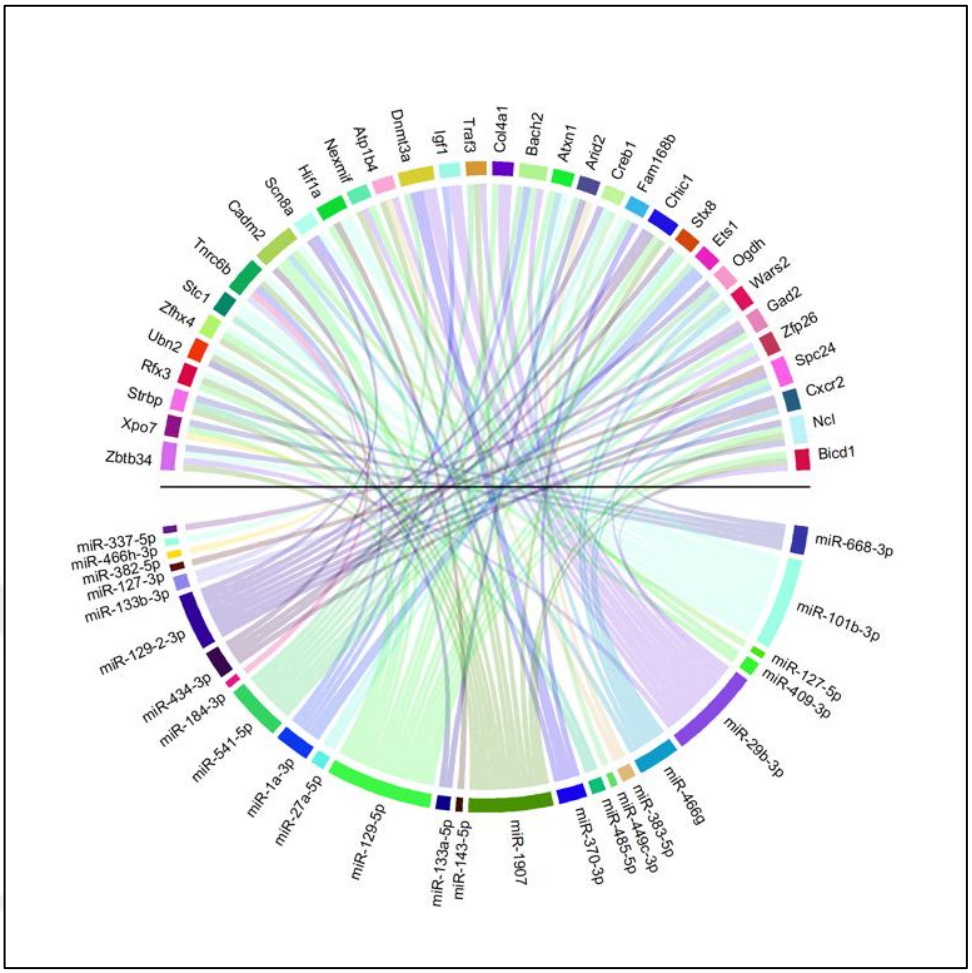

Figure 3.17. Chord diagram of frequently targeted genes of miRNAs significantly expressed in MFP samples

3.13. TOPOLOGICAL PROPERTIES OF CO-EXPRESSION NETWORKS IN THE MFP

Table 3.13. shows the global network characteristics, such as the number of nodes, number of edges, density (ratio of existing versus possible edges), and average clustering coefficient. The density of the co-expression networks of AL and ICR is about 11%, and the density of the co-expression network of CCR is about 9%, meaning that only a small proportion of all node pairs are connected in each inferred network.

Table 3.13. Global network properties of co-expression networks of miRNAs in MFP samples for each dietary group. Columns nodes and edges show the number of nodes and edges in each network

Tissue	**Diet**	**Edges**	**Nodes**	**Clustering**	**Density**
MFP	AL	270	69	0.27	0.11
MFP	CCR	268	74	0.29	0.09
MFP	ICR	268	68	0.28	0.11

The relevant topological properties of each node are its degree, the average degree of its neighbors, and its eigenvector centrality. To illustrate this, Figure 3.18. depicts the distributions of all centrality measures in the networks based on MFP data. The degree distributions of all networks follow a power law, indicating that these networks are indeed scale-free, as expected in biological networks.

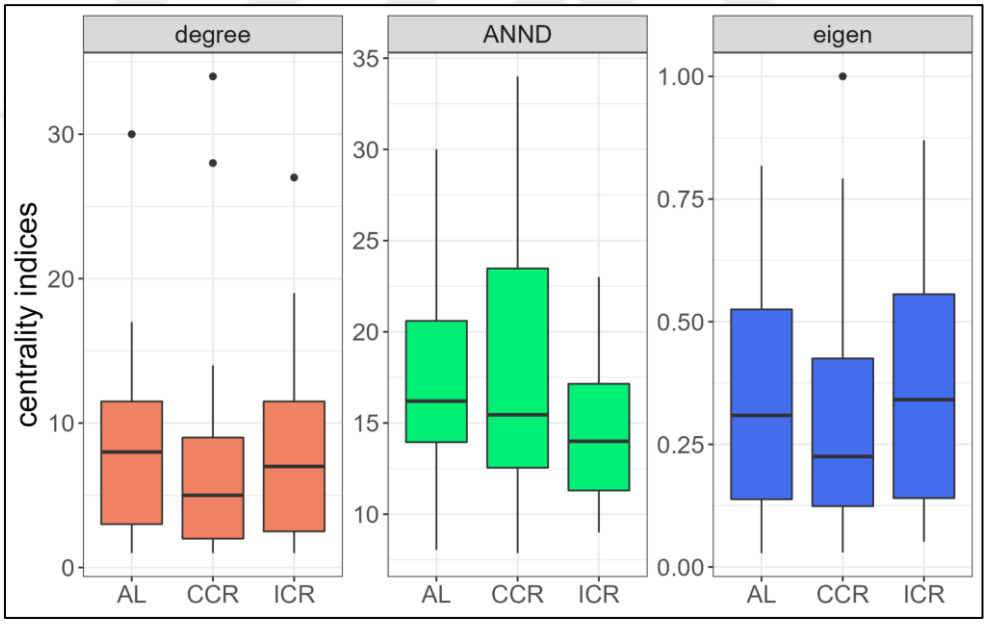

Figure 3.18. Boxplot of centrality indices of co-expression networks of miRNAs in MFP samples for each dietary group. Degree, average nearest neighbor degree (ANND), and eigenvector centrality were measured and visualized as a boxplot. There is no significant change across diets

For MFP, the co-expression network for AL has 69 nodes and 270 edges, for CCR has 74 nodes and 268 edges, and for ICR has 68 nodes and 268 edges. These numbers are similar to the ones found in networks built with data from blood tissue.

3.13.1. Hub miRNAs in the MFP for the AL Group

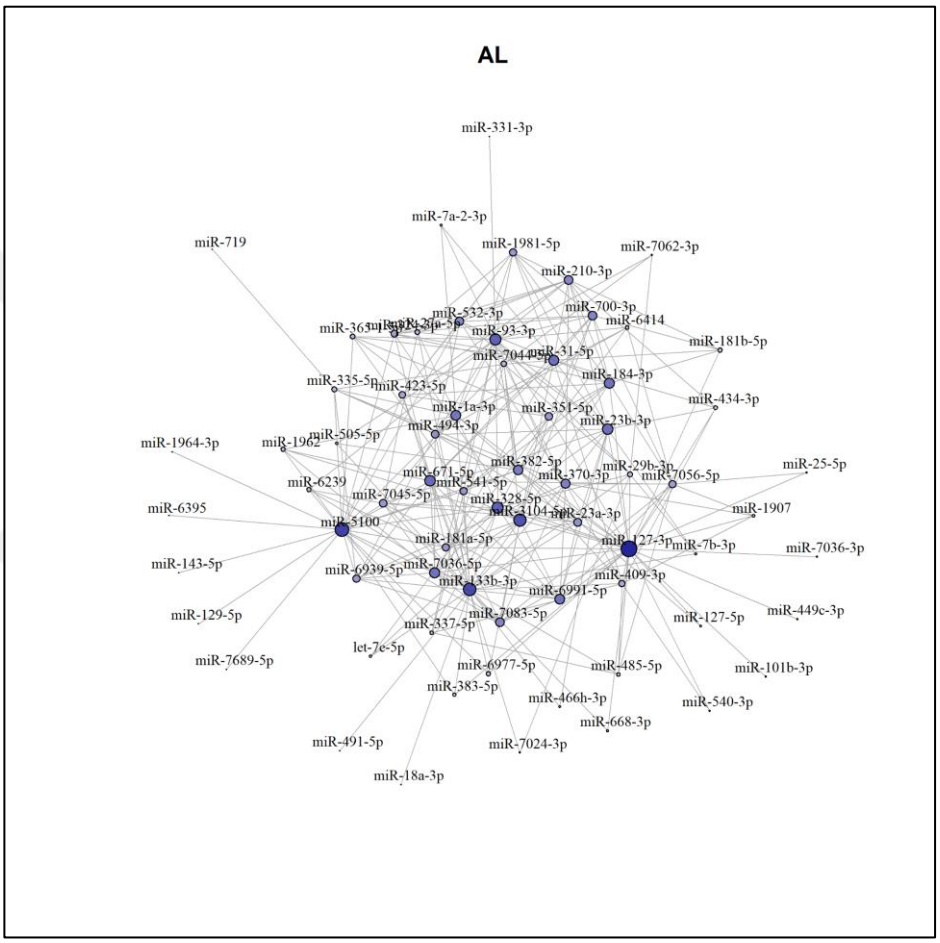

Figure 3.19. Co-expression network of miRNAs in MFP samples for the AL group. The node size is proportional to its eigenvector centrality. Darker nodes have higher eigenvector centrality

The co-expression network in miRNA from MFP tissue under AL diet is shown in Figure 3.19. The centrality indices of each node can be seen in Table 3.14. There are 13 miRNAs identified as hubs. The node with the highest degree and eigenvector centrality corresponds to miR-127-3p. The nodes representing miR-671-5p, miR-382-5p, and miR-210-3p are hubs specific to the co-expression of AL diet in MFP.

Table 3.14. Centrality indices of hubs of co-expression network of miRNAs in MFP samples for the AL group. miRNAs highlighted with bold represent a hub only in the AL group

ranking	**miRNA**	**degree**	**eigenvector centrality**	**ANND**
1	miR-127-3p	30	1.00	7.90
2	miR-5100	26	0.86	8.04
3	miR-133b-3p	26	0.81	7.69
4	miR-3104-5p	17	0.79	12.2
5	miR-93-3p	21	0.72	8.52
6	**miR-671-5p**	**14**	**0.68**	**12.9**
7	miR-23b-3p	15	0.66	11.9
8	miR-31-5p	16	0.65	10.2
9	miR-184-3p	14	0.65	12.5
9	miR-1a-3p	14	0.62	13.1
11	**miR-382-5p**	**15**	**0.60**	**11.9**
12	miR-370-3p	13	0.58	12.9
13	**miR-210-3p**	**13**	**0.55**	**11.1**

3.13.2. Hub miRNAs in the MFP for the CCR Group

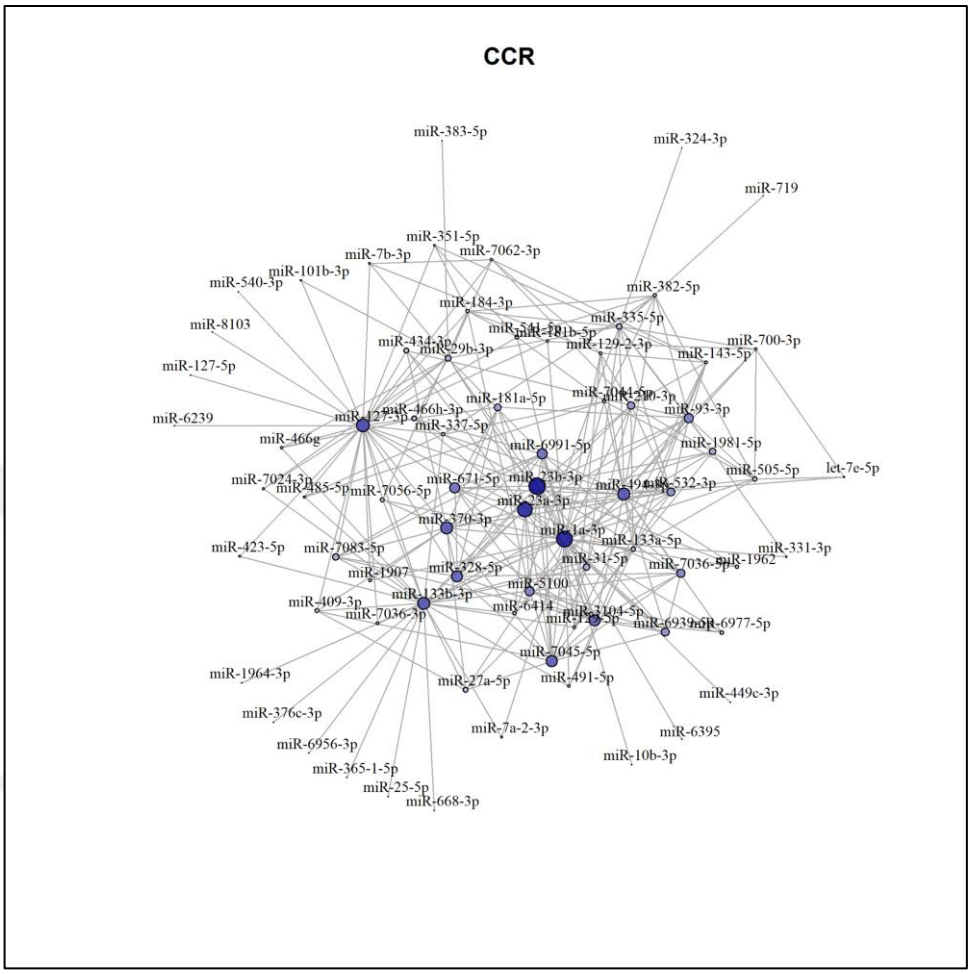

Figure 3.20. Co-expression network of miRNAs in MFP samples for the CCR group. The node size is proportional to its eigenvector centrality. Darker nodes have higher eigenvector centrality

The co-expression network under CCR diet in MFP tissue is shown in Figure 3.20., and the centrality measurements of each node can be seen in Table 3.15. There are 12 miRNAs identified as hubs in CCR co-expression in MFP. The node with highest degree and eigenvector centrality corresponds to miR-23b-3p. The nodes representing miR-7045-5p, miR-29b-3p and miR-miR-335-5p are hubs specific to the CCR co-expression in MFP.

Table 3.15. Centrality indices of hubs of co-expression network of miRNAs in MFP samples for the CCR group. miRNAs highlighted with bold represent a hub only in the CCR group

ranking	**miRNA**	**degree**	**eigenvector centrality**	**ANND**
1	miR-23b-3p	22	1.00	12.8
2	miR-1a-3p	34	0.95	7.65
3	miR-23a-3p	19	0.90	13.4
4	miR-127-3p	31	0.79	7.06
5	miR-133b-3p	28	0.73	7.86
5	miR-370-3p	16	0.73	12.8
7	miR-494-3p	20	0.72	10.6
8	**miR-7045-5p**	**14**	**0.69**	**13.1**
9	miR-3104-5p	13	0.66	12.7
10	miR-93-3p	14	0.55	12.8
11	**miR-29b-3p**	**12**	**0.39**	**11.7**
12	**miR-335-5p**	**15**	**0.36**	**7.87**

3.13.3. Hub miRNAs in the Blood for the ICR Group

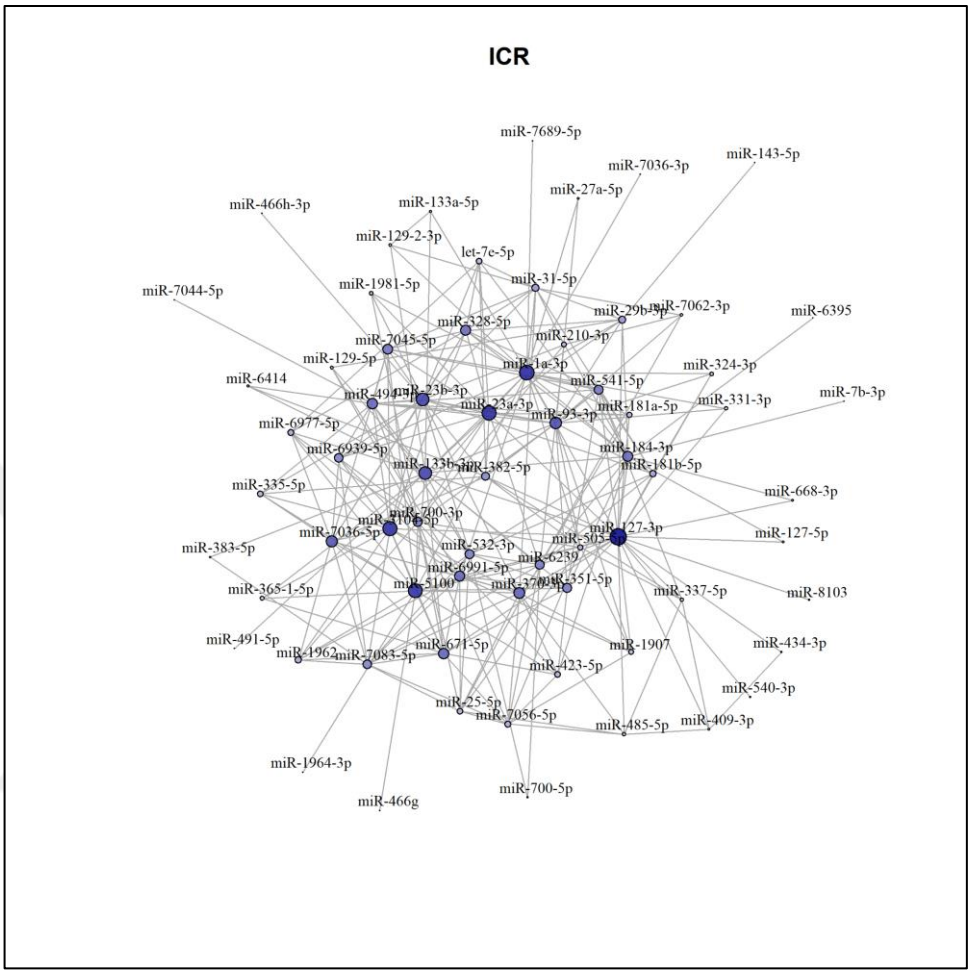

Figure 3.21. Co-expression network of miRNAs in MFP samples for the ICR group. The node size is proportional to its eigenvector centrality. Darker nodes have higher eigenvector centrality

The co-expression network of miRNA from MFP tissue under ICR diet is shown in Figure 3.21., and the centrality measurements of each node can be seen in Table 3.16. There are 17 miRNAs identified as hubs in this network. The node representing miR-127-3p has the highest degree and eigenvector centrality. The nodes representing miR-7036-5p, miR-700-3p, miR-6239 and miR-7083-5p are other hub miRNAs specific to ICR co-expression in MFP.

Table 3.16. Centrality indices of hubs of co-expression network of miRNAs in MFP samples for the ICR group. miRNAs highlighted with bold represent a hub only in the ICR group

ranking	**miRNA**	**degree**	**eigenvector centrality**	**ANND**
1	miR-127-3p	27	1.00	9.44
2	miR-1a-3p	23	0.88	9.83
3	miR-3104-5p	17	0.87	12.7
4	miR-23a-3p	17	0.86	13.5
5	miR-5100	19	0.85	11.5
6	miR-23b-3p	18	0.78	10.7
6	miR-133b-3p	19	0.78	11.1
8	miR-93-3p	18	0.72	10.4
9	**miR-7036-5p**	**14**	**0.69**	**12.0**
10	miR-370-3p	14	0.67	13.2
11	miR-494-3p	14	0.64	11.4
12	miR-6991-5p	13	0.63	12.7
12	miR-184-3p	16	0.62	10.2
14	**miR-700-3p**	**14**	**0.55**	**10.3**
14	**miR-6239**	**13**	**0.55**	**11.6**
16	**miR-7083-5p**	**12**	**0.53**	**11.1**
17	miR-31-5p	11	0.45	10.5

3.13.4. GO Terms Enriched by Hub miRNAs in the MFP

In MFP samples from mice with different types of CR, we investigated which GO terms are enriched by the targets of the hubs of the co-expression network of miRNAs. Figure 3.22. shows the top ten enriched GO terms for hubs in co-expression networks in MFP samples for each dietary group.

The top enriched GO terms in the AL co-expression network are “cardiac muscle contraction”, “in utero embryonic development”, “canonical Wnt signaling pathway”, and “BMP signaling pathway”. The top enriched GO terms in the CCR co-expression network are “negative regulation of glycolytic process”, “response to heat”, “cell population proliferation”, and “negative regulation of protein phosphorylation”. The top enriched GO terms for the ICR are “somatic stem cell division”, “outflow tract septum morphogenesis”, “pharyngeal arch artery morphogenesis”.

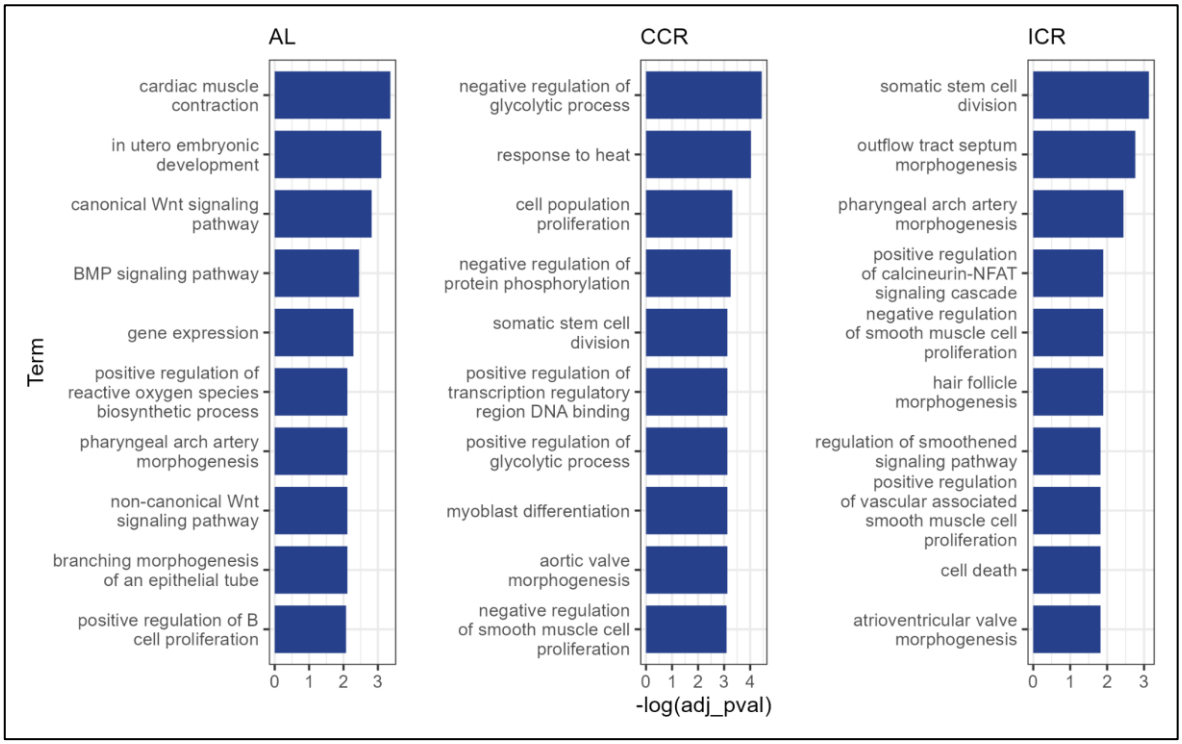

Figure 3.22. Top ten GO terms enriched by the target of hubs in MFP samples for each dietary group. Top ten enriched terms are arranged by the log of the adjusted p-value

3.14. CHANGE OF MIRNA RANKING IN THE MFP

3.14.1. Comparison of miRNA Ranking Between CCR and AL in the MFP

Table 3.17. shows the miRNAs with major change in ranking (either positive or negative) between CCR and AL co-expression networks from MFP samples. The largest increase of ranking (from AL to CCR) corresponds to miR-466h-3p, while the largest decrease of ranking corresponds to miR-324-3p (Table 3.17.).

Table 3.17. Top miRNAs that changed ranking between the CCR and the AL groups in MFP samples. The table is sorted according to change of ranking. A positive change of ranking means the importance of miRNA increases with CCR. A negative change of ranking means the importance of miRNA decreases with CCR

miRNA	**rank under AL**	**rank under CCR**	**change of rank**	**z-score of rank**
miR-466h-3p	53	25	28	2.05
miR-143-5p	62	42	20	1.50
miR-491-5p	67	47	20	1.50
miR-505-5p	47	28	19	1.43
miR-7036-3p	60	41	19	1.43
miR-23a-3p	20	3	17	1.29
miR-129-5p	61	44	17	1.29
miR-434-3p	41	26	15	1.15
miR-494-3p	21	7	14	1.08
miR-7045-5p	22	8	14	1.08
miR-668-3p	51	69	-18	-1.13
miR-382-5p	14	35	-21	-1.34
miR-6239	40	64	-24	-1.54
miR-423-5p	30	55	-25	-1.61
miR-184-3p	10	37	-27	-1.75
miR-383-5p	45	72	-27	-1.75
miR-700-3p	16	46	-30	-1.96
miR-351-5p	23	53	-30	-1.96
miR-365-1-5p	35	67	-32	-2.10
miR-324-3p	29	73	-44	-2.93

3.14.2. Comparison of miRNA Ranking Between ICR and AL in the MFP

Table 3.18. shows the miRNAs with highest change in ranking (positive or negative) between ICR and AL co-expression networks from MFP samples. The biggest increase of ranking (from AL to CCR) corresponds to miR-331-3p. The largest decrease of ranking corresponds to miR-7044-5p.

Table 3.18. Top miRNAs that changed ranking between the ICR and the AL groups in MFP samples. The table is sorted according to the change of ranking. A positive change of ranking means the importance of miRNA increases with ICR. A negative change of ranking means the importance of miRNA decreases with ICR

miRNA	**rank under AL**	**rank under ICR**	**change of rank**	**z-score of rank**
miR-331-3p	68	44	24	2.26
miR-25-5p	54	31	23	2.17
miR-6239	40	21	19	1.80
miR-23a-3p	20	4	16	1.52
miR-129-5p	61	45	16	1.52
let-7e-5p	48	34	14	1.33
miR-181b-5p	39	27	12	1.14
miR-1a-3p	13	2	11	1.05
miR-505-5p	47	36	11	1.05
miR-324-3p	29	41	-12	-1.09
miR-434-3p	41	55	-14	-1.27
miR-1981-5p	25	40	-15	-1.37
miR-31-5p	9	25	-16	-1.46
miR-27a-5p	36	52	-16	-1.46
miR-7b-3p	50	66	-16	-1.46
miR-210-3p	18	37	-19	-1.74

miRNA	rank under AL	rank under ICR	change of rank	z-score of rank
miR-409-3p	31	53	-22	-2.02
miR-7044-5p	32	65	-33	-3.05

3.14.3. GO Terms Enriched by miRNAs with Major Change of Ranking Between Dietary Groups in the MFP

In MFP tissue, the GO terms most enriched by targets of miRNAs changing ranking between CCR with respect to AL are “positive regulation of cytoplasmic translation” and “negative regulation of translation”. The GO terms most enriched with targets of miRNAs that change their relevance between AL and ICR are “photoreceptor cell maintenance” and “positive regulation of chemotaxis” (Figure 3.23.).

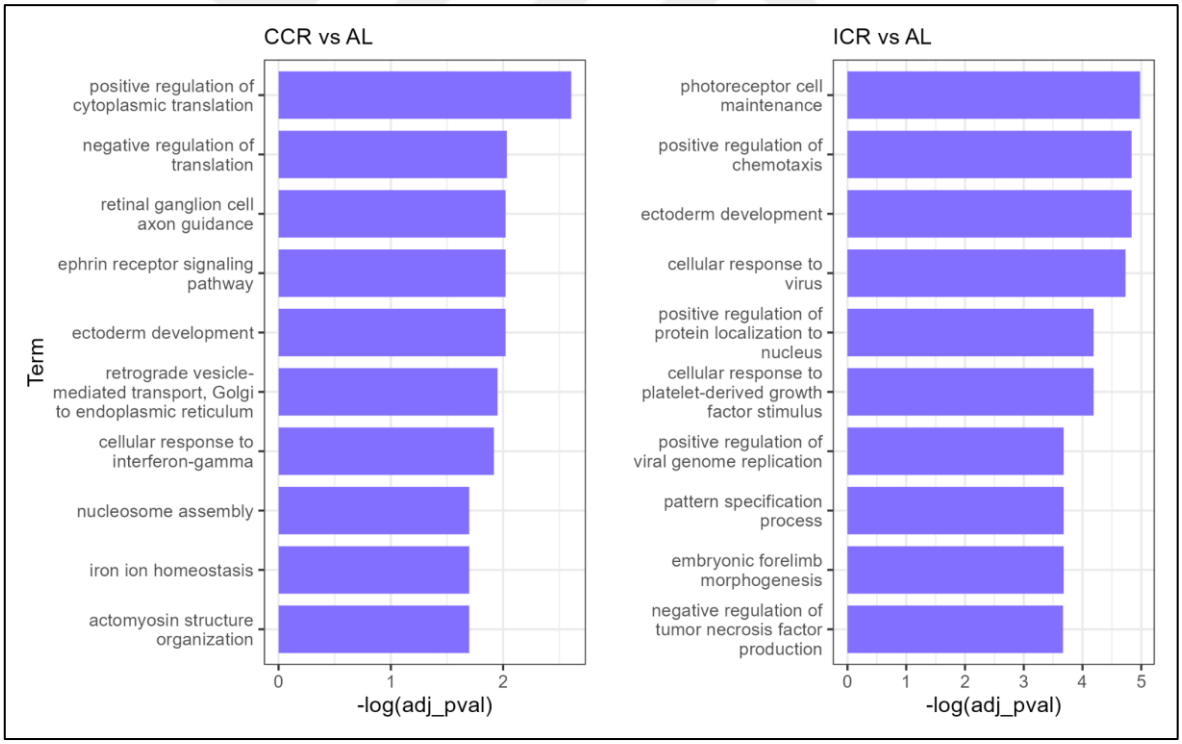

Figure 3.23. Top ten GO terms enriched by targets of miRNAs that changed ranking between dietary groups in blood samples. Enriched GO terms are arranged by adjusted p-value. The length of the bar represents the significance of the term

3.15. CHANGE OF PATHWAY INFLUENCE RANKING IN THE MFP

Table 3.19. and Table 3.20. show the top regulated KEGG pathways by rewired miRNA-target gene connections with the CCR diet in MFP. The “Oocyte meiosis” pathway is the highest differential ranked pathway with CCR in respect to AL followed by the “Pathways of neurodegeneration - multiple diseases”. Other pathways with high differential ranks are similar to neurologic pathways such as “Alzheimer disease”, ”Huntington disease”, and ”Amyotrophic lateral sclerosis.” The “Serotonergic synapse” pathway is the lowest differential ranked pathway with CCR in respect to AL followed by “Cholinergic synapse.”

Table 3.19. Top 20 pathways that increased ranking of influence between the CCR and the AL groups in MFP samples. A positive z score means the importance of pathways increased with the CCR diet, with respect to the AL diet

KEGG pathway	**rank AL**	**rank CCR**	**z score**
Oocyte meiosis	142	55	4.81
Pathways of neurodegeneration - multiple diseases	186	108	4.31
Alzheimer disease	179	109	3.87
Huntington disease	180	110	3.87
Amyotrophic lateral sclerosis	181	111	3.87
Spinocerebellar ataxia	183	114	3.81
Parkinson disease	184	115	3.81
Prion disease	185	116	3.81
Pentose phosphate pathway	131	64	3.70
beta-Alanine metabolism	79	32	2.60
Valine. leucine and isoleucine degradation	97	54	2.38
p53 signaling pathway	117	87	1.66
Fatty acid degradation	72	46	1.44
Citrate cycle (TCA cycle)	256	233	1.27

KEGG pathway	rank AL	rank CCR	z score
Glycosphingolipid biosynthesis - globo and isoglobo series	286	263	1.27
RIG-I-like receptor signaling pathway	99	77	1.22
Platinum drug resistance	141	119	1.22
Viral protein interaction with cytokine and cytokine receptor	231	209	1.22
Taurine and hypotaurine metabolism	233	212	1.16

Table 3.20. Top 20 pathways that decreased ranking of influence between the CCR and the AL groups in MFP samples. A negative z score means the importance of pathways decreased with the CCR diet. with respect to the AL diet

KEGG pathway	rank AL	rank CCR	z score
Cholinergic synapse	88	125	-2.05
Serotonergic synapse	156	193	-2.05
Morphine addiction	152	186	-1.88
Calcium signaling pathway	57	90	-1.82
Cushing syndrome	50	82	-1.77
Neutrophil extracellular trap formation	170	202	-1.77
Melanogenesis	60	91	-1.71
Yersinia infection	91	122	-1.71
B cell receptor signaling pathway	161	192	-1.71
Retrograde endocannabinoid signaling	134	164	-1.66
Wnt signaling pathway	46	75	-1.60
Circadian entrainment	111	140	-1.60
Fc gamma R-mediated phagocytosis	126	155	-1.60
Lysine degradation	137	166	-1.60

KEGG pathway	rank AL	rank CCR	z score
Chronic myeloid leukemia	93	120	-1.49
T cell receptor signaling pathway	149	175	-1.44
Natural killer cell mediated cytotoxicity	122	147	-1.38
Glutamatergic synapse	127	152	-1.38
Neuroactive ligand-receptor interaction	215	240	-1.38

Table 3.21. and Table 3.22. show the top regulated KEGG pathways by rewired miRNA-target gene connections with the ICR diet in MFP. The “Pathways of neurodegeneration - multiple diseases” pathway is the highest differential ranked pathway with CCR in respect to AL followed by the “Huntington disease”. Other high differential ranked pathways are similar to neurologic pathways such as “Spinocerebellar ataxia”, ”Spinocerebellar ataxia”, and ”Amyotrophic lateral sclerosis.” The “Cholinergic synapse” pathway is the lowest differential ranked pathway with ICR in respect to AL followed by “Mitophagy - Animal.”

Table 3.21. Top 20 pathways that increased ranking of influence between the ICR and the AL groups in MFP samples. A positive z score means the importance of pathways increased with the ICR diet, with respect to the AL diet

KEGG pathway	rank AL	rank ICR	z score
Pathways of neurodegeneration - multiple diseases	186	114	4.63
Huntington disease	180	115	4.18
Amyotrophic lateral sclerosis	181	116	4.18
Spinocerebellar ataxia	183	118	4.18
Prion disease	185	120	4.18
Pentose phosphate pathway	131	67	4.12
Alzheimer disease	179	117	3.99
Parkinson disease	184	122	3.99
Oocyte meiosis	142	90	3.35
beta-Alanine metabolism	79	39	2.57

KEGG pathway	rank AL	rank ICR	z score
ECM-receptor interaction	92	66	1.67
Carbon metabolism	203	177	1.67
p53 signaling pathway	117	93	1.54
Citrate cycle (TCA cycle)	256	232	1.54
Necroptosis	98	75	1.48
Tyrosine metabolism	246	223	1.48
Starch and sucrose metabolism	222	201	1.35
Porphyrin and chlorophyll metabolism	271	252	1.22
Toxoplasmosis	129	111	1.16

Table 3.22. Top 20 pathways that decreased ranking of influence between the ICR and the AL groups in MFP samples. A negative z score means the importance of pathways decreased with the ICR diet, with respect to the AL diet

KEGG pathway	rank AL	rank ICR	z score
Cholinergic synapse	88	127	-2.51
Mitophagy - animal	175	207	-2.06
Circadian entrainment	111	142	-2.00
Glycosphingolipid biosynthesis - lacto and neolacto series	55	84	-1.87
Parathyroid hormone synthesis, secretion and action	105	134	-1.87
Autophagy - animal	73	101	-1.80
Serotonergic synapse	156	184	-1.80
Carbohydrate digestion and absorption	216	243	-1.74
Melanogenesis	60	86	-1.67
Morphine addiction	152	178	-1.67
Calcium signaling pathway	57	82	-1.61

KEGG pathway	rank AL	rank ICR	z score
Choline metabolism in cancer	128	153	-1.61
Estrogen signaling pathway	104	128	-1.54
Glutamatergic synapse	127	151	-1.54
Central carbon metabolism in cancer	139	163	-1.54
Th17 cell differentiation	84	107	-1.48
Gap junction	87	110	-1.48
PD-1 checkpoint pathway in cancer	101	124	-1.48
Vascular smooth muscle contraction	107	130	-1.48

4. DISCUSSION

4.1. BRIEF SUMMARY OF INTRODUCTION AND METHOD

To better understand the changes in the miRNA expression profile in blood and MFP tissues, as well as the interaction network between these two tissues in mice fed with different types of CR, a system-level approach was developed in this study. We reconstructed diet-specific co-expression networks for each tissue, and we identified the most relevant miRNAs, GO terms, and KEGG pathways in the context of these networks. Moreover, the relevance of these terms was compared depending on the diet in Section 4.

Differential expression methods have been used to study changes in the quantity of RNAs. However, in the classic differential expression analysis, each miRNA is treated independently, with no consideration given to its interactions with other miRNAs [101]. It is difficult to tell whether the changes are independent or coordinated when two miRNAs are up- or down-regulated at the same time. Moreover, miRNAs may not conduct their functions independently, but the collaboration of distinct miRNAs may be necessary for the effective regulation of gene expression. Therefore, slight modifications in the abundance of miRNAs might result in a notable difference in the physiological condition of cells.

Networks were used to represent interactions between genes or miRNAs of interest [102]. These interactions were used to understand the underlying mechanisms of complicated biological events. Co-expression network analysis, which creates networks of transcripts that tend to activate together across a group of samples, and then investigates and analyzes this network, is a method to extract the role of a gene from gene expression [103]. One way to build a co-expression network directly from gene expression data was to calculate partial correlations between genes, showing genes as nodes and strong correlations as edges. Correlations between miRNA expression levels are caused by regulatory interactions, and knowing which of these correlations are altered in diet-applied tissue versus normal tissue was the first step in identifying the regulatory systems in our work.

The hypothesis that circulating miRNAs might be involved in cell communication was proposed to explain the stable presence of miRNAs in blood [104]. This idea argues that miRNAs are selectively secreted by a cell and influence distant target cells. It is very

important to find biomarkers for better diagnosis of diseases at an early stage. Therefore, miRNAs in the blood are promising for the diagnosis and prognosis of many diseases such as cancer. [105,106].

4.1.1. The Novelty of the Network Analysis

Following the ideas that circulating miRNAs could be used as markers for some diseases, and that the miRNA co-expression network could reveal dietary differences in blood and MFP, we analyzed the miRNA expression and co-expression of both blood and MFP tissue of mice prone to develop breast cancer, revealing shared and specific features. In doing so, we benefited from the robust nature of co-expression networks. In particular, co-expression networks are more resistant to measurement noise than each individual relation, making them more reliable [102]. Several studies have used miRNA co-expression analysis to find important miRNAs in a variety of diseases [107,108]. For example, Chen *et al.* [107] compared healthy aorta samples with samples from thoracic aortic aneurysm patients using co-expression of differentially expressed miRNAs and found that the pathways involved in apoptosis are enriched. They concluded that apoptosis-related miRNAs might be important for the prognosis of thoracic aortic aneurysms. In another study, He *et al.* [108] constructed miRNA co-expression networks to compare specific signatures for each stage of Parkinson's disease. They found that several serum extracellular vesicle-derived miRNAs could be used as biomarkers for Parkinson's disease progression and early detection. However, we are not aware of any study showing how miRNA co-expression varies by CR. To the best of our knowledge, there is no study on the effects of different types of CR on miRNA co-expression in breast cancer model mice.

4.2. INTERPRETATION OF RESULTS

4.2.1. miRNA Expression is Tissue-specific

In the present thesis, to study the effects of different types of CR and/or aging on miRNA profile in MFP and blood samples, mice were applied to different types of CR from week 10 (baseline) up to week 81. We analyzed the expression of miRNA in MFP and blood samples

taken from mice subject to different types of CR from week 10 (baseline) up to week 81 using Affymetrix miRNA 4.1 Array Strip microarrays. The main source of variation of miRNA expression is the tissue type. For a given tissue (either blood or MFP), miRNA expression was highly correlated (r = 0.96) in the same tissue of animals regardless of their dietary group (Figure 3.5.). On the other hand, the correlation coefficients between different tissues in the same animal were always under 62%. This reveals that miRNA expression is more modulated by the type of tissue than the type of diet. In a similar study, Ferreira *et al.* [109] have also reported that gene expression profiles of mice throughout aging appear to be clustered by tissue (brain, heart, liver, muscle, and pancreas samples) in their principal component analysis. They also reported that the highest variation was in different tissue types when effects of tissue, age, and sex were considered.

In the current study, miRNA expression levels with respect to their tissue-specific baselines were analyzed considering that it is more affected by tissue type than diet. The expression of each miRNA was modeled by a linear model with three independent variables: age, diet, and tissue. The coefficients of the fitted model correspond to the contribution of each condition to the miRNA expression, using the tissue-specific baseline as a reference. A significantly expressed miRNA is one where its expression in a given condition is significantly different from the corresponding tissue-specific baseline. Surprisingly, we did not find any miRNA that was significantly expressed in both blood and MFP. As a result of this analysis, we showed that each dietary condition has a specific set of significantly expressed miRNAs for each tissue (Figure 3.6.). The largest number of significantly expressed miRNAs was seen in old-aged mice compared to the other groups. Figure 4.1. shows that 72% of significantly expressed miRNAs are expressed in the old-aged AL and CCR group of mice. These results indicate that aging has more effect than diet on the number of significantly expressed miRNAs (Figure 4.1.). Also, most miRNAs significantly expressed were unique to one group (for example CCR.81), while the rest were significantly expressed in more than one group (Figure 4.1.).

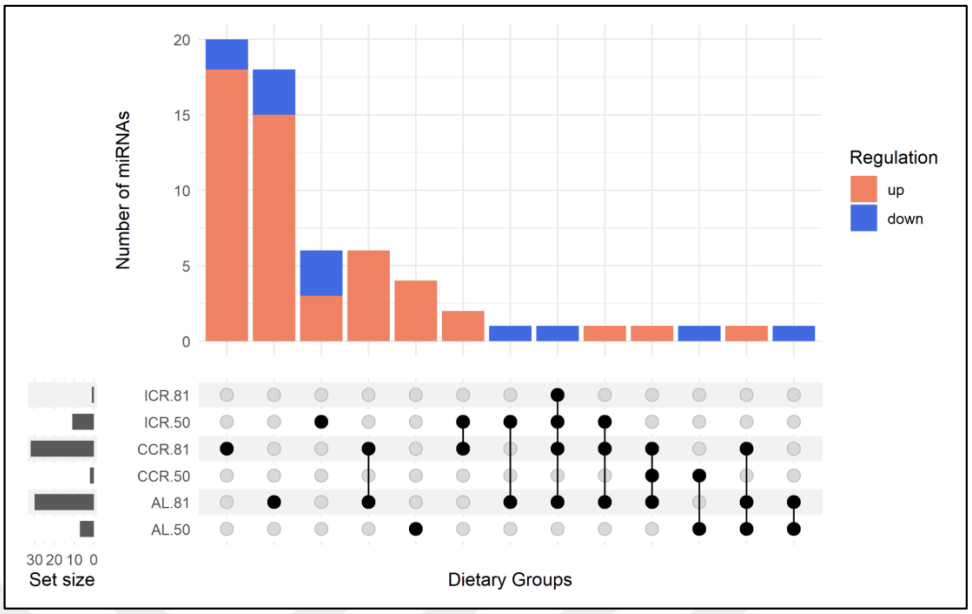

Figure 4.1. The upset plot of miRNAs showing significantly expressed in blood for middle-aged (50) and old-aged (81) mice. This is the same diagram as Figure 3.7., shown here for convenience

4.2.2. Upregulated miRNAs might be the key mediators in the CCR diet

There were 63 miRNAs that were significantly expressed in blood samples. Among these miRNAs and their targets, the CR and cancer-related ones are the focus of the present thesis since our lab has been studying the roles of CR in cancer development for the past 15-20 years [110,111]. For example, the miRNA miR-494-3p is upregulated in mice fed with the CCR diet at both ages (week 50 and 81). Sun *et al.* have shown that upregulation of miR-494-3p induced the expression of HIF-1α, which is reported to be involved in breast cancer biology, including angiogenesis, stem cell maintenance, metabolic reprogramming, epithelial-to-mesenchymal transition, metastasis, hypoxia-induced apoptosis, and resistance to radiation therapy and chemotherapy [112]. In addition, in human breast cancer, a high level of HIF-1α at diagnosis predicts early relapse and metastasis, and it is associated with poor clinical outcomes [113]. Other studies have also reported that miR-494-3p is downregulated in breast cancer cells, which regulates the CXCR4-mediated Wnt/B-catenin signaling pathway [114]. On the contrary, miR-494-3p expression is downregulated in glioma cells, which leads to inhibition of invasion and proliferation while promoting apoptosis by upregulating the PTEN gene in human brain cancer [115]. Considering that the

CCR diet is associated with reduced tumor incidence in our previous studies, miR-494-3p might be a key regulator of cancer development in the preventive effects of CCR.

Another miRNA that was examined is miR-742-5p, which is downregulated in the three dietary groups at old age. There is little information about this miRNA in the literature. To the best of our knowledge, there is no study relating miR-742-5p to cancer, CR, or aging in breast cancer model mice. The Hdac2 gene was found to be among the predicted targets of miR-742-5p. In this context, histone deacetylases (HDACs) are epigenetic controllers that regulate transcription, protein-DNA interactions, chromatin shape, and the histone tail [116]. Genetic lifespan experiments with HDACs in animal models have shown that treatment with HDAC inhibitors extended lifespan [117,118]. Also, according to recent research, abnormal regulation of many HDACs resulted in cancer [119]. For example, Song *et al.* reported that HDAC2 protein is upregulated in gastric cancer, compared to normal gastric mucosa adjacent to each tumor and HDAC2 regulation may play an important role in the aggressiveness of human gastric cancer [120]. The present thesis is the first one to report potential targets of miR-742-5p (full list in Section 6). miR-742-5p might be a potential circulating biomarker for aging-related diseases since the expression level of miR-742-5p is downregulated through aging.

In the present thesis, there was not a significant difference in the global network properties between diets in the blood samples (Figure 3.9.). All co-expression networks had a similar density of approximately 0.1. Nevertheless, the AL co-expression network had the highest number of nodes and edges, while the ICR co-expression network had the lowest one. Thus, these results revealed that dietary intervention reduces the size of miRNA–miRNA interaction networks in the blood. In the literature, there is no similar study to discuss these results. One strategy to find relevant miRNAs in a co-expression network is to look for the ones represented by highly connected nodes. Each node in the network can be connected to many other nodes (that is, to its neighbors), and its degree is the number of such neighbors. The nodes having a degree higher than the average degree of their neighbors is called a *hub*. Because the functionality of networks typically depends more on hubs than other nodes, the miRNAs represented by hub nodes have been chosen to be discussed [103].

This thesis shows that different diets often share the same hub miRNAs. Among hub miRNAs in each dietary group, miR-31-5p and miR-5100 have a high rank in every dietary group in blood tissue (Table 4.1.). This suggest that these miRNAs are constitutive to the

mechanism of aging since they are important in all cases independent of any dietary intervention. Recent studies have reported both positive and negative relationships between miR-31-5p expression and cancer progression [121,122]. Specifically, Shen *et al.* [122] reported that overexpression of miR-31-5p increased the apoptosis and sensitivity of triple-negative breast cancer (TNBC) cells (MDA-MB-231 and MDA-MB-468) to taxol and cisplatin drugs. On the contrary, in the study using human cohort data, Mi *et al.* [121] reported that miR-31-5p is associated with poor prognosis of colon cancer patients, which in turn regulates macrophage polarization by targeting the TSN1 gene. In addition, miR-31-5p was a circulatory biomarker for the diagnosis of oral cancer [123]. In line with the previous findings, it is likely that miR-31-5p plays a role in the preventive effects of CR in breast cancer development. However, this needs to be confirmed by wet lab experiments. Like miR-31-5p studies, similar findings have been reported for miR-5100 as well. In this context, studies have shown that the expression of miR-5100 inhibits the apoptosis of gastric [124], lung [125], and oral cancer cells [126]. Also, it was reported that miR-5100 may play a potential role in lung cancer metastasis since miR-5100 was carried in exosomes derived from bone marrow [127].

Table 4.1. Hub miRNAs and their rankings in blood samples for each dietary group

	AL			**CCR**			**ICR**		
miRNA	**rank**	**hub**	**eigen**	**rank**	**hub**	**eigen**	**rank**	**hub**	**eigen**
miR-31-5p	3	**1**	0.956	1	**1**	1.000	2	**1**	0.989
miR-5100	5	**1**	0.898	3	**1**	0.734	3	**1**	0.953
miR-6239	4	**1**	0.900	4	**1**	0.732	4	**1**	0.911
miR-181a-5p	6	**1**	0.878	5	**1**	0.729	1	**1**	1.000
miR-494-3p	1	**1**	1.000	2	**1**	0.949	20	0	0.558
miR-6991-5p	1	**1**	1.000	19	**1**	0.463	6	**1**	0.875
miR-23a-3p	11	**1**	0.707	10	**1**	0.577	7	**1**	0.816
let-7e-5p	7	**1**	0.839	17	**1**	0.484	5	**1**	0.883
miR-93-3p	12	0	0.699	9	**1**	0.588	9	**1**	0.736

	AL			**CCR**			**ICR**		
miR-484	8	**1**	0.764	11	**1**	0.572	13	**1**	0.658
miR-210-3p	19	**1**	0.596	7	**1**	0.664	11	**1**	0.699
miR-532-3p	9	**1**	0.761	15	**1**	0.507	18	0	0.588
miR-505-5p	21	**1**	0.562	6	**1**	0.709	19	**1**	0.568
miR-328-5p	27	0	0.470	16	**1**	0.488	16	**1**	0.593
miR-3104-5p	10	**1**	0.754	27	0	0.382	25	0	0.499
miR-423-5p	26	**1**	0.503	26	**1**	0.403	10	**1**	0.732
miR-6395	32	0	0.439	39	0	0.264	8	**1**	0.772

The GO terms involved in immune response and inflammation are significantly enriched (adjusted *p*-value<0.01) by the targets of the hub miRNAs in all dietary groups. The terms “cytokine-mediated signaling pathway”, “leukocyte tethering or rolling”, and “negative regulation of immune response” were enriched with a *p*-value under 0.01 in each dietary group (Figure 3.13.). In addition, the “type I interferon signaling pathway” is enriched only in the AL diet group. Chronic inflammation is widely acknowledged to be a factor in the promotion of cancer [40]. Moreover, research has shown that CR lowers the levels of inflammatory cytokines in circulation and the activity of inflammatory signaling [27].

Furthermore, in the present thesis, some GO terms such as “positive regulation of stress-activated MAPK cascade”, “positive regulation of protein autophosphorylation”, and “phagocytosis” are enriched only by targets of hubs in CCR and ICR dietary groups but not in the AL dietary group. In other words, these GO terms are associated with reduced calorie intake. These three terms are relevant to the present thesis. First, MAPKs are part of the stress response pathways activated by cellular stress caused by substances such as inflammatory cytokines, that mediate cell growth or cell death inhibition [128]. Second, autophosphorylation of ERBB2 plays an essential role in biological signal transmissions, such as progression, metastasis, and resistance of HER2+ breast cancer [129]. Lastly, phagocytosis is the initial stage in host defense and inflammation; it is necessary for the elimination of old cells that die on a daily basis; it is required for tissue remodeling [130]. These results suggest that the hub miRNAs in the blood of aging mice affect biological processes related to inflammation, and that the CR might modify the process of aging and

cancer development by regulating MAPK and phagocytosis pathways in addition to other inflammatory pathways.

The second criteria to select relevant nodes is to consider some centrality index. There are several centrality indices that can be calculated for every node in a specific network. For instance, the node degree is a centrality index, but there are others. Here we consider the so-called *eigenvector centrality*, which is a number between zero and one, proportional to the stationary distribution (long-term probability) of a random walk through the network. The miRNAs with high eigenvector centrality are important because their presence is essential for the operation of the network. Losing a central node would disrupt the network connectivity. This leads to a major reorganization of the miRNA network. To facilitate the interpretation of eigenvector centrality, we use it to order the nodes and *rank* them. The node with *rank one* is the one with the highest eigenvector centrality. The least central node will have the largest rank value. Lower rank values are more important.

In the following sections, we will use the rank to indicate how important every miRNA is in each particular diet. Our hypothesis is that, even though the set of hub miRNAs were nearly identical across dietary conditions, the change in the rank of these miRNAs might be significant. Although the distribution of a null hypothesis for this change is complex and beyond the scope of this thesis, we used a rule-of-thumb criteria. We centered and scaled the raw change-of-score using the empirical mean and standard deviation, obtaining a z-score. We selected all miRNAs with an absolute z-score above 1.0 as *significantly re-ranked miRNAs*.

The miRNA miR-374c-3p had a high rank in the CCR diet (rank of 49) and a low rank in the AL diet (rank of 75). The miRNA miR-374c-3p is the one with the largest increase in ranking between the CCR and AL dietary groups. In this context, Bian *et al.* [131] revealed that miR-374 could be a possible biomarker for choosing the best course of treatment for cancer, due to its role in the malignant characteristics of colon and gastric cancer, including proliferation, apoptosis, invasion, and metastasis, by suppressing the Wnt signaling pathway.

Another case is miR-144-3p, which had a low rank in the CCR diet (rank of 58) and a high rank in the AL diet (rank of 14), and is the miRNA with the largest decrease in ranking between the two dietary groups. This change of ranking indicates that there are more miRNAs interacting with miR-144-3p in the AL diet than in CR diets. It is possible that these

interactions inhibit the activity of miR-144-3p directly or indirectly, so CR diets reduce these interactions and enable the role of miR-144-3p in the regulation of proliferation of various types of cancer cells, since the inhibitory roles of miR-144-3p in lung [132] and cervical cancer [133] was reported. On the other hand, miR-144-3p has been shown to be a biomarker for diabetes that might interfere with insulin signaling and control adipogenesis [134].

Furthermore, in the present thesis, the miRNA miR-505-5p is significantly expressed in the blood of mice fed with both AL and CCR diets. However, miR-505-5p is the hub miRNA only in the CCR diet co-expression network, as seen in Figure 4.2. Its centrality was also significantly higher under the CCR diet (ranking of 6) compared to the AL diet (ranking of 21). In this context, Zhu *et al.* [135] reported that miR-505-5p is expressed in both basal human and mouse mammary tumors. This might suggest that the CCR diet regulates the neighbors of miR-505-5p more than the AL diet to prevent its proliferative effect on cancerous tissues [136].

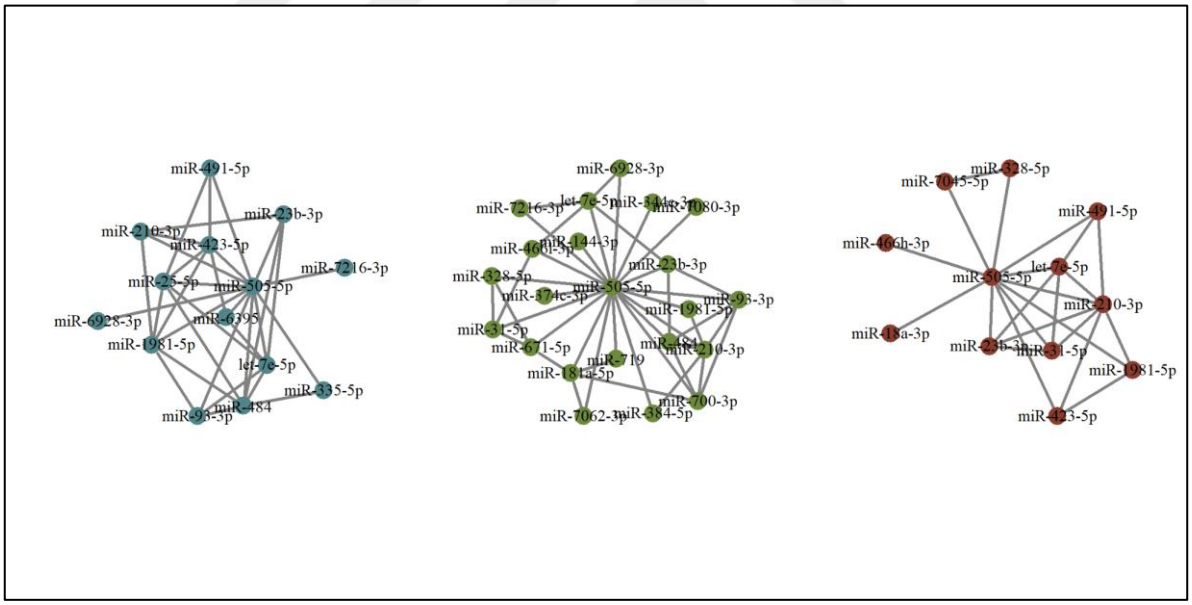

Figure 4.2. Neighbors of miR-505-5p in blood samples for each dietary group. The left subgraph is taken from the network built using miRNA expression from AL-fed mice. The center subgraph corresponds to the CCR diet, and the right one corresponds to the ICR diet

The miRNA miR-668-3p had a high rank in the ICR diet (rank of 44) and a low rank in the AL diet (rank of 74). Recent studies have reported that miR-668-3p acts together with long noncoding RNA circ_0014717 to control tumor growth in liver cancer targeting the human

BTG2 gene [137] and reduce the effect of radiotherapy in breast cancer cell lines [138]. The miRNA miR-6939-5p had a low rank in the ICR diet (rank of 58) and a high rank in the AL diet (rank of 14) and is the miRNA with the largest decrease in ranking between the two diets. Although there is no direct study on miR-6939-5p in the literature, some predicted target genes, such as Ajuba [139], Gdp2 [140], and Josd2 [141], make it a potential research subject in cancer and other metabolic diseases.

In the following paragraphs, the effects of CR on miRNA expression in the MFP will be discussed. Most of the significant miRNA expression occurred in both middle-aged and old-aged mice fed with the CCR diet. Thirteen miRNAs were significantly expressed in middle-aged mice fed with the CCR diet. Of them, ten miRNAs were significantly expressed only in this condition (Table 4.2.). The other three miRNAs, miR-409-3p, miR-540-3p, and miR-127-3p, were also significantly expressed in some of the other conditions. These miRNAs were downregulated in all diets, with the exception of miR-127-3p, which is not significantly expressed in old-aged mice fed with CCR (Table 4.2.). Previous studies on skeletal muscle of aging mice have shown that miR-127-3p and miR-540-3p are downregulated with age they could contribute to muscle aging through the regulation of transcription [142]. These miRNAs are downregulated in all conditions, indicating that they might be related to MFP aging. In one study, Zhang *et al.* reported that miR-409-3p is downregulated in breast cancer cell line, and functions as a tumor suppressor through downregulating Akt1 [144].

Table 4.2. Significant miRNAs in MFP samples for each dietary group. Cells with zero indicate non-significant expression. Cells with one indicate significant upregulation and minus one indicate significant downregulation

	AL		**CCR**		**ICR**	
miRNA	**50**	**81**	**50**	**81**	**50**	**81**
miR-409-3p	**-1**	**-1**	**-1**	**-1**	**-1**	**-1**
miR-540-3p	**-1**	**-1**	**-1**	**-1**	**-1**	**-1**
miR-127-3p	**-1**	**-1**	**-1**	0	**-1**	**-1**
miR-29b-3p	0	0	**1**	0	0	0
miR-101b-3p	0	0	**1**	0	0	0

	AL		**CCR**		**ICR**	
miR-466g	0	0	**1**	0	0	0
miR-466h-3p	0	0	**1**	0	0	0
miR-8103	0	0	**1**	0	0	0
miR-7024-3p	0	0	**1**	0	0	0
miR-383-5p	0	0	**1**	0	0	0
miR-7062-3p	0	0	**1**	0	0	0
miR-7b-3p	0	0	**1**	0	0	0
miR-449c-3p	0	0	**1**	0	0	0

These ten CCR-specific miRNAs are upregulated. Several of them may contribute to the anti-cancer and cardioprotective effects of the CCR diet (for the full list, see the Appendix). For instance, miR-383-5p is upregulated with CCR and, by controlling the expression of genes associated with apoptosis and downregulating genes associated with metastasis, miR-383-5p decreased the viability and migration of breast cancer cells [145]. In the same study, the authors showed that miR-383-5p has the ability to significantly increase the release of pro-inflammatory cytokines and regulate the PD-L1 expression.

One of the significantly upregulated miRNAs, miR-29b-3p, has the largest fold change in CCR. It has been shown that miR-29b-3p has a cardioprotective role in male C57Bl/6 mice that received a 30% CCR diet through downstream targets of Col1a1, Mmp2, and Itg6 [146]. Another study found that miR-29b controls cell proliferation and tumor progression in both ER-negative and ER-positive breast cancer cells by regulating the NF-Kβ and p53 pathways as a consequence of p53 phosphorylation activation [147].

The miRNA miR-129-5p was upregulated in mice fed with CCR of old-aged mice. Luan *et al.* [148] showed that miR-129-5p was downregulated in MCF-7 breast cancer cells and modified epithelial-to-mesenchymal transition (EMT) and drug resistance by targeting the SOX4 and EZH1 gene. Another study also showed that upregulation of miR-129-5p suppressed tumor cell proliferation by targeting the CBX4 gene [149]. Considering that this miRNA is upregulated in our results, the CCR diet may show its protective effect, especially against breast cancer by regulating miR-129-5p.

4.2.3. Significantly Expressed miRNAs are also Hubs in MFP

We did not find significant differences between global network properties between dietary groups, neither in MFP nor in blood tissue. Moreover, the global topological properties of co-expression networks in MFP are almost identical to those in blood. Unlike blood, the co-expression network of miRNAs for the CCR diet had a larger size compared to other dietary conditions in MFP.

The miRNAs with the largest upregulation also had a high degree (Table 3.15., Appendix A). For instance, miR-127-3p has the largest downregulation for all diets in MFP tissue, and it has a high degree in the corresponding co-expression networks. Chen *et al.* [150] also reported that hub genes in skin cancer had also a large differential expression. On the other hand, Dewey *et al.* reported contradicting results [151]. According to this study, known fetal gene markers that were upregulated in gene co-expression networks shared by developing and diseased myocardium were not hub genes. This might be because the regulatory processes affect gene and miRNA expression profiles differently during development and aging.

We have seen that, as in blood, some hub miRNAs are common to all diet-specific networks in MFP tissue (Table 4.3.). The miRNAs miR-127-3p and miR-133b-3p were hubs with high centrality in every diet. As discussed in the previous sections, miR-127-3p decreases with age in every diet. Various studies have found that miR-133b-3p affects diabetic insulin resistance by regulating the GLU4 gene [152], and plays a role in tumor proliferation by directly targeting TGF in various cancers such as brain and breast cancer [153,154]. The fact that these miRNAs (miR-127-3p and miR-133b-3p) were a hub in all diets, it might be required further investigation of their diet-specific effects.

Table 4.3. Hub miRNAs and their rankings in MFP samples for each dietary group

	AL			**CCR**			**ICR**		
miRNA	**rank**	**hub**	**eigen**	**rank**	**hub**	**eigen**	**rank**	**hub**	**eigen**
miR-127-3p	1	**1**	1.000	4	**1**	0.792	1	**1**	1.000
miR-23b-3p	8	**1**	0.666	1	**1**	1.000	6	**1**	0.786

	AL			**CCR**			**ICR**		
miR-133b-3p	3	**1**	0.818	5	**1**	0.734	7	**1**	0.781
miR-3104-5p	4	**1**	0.792	10	**1**	0.664	3	**1**	0.870
miR-1a-3p	13	**1**	0.620	2	**1**	0.958	2	**1**	0.886
miR-5100	2	**1**	0.867	13	0	0.554	5	**1**	0.852
miR-23a-3p	20	0	0.505	3	**1**	0.901	4	**1**	0.865
miR-93-3p	5	**1**	0.727	14	**1**	0.550	8	**1**	0.722
miR-671-5p	7	**1**	0.680	11	0	0.627	11	0	0.652
miR-370-3p	15	**1**	0.586	6	**1**	0.731	10	**1**	0.670
miR-7036-5p	11	0	0.643	15	0	0.515	9	**1**	0.697
miR-6991-5p	12	0	0.635	12	0	0.626	13	**1**	0.636
miR-494-3p	21	0	0.495	7	**1**	0.729	12	**1**	0.641
miR-7045-5p	22	0	0.487	8	**1**	0.698	16	0	0.599
miR-31-5p	9	**1**	0.656	20	0	0.409	25	**1**	0.451
miR-7083-5p	17	0	0.556	21	0	0.394	23	**1**	0.532
miR-184-3p	10	**1**	0.653	37	0	0.225	15	**1**	0.620
miR-210-3p	18	**1**	0.555	18	0	0.478	37	0	0.319
miR-382-5p	14	**1**	0.606	35	0	0.233	24	0	0.502
miR-700-3p	16	0	0.567	46	0	0.180	19	**1**	0.557
miR-29b-3p	34	0	0.334	23	**1**	0.392	26	0	0.448
miR-335-5p	33	0	0.338	24	**1**	0.362	32	0	0.360
miR-6239	40	0	0.283	62	0	0.064	21	**1**	0.550

We identified some miRNAs that are specific to each diet. For instance, miR-7045-5p is a hub miRNA present only in the CCR diet (Table 3.15.), and there is no literature about the effects of miR-7045-5p on CR or cancer. Thus, we focused on one predicted target gene of miR-7045-5p that is Mdn1. This gene belongs to the AAA-ATPases family, which is involved in pre-60S ribosome maturation [155]. In one study, MDN1 was described to be a high-frequency mutation gene in breast cancer, and to have an impact on a variety of

biological processes, including drug metabolism and the RTK-Ras pathway [156]. This miRNA, together with other potential miRNAs, might explain the lower tumor incidence in the CCR group.

Another example of a hub specific to the ICR co-expression network is miR-3104-5p. Since studies on this miRNA are limited, we focused on its predicted targets. One of the predicted targets of miR-3104-5p is Map3k10. It has been demonstrated that Map3k10 is significantly expressed in peripheral insulin-responsive tissues, including adipose tissue, liver, and muscle [157]. A higher risk of different cancers is linked to being overweight or obese. It is also known that dysregulation of insulin metabolism, including insulin resistance, diabetes and obesity are disorders that are closely related to cancer. The evidence suggests that dysregulation of cholesterol synthesis due to limited insulin action may have a causal role in linking diabetes and cancer [158].

We found that hub miRNAs in the AL diet are enriched in the GO term “Wnt signaling pathway”. The same GO term was also enriched in the AL diet in blood. The Wnt pathway is a fundamental signaling pathway that performs a variety of critical activities during development and adult homeostasis [159]. Wnt pathways, both canonical and non-canonical, are involved in ductal growth throughout puberty and adult mammary epithelial maintenance. It also plays an important part in the development of breast cancer which loss of Wnt promotes the migration and invasion of breast cancer without affecting apoptosis or proliferation [160]. This pathway could be a target for anti-aging and aging-related disease treatment strategies due to the high regulation of miRNAs with the AL diet. In CCR, many highly enriched GO terms were related to cell proliferation, inflammation, and glucose homeostasis. Effect of CR on inflammation and glucose homeostasis was already discussed previously. Hsieh *et al.* showed that a 33% CR for varying durations of time (two weeks, one month and two months) inhibits epidermal cell, mammary epithelial cell and T cell proliferation in mice [161].

The miRNA that changed most of its centrality ranking in the CCR diet compared to the AL diet was miR-466h-3p. Although there are not many studies on miR-466h-3p, it has been shown in a study that it may be related to apoptosis [162].

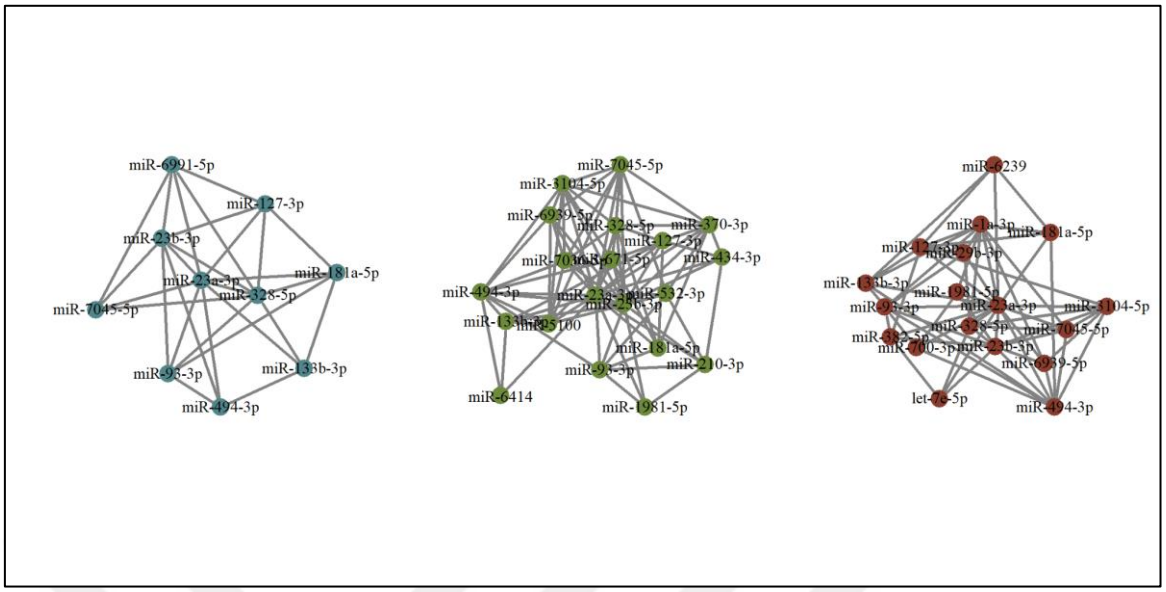

Figure 4.3. Neighbors of miR-23a-3p in MFP samples for each dietary group. The left subgraph is taken from the network built using miRNA expression from AL-fed mice. The center subgraph corresponds to the CCR diet, and the right one corresponds to the ICR diet

While miR-23a-3p was not a hub miRNA in the AL diet, it is a hub in the other two dietary interventions (Figure 4.3.). Many studies have shown that this miRNA has an important role in cancer and energy metabolism [163]. For instance, researchers have shown that overexpression of miR-23a in hepatic cells (Hep1-6) increased intracellular triglyceride levels and increased the expression of Srebp-1c and Fas [164]. In another study, it has been shown that upregulation of miR-23a by interleukin-6 and Stat3 promoted hepatocellular carcinoma by altering glucose homeostasis [165]. Thus, regulation of miR-23a-3p might be essential to the beneficial effects of CR.

4.2.4. Some Hubs are Common in Both Tissues

Although no miRNAs are significantly expressed concurrently across tissues, some hub miRNAs were seen in both blood and MFP co-expression networks. The miRNA miR-494-3p, which was hub miRNA in AL and CCR in blood, was also hub miRNA in CCR and ICR in MFP. The miRNA miR-31-5p, which was hub miRNA in every diet in blood, was also hub miRNA in AL and CCR in MFP (Table 4.3.). On the other hand, some hub miRNAs are tissue specific. The miRNA miR-181a-5p is a hub miRNA only seen in blood. The miRNA

miR-127-3p, on the other hand, was observed to be a hub miRNA specific only to the MFP. Effects of hub miRNAs present in both blood and MFP tissues should be investigated in future studies.

4.2.5. Pathway Influence

Diet-specific miRNA interactions may have a distinct effect on genes in the pathways. A pathway influence analysis sensitive to co-expression network topologies can be performed by stating that miRNAs influencing high-importance hub genes have a significant impact on that pathway [99]. Thus, pathways influenced differently between diets would become a measure of the overall impact of networks on pathways. We found this impact by calculating the sum of eigenvector centrality of the genes in a given KEGG pathway.

Metabolic and regulatory pathways are represented by directed networks. The influence of a co-expression network on a pathway takes into consideration all nodes in both networks and evaluates the eigenvector centrality of the nodes representing the genes predicted as targets of all miRNAs in the co-expression network. The influence value (of a diet-specific co-expression network into a KEGG pathway) is the sum of the eigenvector centralities of the target genes. It depends on the structure of both networks. In order to reveal the pathways that change with diet, we ranked pathways according to their influence score. Here we discuss the pathways with the highest influence score with respect to the AL diet.

We found that some KEGG pathways are highly influenced by all diet-specific co-expression networks. The KEGG pathways “Phosphatidylinositol signaling system” and “Inositol phosphate metabolism” were highly influenced by all miRNA co-expression networks, with a high influence score in all cases. Phosphatidylinositols have a variety of effects on organisms including cell migration, proliferation, survival, and differentiation. Phosphatidylinositols influence a huge range of cell signaling across the cell membrane and cytoplasm, with high-affinity connections between PKC, PKB, PLC, and PDK1 [166]. Another pathway with a high influence score in all co-expression networks is the “MAPK signaling pathway”. MAPKs are enzymes that have been shown to play an important role in extracellular signal transduction to the nucleus. MAPK was found as a significant mechanism connected to weight control and cancer prevention in one study done with rats fed with 40% CR [167].

In blood, the influence of pathways such as the “Glucagon signaling pathway”, “Breast cancer” and “mTOR signaling pathway” increased with the CCR diet with respect to the AL diet. These findings show that the CCR diet alters miRNA interactions in the blood in a way that affects cancer metabolism. Interestingly, in MFP many differential pathways are related to neurodegeneration. Among many others, the “p53 signaling pathway” increased its importance with the CR diet. Roles of p53 in cancer biology were well-defined, and mutated in most samples from some of the most aggressive malignancies, including triple-negative breast cancer [34].

4.3. LIMITATIONS

Network prediction methods based on correlations do not determine the direction of the interaction between miRNAs. Without additional information on the directionality of interactions, it is hard to conclude the underlying regulatory network, which is characterized by its directionality [168]. To know how the miRNAs regulate each other, it is necessary to incorporate the interactions with other non-coding RNAs and transcription factors into the miRNA-miRNA network. Nevertheless, the co-expression network is useful to extract some information about the structure of the underlying regulatory network. It is essential to develop the relevant theoretical and practical tools for this.

GGM may introduce spurious artifacts in the predicted networks. In simple terms, these methods look for the smallest number of edges that is compatible with the experimental covariance. To avoid some of these possible artifacts, we fitted all the networks at the same time trying to control the number of edges in each network and, simultaneously, the number of remodeled edges.

The reconstructed networks depend on some hyperparameters (usually called lambda) that must be chosen carefully, again to avoid artifacts. We chose these hyperparameters by testing many values and evaluating them with the classical AIC. This again should reduce the number of artifacts. There are other criteria to select the hyperparameters, such as the (Extended) Bayesian Information Criteria, which may give different predicted networks, still compatible with the experimental data under the respective criteria. With the information we have, we cannot decide which is better. In fact, all these criteria are widely used in this and other scientific and technical domains.

Moreover, since the experimental data includes a large amount of noise and natural variability, there is a possibility that some of the edges predicted do not correspond to the real relationships, but instead, just reflect the noise. This could be mitigated with larger sample sizes. Nevertheless, most of the network structure is probably correct.

Another limitation is the lack of mRNA expression data in the same animals, or at least the same conditions of the analysis. We determined the genes affected by miRNAs using public miRNA-target gene databases, which may be incomplete or inaccurate. Based on these predicted target genes, we revealed the pathways most influenced by each miRNA co-expression network. Again, it could not be tested whether the affected pathways are actually influenced by miRNAs.

5. CONCLUSION

CR explicitly delays aging-related diseases. In relation to that, the impact of post transcriptional epigenetic control by miRNAs on the onset and progression of various malignancies have been demonstrated. This thesis evaluated the effect of CR on miRNA expression in the blood due to its biomarker feature and in the MFP as it is expected to develop cancer. We have shown that miRNA expression is most altered by tissue type. However, when we compare it with the tissue-specific baseline, there is no miRNA that is commonly expressed in both tissues. This shows that the tissue-specific effects of miRNA expression should be considered in future studies, just as in gene expression. The CCR diet affects more miRNA in each tissue other than the AL and ICR diets. It has been shown here that upregulation of miRNAs such as miR-31-5p and miR-494-3p in blood and miR-133a/b and miR-1a-3p in MFP may play a role in the protective effect of CR against cancer.

For co-expression analysis, these significant miRNAs were chosen, and networks were built for each diet and tissue. We have shown that although the networks have different numbers of interactions, we could not find any difference in their global properties. On the other hand, we have shown that some hub miRNAs were different. We ranked these miRNAs according to their eigenvector centrality and examined how this ranking changed in diets. When compared with AL diet, the importance of miR-374c-3p in blood and miR-466h-3p in MFP increased for CCR; For ICR, we found increased importance of miR-668-3p in blood and miR-331-3p in MFP.

Finally, we showed that the miRNAs we found might be involved in biological processes that are intensely related to inflammation. In addition, we showed that some pathways, such as the “Phosphatidylinositol signaling system”, “focal adhesion” and the “MAPK signaling pathway”, are commonly influenced in all diets and tissues. We have shown that these pathways can be modulated by CR via miRNAs. We have identified some necessary strategies to better understand these findings in the future. That is, mRNA expression data from corresponding diets and tissues must be integrated with the data we analyzed. In addition, motif analysis may be appropriate to identify differential interactions (modules) between networks.

REFERENCES

1. Wyss-Coray T. Ageing, neurodegeneration and brain rejuvenation. *Nature*. 2016;539 (7628): 180–6.

2. Carmona JJ, Michan S. Biology of Healthy Aging and Longevity. *Rev Invest Clin*. 2016;68(1):7-16.

3. Almendáriz-Palacios C, Mousseau DD, Eskiw CH, Gillespie ZE. Still Living Better through Chemistry: An Update on Caloric Restriction and Caloric Restriction Mimetics as Tools to Promote Health and Lifespan. *International Journal of Molecular Sciences.* 2020;21 (23): E9220.

4. López-Lluch G, Navas P. Calorie restriction as an intervention in ageing. *The Journal of Physiology*. 2016;594 (8): 2043–60.

5. Martin B, Mattson MP, Maudsley S. Caloric restriction and intermittent fasting: Two potential diets for successful brain aging. *Ageing Research Reviews.* 2006;5 (3): 332–53.

6. Weindruch R, Walford RL, Fligiel S, Guthrie D. The Retardation of Aging in Mice by Dietary Restriction: Longevity, Cancer, Immunity and Lifetime Energy Intake. *The Journal of Nutrition.* 1986;116 (4): 641–54.

7. Szafranski K. Non-coding RNA in neural function, disease, and aging. *Frontiers in Genetics*. 2015;6.

8. Lau NC, Lim LP, Weinstein EG, Bartel DP. An Abundant Class of Tiny RNAs with Probable Regulatory Roles in *Caenorhabditis elegans*. *Science*. 2001;294 (5543): 858–62.

9. Sayed D, Abdellatif M. MicroRNAs in development and disease. *Physiological Reviews*. 2011;91 (3): 827–87.

10. Ross SA, Davis CD. MicroRNA, nutrition, and cancer prevention. *Advances in Nutrition*. 2011;2 (6): 472–85.

11. Huntley RP, Kramarz B, Sawford T, Umrao Z, Kalea A, Acquaah V, et al. Expanding the horizons of microRNA bioinformatics. *RNA*. 2018;24 (8): 1005–17.

12. Croce CM. Causes and consequences of microRNA dysregulation in cancer. *Nature Reviews Genetics*. 2009;10 (10): 704–14.

13. Hawkins PG, Morris KV. RNA and transcriptional modulation of gene expression. *Cell Cycle*. 2008;7 (5): 602–7.

14. Speakman JR, Mitchell SE. Caloric restriction. *Molecular Aspects of Medicine*. 2011;32 (3): 159–221.

15. Fontana L, Meyer TE, Klein S, Holloszy JO. Long-term calorie restriction is highly effective in reducing the risk for atherosclerosis in humans. *Proceedings of the National Academy of Sciences of the United States of America*. 2004;101 (17): 6659–63.

16. Meynet O, Ricci J-E. Caloric restriction and cancer: Molecular mechanisms and clinical implications. *Trends in Molecular Medicine*. 2014;20 (8): 419–27.

17. Heilbronn LK, Jonge L de, Frisard MI, DeLany JP, Larson-Meyer DE, Rood J, et al. Effect of 6-Month Calorie Restriction on Biomarkers of Longevity, Metabolic Adaptation, and Oxidative Stress in Overweight Individuals: A Randomized Controlled Trial. *JAMA*. 2006;295 (13): 1539.

18. Hadem IKH, Majaw T, Kharbuli B, Sharma R. Beneficial effects of dietary restriction in aging brain. *Journal of Chemical Neuroanatomy*. 2019;95: 123–33.

19. Maroofi M, Nasrollahzadeh J. Effect of intermittent versus continuous calorie restriction on body weight and cardiometabolic risk markers in subjects with overweight or obesity and mild-to-moderate hypertriglyceridemia: A randomized trial. *Lipids in Health and Disease*. 2020;19 (1): 216.

20. Meydani SN, Das SK, Pieper CF, Lewis MR, Klein S, Dixit VD, et al. Long-term moderate calorie restriction inhibits inflammation without impairing cell-mediated immunity: A randomized controlled trial in non-obese humans. *Aging*. 2016;8 (7): 1416–31.

21. Cabelof D. Caloric restriction promotes genomic stability by induction of base excision repair and reversal of its age-related decline. *DNA Repair*. 2003;2 (3): 295–307.

22. Civitarese AE, Carling S, Heilbronn LK, Hulver MH, Ukropcova B, Deutsch WA, et al. Calorie restriction increases muscle mitochondrial biogenesis in healthy humans. *PLoS medicine*. 2007;4 (3): e76.

23. Wang W, Cai G, Chen X. Dietary restriction delays the secretion of senescence associated secretory phenotype by reducing DNA damage response in the process of renal aging. *Experimental Gerontology*. 2018;107: 4–10.

24. Wahl D, LaRocca TJ. Transcriptomic Effects of Healthspan-Promoting Dietary Interventions: Current Evidence and Future Directions. *Frontiers in Nutrition*. 2021; 8: 712129.

25. Derous D, Mitchell SE, Green CL, Wang Y, Han JDJ, Chen L, et al. The Effects of Graded Levels of Calorie Restriction: X. Transcriptomic Responses of Epididymal Adipose Tissue. *The Journals of Gerontology*: Series A. 2018;73 (3): 279–88.

26. Wahl D, Cogger VC, Solon-Biet SM, Waern RVR, Gokarn R, Pulpitel T, et al. Nutritional strategies to optimise cognitive function in the aging brain. *Ageing Research Reviews*. 2016;31: 80–92.

27. Harvey AE, Lashinger LM, Otto G, Nunez NP, Hursting SD. Decreased systemic IGF-1 in response to calorie restriction modulates murine tumor cell growth, nuclear factor-κB activation, and inflammation-related gene expression. *Molecular Carcinogenesis*. 2013;52 (12): 997–1006.

28. Mattson MP, Longo VD, Harvie M. Impact of intermittent fasting on health and disease processes. *Ageing Research Reviews*. 2017;39: 46–58.

29. Collins N, Han S-J, Enamorado M, Link VM, Huang B, Moseman EA, et al. The Bone Marrow Protects and Optimizes Immunological Memory during Dietary Restriction. *Cell*. 2019;178 (5): 1088–1101.e15.

30. Chausse B, Vieira-Lara MA, Sanchez AB, Medeiros MHG, Kowaltowski AJ. Intermittent Fasting Results in Tissue-Specific Changes in Bioenergetics and Redox State. Gueven N, editor. *PLOS ONE*. 2015;10 (3): e0120413.

31. Sharples AP, Hughes DC, Deane CS, Saini A, Selman C, Stewart CE. Longevity and skeletal muscle mass: The role of IGF signalling, the sirtuins, dietary restriction and protein intake. *Aging Cell*. 2015;14 (4): 511–23.

32. Weir HJ, Yao P, Huynh FK, Escoubas CC, Goncalves RL, Burkewitz K, et al. Dietary Restriction and AMPK Increase Lifespan via Mitochondrial Network and Peroxisome Remodeling. *Cell Metabolism*. 2017;26 (6): 884–896.e5.

33. Duszka K, Gregor A, Guillou H, König J, Wahli W. Peroxisome Proliferator-Activated Receptors and Caloric Restriction-Common Pathways Affecting Metabolism, Health, and Longevity. *Cells*. 2020;9 (7): E1708.

34. Muñoz-Pinedo C, El Mjiyad N, Ricci J-E. Cancer metabolism: Current perspectives and future directions. *Cell Death & Disease*. 2012;3: e248.

35. Warburg O. On the origin of cancer cells. *Science*. 1956;123 (3191): 309–14.

36. Avgerinos KI, Spyrou N, Mantzoros CS, Dalamaga M. Obesity and cancer risk: Emerging biological mechanisms and perspectives. *Metabolism: Clinical and Experimental*. 2019;92: 121–35.

37. Debras C, Chazelas E, Srour B, Kesse-Guyot E, Julia C, Zelek L, et al. Total and added sugar intakes, sugar types, and cancer risk: Results from the prospective NutriNet-Santé cohort. *The American Journal of Clinical Nutrition*. 2020;112 (5): 1267–79.

38. Brandhorst S, Longo VD. Fasting and Caloric Restriction in Cancer Prevention and Treatment. *Metabolism in Cancer*. *Recent Results in Cancer Research*. 2016; 207: 241–66.

39. Mercken EM, Crosby SD, Lamming DW, JeBailey L, Krzysik-Walker S, Villareal DT, et al. Calorie restriction in humans inhibits the PI3K/AKT pathway and induces a younger transcription profile. *Aging Cell*. 2013;12 (4): 645–51.

40. Piotrowski I, Kulcenty K, Suchorska W. Interplay between inflammation and cancer. *Reports of Practical Oncology & Radiotherapy*. 2020;25 (3): 422–7.

41. Ricciotti E, FitzGerald GA. Prostaglandins and inflammation. *Arteriosclerosis, Thrombosis, and Vascular Biology*. 2011;31 (5): 986–1000.

42. Maegawa S, Lu Y, Tahara T, Lee JT, Madzo J, Liang S, et al. Caloric restriction delays age-related methylation drift. *Nature Communications*. 2017;8 (1): 539.

43. Wood SH, Dam S van, Craig T, Tacutu R, O'Toole A, Merry BJ, et al. Transcriptome analysis in calorie-restricted rats implicates epigenetic and post-translational mechanisms in neuroprotection and aging. *Genome Biology*. 2015;16 (1): 285.

44. Schneider A, Dhahbi JM, Atamna H, Clark JP, Colman RJ, Anderson RM. Caloric restriction impacts plasma microRNAs in rhesus monkeys. *Aging Cell*. 2017; 16 (5): 1200–3.

45. Hahn O, Grönke S, Stubbs TM, Ficz G, Hendrich O, Krueger F, et al. Dietary restriction protects from age-associated DNA methylation and induces epigenetic reprogramming of lipid metabolism. *Genome Biology*. 2017;18 (1): 56.

46. Hernández-Saavedra D, Moody L, Xu GB, Chen H, Pan Y-X. Epigenetic Regulation of Metabolism and Inflammation by Calorie Restriction. *Advances in Nutrition*. 2019;10 (3): 520–36.

47. Campión J, Milagro FI, Goyenechea E, Martínez JA. TNF-alpha promoter methylation as a predictive biomarker for weight-loss response. *Obesity*. 2009;17 (6): 1293–7.

48. Cordero P, Campion J, Milagro FI, Goyenechea E, Steemburgo T, Javierre BM, et al. Leptin and TNF-alpha promoter methylation levels measured by MSP could predict the response to a low-calorie diet. *Journal of Physiology and Biochemistry*. 2011;67 (3): 463–70.

49. Fontana L, Partridge L. Promoting health and longevity through diet: From model organisms to humans. *Cell*. 2015;161 (1): 106–18.

50. Sharma N, Castorena CM, Cartee GD. Tissue-specific responses of IGF-1/insulin and mTOR signaling in calorie restricted rats. *PloS One*. 2012; 7 (6): e38835.

51. Treiber T, Treiber N, Meister G. Regulation of microRNA biogenesis and its crosstalk with other cellular pathways. *Nature Reviews Molecular Cell Biology*. 2019;20 (1): 5–20.

52. Huntzinger E, Izaurralde E. Gene silencing by microRNAs: Contributions of translational repression and mRNA decay. *Nature Reviews Genetics*. 2011;12 (2): 99–110.

53. Ha M, Kim VN. Regulation of microRNA biogenesis. *Nature Reviews Molecular* Cell Biology. 2014; 15 (8): 509–24.

54. Kobayashi H, Tomari Y. RISC assembly: Coordination between small RNAs and Argonaute proteins. *Biochimica Et Biophysica Acta*. 2016;1859 (1): 71–81.

55. Kim Y-K, Wee G, Park J, Kim J, Baek D, Kim J-S, et al. TALEN-based knockout library for human microRNAs. *Nature Structural & Molecular Biology*. 2013;20 (12): 1458–64.

56. Jonas S, Izaurralde E. Towards a molecular understanding of microRNA-mediated gene silencing. *Nature Reviews Genetics*. 2015;16 (7): 421–33.

57. Meijer HA, Kong YW, Lu WT, Wilczynska A, Spriggs RV, Robinson SW, et al. Translational repression and eIF4A2 activity are critical for microRNA-mediated gene regulation. *Science*. 2013;340 (6128): 82–5.

58. Eulalio A, Tritschler F, Izaurralde E. The GW182 protein family in animal cells: New insights into domains required for miRNA-mediated gene silencing. *RNA*. 2009;15 (8): 1433–42.

59. Abraham KJ, Ostrowski LA, Mekhail K. Non-Coding RNA Molecules Connect Calorie Restriction and Lifespan. *Journal of Molecular Biology*. 2017;429 (21): 3196–214.

60. Calvopina D, Coleman M, Lewindon P, Ramm G. Function and Regulation of MicroRNAs and Their Potential as Biomarkers in Paediatric Liver Disease. *International Journal of Molecular Sciences*. 2016;17 (11): 1795.

61. Kogure A, Uno M, Ikeda T, Nishida E. The microRNA machinery regulates fasting-induced changes in gene expression and longevity in Caenorhabditis elegans. *Journal of Biological Chemistry*. 2017;292 (27): 11300–9.

62. Gendron CM, Pletcher SD. MicroRNAs mir-184 and let-7 alter Drosophila metabolism and longevity. *Aging Cell*. 2017; 16 (6): 1434–8.

63. Dhahbi JM, Spindler SR, Atamna H, Yamakawa A, Guerrero N, Boffelli D, et al. Deep sequencing identifies circulating mouse miRNAs that are functionally implicated in manifestations of aging and responsive to calorie restriction. *Aging*. 2013;5 (2): 130–41.

64. Victoria B, Dhahbi JM, Nunez Lopez YO, Spinel L, Atamna H, Spindler SR, et al. Circulating microRNA signature of genotype-by-age interactions in the long-lived Ames dwarf mouse. *Aging Cell*. 2015;14 (6): 1055–66.

65. Makwana K, Patel SA, Velingkaar N, Ebron JS, Shukla GC, Kondratov RVKV. Aging and calorie restriction regulate the expression of miR-125a-5p and its target genes Stat3, Casp2 and Stard13. *Aging*. 2017;9 (7): 1825–43.

66. Ørom UA, Lim MK, Savage JE, Jin L, Saleh AD, Lisanti MP, et al. MicroRNA-203 regulates caveolin-1 in breast tissue during caloric restriction. *Cell Cycle*. 2012;11 (7): 1291–5.

67. Devlin KL, Sanford T, Harrison LM, LeBourgeois P, Lashinger LM, Mambo E, et al. Stage-Specific MicroRNAs and Their Role in the Anticancer Effects of Calorie Restriction in a Rat Model of ER-Positive Luminal Breast Cancer. *PLOS ONE*. 2016;11 (7): e0159686.

68. Dokholyan NV. Computational Modeling of Biological Systems: From Molecules to Pathways. Springer New York; 2012.

69. Ideker T, Ozier O, Schwikowski B, Siegel AF. Discovering regulatory and signalling circuits in molecular interaction networks. Bioinformatics (Oxford, England). 2002; 18 Suppl 1: S233–240.

70. Saw PE, Xu X, Chen J, Song E-W. Non-coding RNAs: The new central dogma of cancer biology. *Science China Life Sciences*. 2021;64 (1): 22–50.

71. Zhou Y, Ferguson J, Chang JT, Kluger Y. Inter- and intra-combinatorial regulation by transcription factors and microRNAs. *BMC genomics*. 2007;8: 396.

72. Li H. Inferring regulatory networks. *Frontiers in Bioscience*. 2008; 13 (13): 263.

73. He B, Tan K. Understanding transcriptional regulatory networks using computational models. *Current Opinion in Genetics & Development*. 2016;37: 101–8.

74. Serin EAR, Nijveen H, Hilhorst HWM, Ligterink W. Learning from Co-expression Networks: Possibilities and Challenges. *Frontiers in Plant Science*. 2016;7.

75. Kiss HJM, Mihalik A, Nánási T, Ory B, Spiró Z, Soti C, et al. Ageing as a price of cooperation and complexity: Self-organization of complex systems causes the gradual deterioration of constituent networks. *BioEssays: News and Reviews in Molecular, Cellular and Developmental Biology*. 2009;31 (6): 651–64.

76. Peysselon F, Ricard-Blum S. Understanding the biology of aging with interaction networks. *Maturitas*. 2011;69 (2): 126–30.

77. Lorenz DR, Cantor CR, Collins JJ. A network biology approach to aging in yeast. Proceedings of the National Academy of Sciences. 2009;106 (4): 1145–50. Available from: http://www.pnas.org/cgi/doi/10.1073/pnas.0812551106

78. Martínez-Reyes I, Chandel NS. Cancer metabolism: Looking forward. *Nature Reviews Cancer*. 2021;21 (10): 669–80.

79. Yan W, Xue W, Chen J, Hu G. Biological Networks for Cancer Candidate Biomarkers Discovery. *Cancer Informatics*. 2016;15s3: CIN.S39458.

80. Cui Q. A network of cancer genes with co-occurring and anti-co-occurring mutations. *PloS One*. 2010;5 (10): e13180.

81. Zhang P, Ma Y, Wang F, Yang J, Liu Z, Peng J, et al. Comprehensive gene and microRNA expression profiling reveals the crucial role of hsa-let-7i and its target genes in colorectal cancer metastasis. *Molecular Biology Reports*. 2012;39 (2): 1471–8.

82. Sehgal V, Seviour EG, Moss TJ, Mills GB, Azencott R, Ram PT. Robust Selection Algorithm (RSA) for Multi-Omic Biomarker Discovery; Integration with Functional Network Analysis to Identify miRNA Regulated Pathways in Multiple Cancers. *PLoS ONE*. 2015; 10.

83. Pierson E, the GTEx Consortium, Koller D, Battle A, Mostafavi S. Sharing and Specificity of Co-expression Networks across 35 Human Tissues. Rigoutsos I, editor. *PLOS Computational Biology*. 2015;11 (5): e1004220.

84. Carvalho BS, Irizarry RA. A framework for oligonucleotide microarray preprocessing. *Bioinformatics*. 2010;26 (19): 2363–7.

85. Irizarry RA. Summaries of Affymetrix GeneChip probe level data. *Nucleic Acids Research*. 2003;31 (4): 15e–15.

86. Ritchie ME, Phipson B, Wu D, Hu Y, Law CW, Shi W, et al. Limma powers differential expression analyses for RNA-sequencing and microarray studies. *Nucleic Acids Research*. 2015;43 (7): e47–7.

87. Smyth GK. Linear Models and Empirical Bayes Methods for Assessing Differential Expression in Microarray Experiments. *Statistical Applications in Genetics and Molecular Biology*. 2004;3 (1): 1–25.

88. Conway JR, Lex A, Gehlenborg N. UpSetR: An R package for the visualization of intersecting sets and their properties. Hancock J, editor. *Bioinformatics*. 2017;33 (18): 2938–40.

89. Godard P, Eyll J van. Pathway analysis from lists of microRNAs: Common pitfalls and alternative strategy. *Nucleic Acids Research*. 2015;43 (7): 3490–7.

90. Menéndez P, Kourmpetis YAI, Braak CJF ter, Eeuwijk FA van. Gene regulatory networks from multifactorial perturbations using Graphical Lasso: Application to the DREAM4 challenge. *PloS One*. 2010;5 (12): e14147.

91. Danaher P, Wang P, Witten DM. The joint graphical lasso for inverse covariance estimation across multiple classes. *Journal of the Royal Statistical Society*. 2014; 76 (2): 373–97.

92. John B, Enright AJ, Aravin A, Tuschl T, Sander C, Marks DS, et al. Human microRNA targets. *PLoS biology*. 2004; 2 (11): e363.

93. Krek A, Grün D, Poy MN, Wolf R, Rosenberg L, Epstein EJ, et al. Combinatorial microRNA target predictions. *Nature Genetics*. 2005;37 (5): 495–500.

94. Lewis BP, Shih I, Jones-Rhoades MW, Bartel DP, Burge CB. Prediction of Mammalian MicroRNA Targets. *Cell*. 2003;115 (7): 787–98.

95. Maragkakis M, Alexiou P, Papadopoulos GL, Reczko M, Dalamagas T, Giannopoulos G, et al. Accurate microRNA target prediction correlates with protein repression levels. *BMC Bioinformatics*. 2009;10 (1): 295.

96. Wong N, Wang X. miRDB: An online resource for microRNA target prediction and functional annotations. *Nucleic Acids Research*. 2015;43 (D1): D146–52.

97. Huang H-Y, Lin Y-C-D, Li J, Huang K-Y, Shrestha S, Hong H-C, et al. miRTarBase 2020: Updates to the experimentally validated microRNA–target interaction database. *Nucleic Acids Research*. 2020;48(D1):D148–54.

98. Gu Z, Gu L, Eils R, Schlesner M, Brors B. Circlize implements and enhances circular visualization in R. *Bioinformatics*. 2014;30 (19): 2811–2.

99. Li C, Dinu V. miR2Pathway: A novel analytical method to discover MicroRNA-mediated dysregulated pathways involved in hepatocellular carcinoma. *Journal of Biomedical Informatics*. 2018;81: 31–40.

100. Sales G, Calura E, Cavalieri D, Romualdi C. Graphite - a Bioconductor package to convert pathway topology to gene network. *BMC Bioinformatics*. 2012;13 (1): 20.

101. Choi JK, Yu U, Yoo OJ, Kim S. Differential coexpression analysis using microarray data and its application to human cancer. *Bioinformatics*. 2005;21 (24): 4348–55.

102. Villa-Vialaneix N, Liaubet L, Laurent T, Cherel P, Gamot A, SanCristobal M. The Structure of a Gene Co-Expression Network Reveals Biological Functions Underlying eQTLs. *PLoS ONE*. 2013;8 (4): e60045.

103. Dam S van, Võsa U, Graaf A van der, Franke L, Magalhães JP de. Gene co-expression analysis for functional classification and gene-disease predictions. *Briefings in Bioinformatics*. 2018;19 (4): 575–92.

104. Weber JA, Baxter DH, Zhang S, Huang DY, How Huang K, Jen Lee M, et al. The MicroRNA Spectrum in 12 Body Fluids. *Clinical Chemistry*. 2010;56 (11): 1733–41.

105. Galvão-Lima LJ, Morais AHF, Valentim RAM, Barreto EJSS. miRNAs as biomarkers for early cancer detection and their application in the development of new diagnostic tools. *BioMedical Engineering OnLine*. 2021;20 (1): 21.

106. Kaneto CM, Nascimento JS, Prado MSJG, Mendonça LSO. Circulating miRNAs as biomarkers in cardiovascular diseases. *European Review for Medical and Pharmacological Sciences*. 2019;23 (5): 2234–43.

107. Chen S, Ji L, Chen M, Yang D, Zhou J, Zheng Y. Weighted miRNA co-expression network reveals potential roles of apoptosis related pathways and crucial genes in thoracic aortic aneurysm. *Journal of Thoracic Disease*. 2021;13 (5): 2776–89.

108. He S, Huang L, Shao C, Nie T, Xia L, Cui B, et al. Several miRNAs derived from serum extracellular vesicles are potential biomarkers for early diagnosis and progression of Parkinson's disease. *Translational Neurodegeneration*. 2021;10 (1): 25.

109. Ferreira M, Francisco S, Soares AR, Nobre A, Pinheiro M, Reis A, et al. Integration of segmented regression analysis with weighted gene correlation network analysis identifies genes whose expression is remodeled throughout physiological aging in mouse tissues. *Aging*. 2021;13 (14): 18150–90.

110. Dogan S, Rogozina OP, Lokshin AE, Grande JP, Cleary MP. Effects of chronic vs. Intermittent calorie restriction on mammary tumor incidence and serum adiponectin

and leptin levels in MMTV-TGF-α mice at different ages. *Oncology Letters*. 2010;1 (1): 167–76.

111. Dogan S, Cicekdal MB, Özorhan Ü, Karabiyik G, Kazan BT, Ekici ID, et al. Roles of Adiponectin and Leptin Signaling Related microRNAs in The Preventive Effects of Calorie Restriction in Mammary Tumor Development. *Applied Physiology, Nutrition, and Metabolism*. 2021;46 (8): 866-876.

112. Sun G, Zhou Y, Li H, Guo Y, Shan J, Xia M, et al. Over-expression of microRNA-494 up-regulates hypoxia-inducible factor-1 alpha expression via PI3K/Akt pathway and protects against hypoxia-induced apoptosis. *Journal of Biomedical Science*. 2013;20 (1): 100.

113. Masoud GN, Li W. HIF-1α pathway: Role, regulation and intervention for cancer therapy. *Acta Pharmaceutica Sinica B*. 2015;5 (5): 378–89.

114. Song L, Liu D, Wang B, He J, Zhang S, Dai Z, et al. miR-494 suppresses the progression of breast cancer in vitro by targeting CXCR4 through the Wnt/β-catenin signaling pathway. *Oncology Reports*. 2015;34 (1): 525–31.

115. Li X, Wang H, Wu Z, Yang T, Zhao Z, Chen G, et al. miR-494-3p Regulates Cellular Proliferation, Invasion, Migration, and Apoptosis by PTEN/AKT Signaling in Human Glioblastoma Cells. *Cellular and Molecular Neurobiology*. 2015;35 (5): 679–87.

116. Yoon S, Eom GH. HDAC and HDAC Inhibitor: From Cancer to Cardiovascular Diseases. *Chonnam Medical Journal*. 2016; 52 (1): 1.

117. Pasyukova EG, Vaiserman AM. HDAC inhibitors: A new promising drug class in anti-aging research. *Mechanisms of Ageing and Development*. 2017;166: 6–15.

118. Jones MJ, Goodman SJ, Kobor MS. DNA methylation and healthy human aging. *Aging Cell*. 2015;14 (6): 924–32.

119. Li G, Tian Y, Zhu W-G. The Roles of Histone Deacetylases and Their Inhibitors in Cancer Therapy. *Frontiers in Cell and Developmental Biology*. 2020;8: 576946.

120. Song J, Noh JH, Lee JH, Eun JW, Ahn YM, Kim SY, et al. Increased expression of histone deacetylase 2 is found in human gastric cancer. *APMIS*. 2005;113 (4): 264–8.

121. Mi B, Li Q, Li T, Liu G, Sai J. High miR-31-5p expression promotes colon adenocarcinoma progression by targeting TNS1. *Aging*. 2020;12 (8): 7480–90.

122. Shen X, Lei J, Du L. miR-31-5p may enhance the efficacy of chemotherapy with Taxol and cisplatin in TNBC. *Experimental and Therapeutic Medicine.* 2020;19 (1): 375–83.

123. Lu Z, He Q, Liang J, Li W, Su Q, Chen Z, et al. miR-31-5p Is a Potential Circulating Biomarker and Therapeutic Target for Oral Cancer. *Molecular Therapy Nucleic Acids*. 2019;16: 471–80.

124. Zhang H-M, Li H, Wang G-X, Wang J, Xiang Y, Huang Y, et al. MKL1/miR-5100/CAAP1 loop regulates autophagy and apoptosis in gastric cancer cells. *Neoplasia*. 2020;22 (5): 220–30.

125. Huang H, Jiang Y, Wang Y, Chen T, Yang L, He H, et al. miR-5100 promotes tumor growth in lung cancer by targeting Rab6. *Cancer Letters*. 2015;362 (1): 15–24.

126. Shi J, Bao X, Liu Z, Zhang Z, Chen W, Xu Q. Serum miR-626 and miR-5100 are Promising Prognosis Predictors for Oral Squamous Cell Carcinoma. *Theranostics*. 2019; 9 (4): 920–31.

127. Zhang X, Sai B, Wang F, Wang L, Wang Y, Zheng L, et al. Hypoxic BMSC-derived exosomal miRNAs promote metastasis of lung cancer cells via STAT3-induced EMT. *Molecular Cancer*. 2019;18 (1): 40.

128. Sinkala M, Nkhoma P, Mulder N, Martin DP. Integrated molecular characterisation of the MAPK pathways in human cancers reveals pharmacologically vulnerable mutations and gene dependencies. *Communications Biology*. 2021;4 (1): 9.

129. Iqbal N, Iqbal N. Human Epidermal Growth Factor Receptor 2 (HER2) in Cancers: Overexpression and Therapeutic Implications. *Molecular Biology International*. 2014; 2014: 852748.

130. Aderem A. Phagocytosis and the Inflammatory Response. *The Journal of Infectious Diseases*. 2003;187 (s2): S340–5.

131. Bian H, Zhou Y, Zhou D, Zhang Y, Shang D, Qi J. The latest progress on miR-374 and its functional implications in physiological and pathological processes. *Journal of Cellular and Molecular Medicine*. 2019; 23 (5): 3063–76.

132. Sun Y, Liu Z, Huang L, Shang Y. MiR-144-3p inhibits the proliferation, migration and invasion of lung adenocargen cancer cells by targeting COL11A1. *Journal of Chemotherapy*. 2021;33 (6): 409–19.

133. Wu J, Zhao Y, Li F, Qiao B. MiR-144-3p: A novel tumor suppressor targeting MAPK6 in cervical cancer. *Journal of Physiology and Biochemistry*. 2019;75 (2): 143–52.

134. Liang Y-Z, Dong J, Zhang J, Wang S, He Y, Yan Y-X. Identification of Neuroendocrine Stress Response-Related Circulating MicroRNAs as Biomarkers for Type 2 Diabetes Mellitus and Insulin Resistance. *Frontiers in Endocrinology*. 2018;9: 132.

135. Zhu M, Yi M, Kim CH, Deng C, Li Y, Medina D, et al. Integrated miRNA and mRNA expression profiling of mouse mammary tumor models identifies miRNA signatures associated with mammary tumor lineage. *Genome Biology*. 2011; 12 (8): R77.

136. Wang T, Zhang H, Wang H, Chang C, Huang F, Zhang L. MiR-505-5p inhibits proliferation and promotes apoptosis of osteosarcoma cells via regulating RASSF8 expression. *Journal of BUON*. 2021;26 (2): 599–605.

137. Ma H, Huang C, Huang Q, Li G, Li J, Huang B, et al. Circular RNA circ_0014717 Suppresses Hepatocellular Carcinoma Tumorigenesis Through Regulating miR-668-3p/BTG2 Axis. *Frontiers in Oncology*. 2021;10: 592884.

138. Luo M, Ding L, Li Q, Yao H. miR-668 enhances the radioresistance of human breast cancer cell by targeting IκBα. *Breast Cancer*. 2017;24 (5): 673–82.

139. Li X, Zhao G, Mi X, Xu T, Li X, Liu B. Ajuba Overexpression Promotes Breast Cancer Chemoresistance and Glucose Uptake through TAZ-GLUT3/Survivin Pathway. *BioMed Research International*. 2022; 2022: 3321409.

140. Langston PK, Nambu A, Jung J, Shibata M, Aksoylar HI, Lei J, et al. Glycerol phosphate shuttle enzyme GPD2 regulates macrophage inflammatory responses. *Nature Immunology*. 2019;20 (9): 1186–95.

141. Lei H, Yang L, Wang Y, Zou Z, Liu M, Xu H, et al. JOSD2 regulates PKM2 nuclear translocation and reduces acute myeloid leukemia progression. *Experimental Hematology & Oncology*. 2022;11 (1): 42.

142. Kim JY, Park Y-K, Lee K-P, Lee S-M, Kang T-W, Kim H-J, et al. Genome-wide profiling of the microRNA-mRNA regulatory network in skeletal muscle with aging. *Aging*. 2014;6 (7): 524–44.

143. Zhang G, Liu Z, Xu H, Yang Q. miR-409-3p suppresses breast cancer cell growth and invasion by targeting Akt1. *Biochemical and Biophysical Research Communications*. 2016;469 (2): 189–95.

144. Li W, Lin J, Huang J, Chen Z, Sheng Q, Yang F, et al. MicroRNA-409-5p inhibits cell proliferation, and induces G_2 /M phase arrest and apoptosis by targeting DLGAP5 in ovarian cancer cells. *Oncology Letters*. 2022;24 (2): 261.

145. Azarbarzin S, Hosseinpour-Feizi MA, Banan Khojasteh SM, Baradaran B, Safaralizadeh R. MicroRNA -383-5p restrains the proliferation and migration of breast cancer cells and promotes apoptosis via inhibition of PD-L1. *Life Sciences*. 2021;267: 118939.

146. Noyan H, El-Mounayri O, Isserlin R, Arab S, Momen A, Cheng HS, et al. Cardioprotective Signature of Short-Term Caloric Restriction. *PLOS ONE*. 2015;10 (6): e0130658.

147. Zhao H, Wilkie T, Deol Y, Sneh A, Ganju A, Basree M, et al. miR-29b defines the pro-/anti-proliferative effects of S100A7 in breast cancer. *Molecular Cancer*. 2015;14 (1): 11.

148. Luan Q-X, Zhang B-G, Li X-J, Guo M-Y. MiR-129-5p is downregulated in breast cancer cells partly due to promoter H3K27m3 modification and regulates epithelial-mesenchymal transition and multi-drug resistance. *European Review for Medical and Pharmacological Sciences*. 2016;20 (20): 4257–65.

149. Meng R, Fang J, Yu Y, Hou LK, Chi JR, Chen AX, et al. miR-129-5p suppresses breast cancer proliferation by targeting CBX4. *Neoplasma*. 2018; 65 (4): 572–8.

150. Chen H, Yang J, Wu W. Seven key hub genes identified by gene co-expression network in cutaneous squamous cell carcinoma. *BMC cancer*. 2021;21 (1): 852.

151. Dewey FE, Perez MV, Wheeler MT, Watt C, Spin J, Langfelder P, et al. Gene Coexpression Network Topology of Cardiac Development, Hypertrophy, and Failure. Circulation: *Cardiovascular Genetics*. 2011;4 (1): 26–35.

152. Esteves JV, Enguita FJ, Machado UF. MicroRNAs-Mediated Regulation of Skeletal Muscle GLUT4 Expression and Translocation in Insulin Resistance. *Journal of Diabetes Research*. 2017; 2017: 7267910.

153. Wang H, Li H, Jiang Q, Dong X, Li S, Cheng S, et al. HOTAIRM1 Promotes Malignant Progression of Transformed Fibroblasts in Glioma Stem-Like Cells Remodeled Microenvironment via Regulating miR-133b-3p/TGFβ Axis. *Frontiers in Oncology*. 2021; 11: 603128.

154. Chen H-W, Lai Y-C, Rahman MM, Husna AA, Hasan MN, Miura N. Micro RNA differential expression profile in canine mammary gland tumor by next generation sequencing. *Gene*. 2022;818: 146237.

155. Raman N, Weir E, Müller S. The AAA ATPase MDN1 Acts as a SUMO-Targeted Regulator in Mammalian Pre-ribosome Remodeling. *Molecular Cell*. 2016;64 (3): 607–15.

156. Hao S, Huang M, Xu X, Wang X, Huo L, Wang L, et al. MDN1 Mutation Is Associated With High Tumor Mutation Burden and Unfavorable Prognosis in Breast Cancer. *Frontiers in Genetics*. 2022;13: 857836.

157. Kant S, Barrett T, Vertii A, Noh YH, Jung DY, Kim JK, et al. Role of the Mixed-Lineage Protein Kinase Pathway in the Metabolic Stress Response to Obesity. *Cell Reports*. 2013;4 (4): 681–8.

158. Larsson SC, Mantzoros CS, Wolk A. Diabetes mellitus and risk of breast cancer: A meta-analysis. *International Journal of Cancer*. 2007;121 (4): 856–62.

159. Abreu de Oliveira WA, El Laithy Y, Bruna A, Annibali D, Lluis F. Wnt Signaling in the Breast: From Development to Disease. *Frontiers in Cell and Developmental Biology*. 2022; 10: 884467.

160. Xu X, Zhang M, Xu F, Jiang S. Wnt signaling in breast cancer: Biological mechanisms, challenges and opportunities. *Molecular Cancer*. 2020;19 (1): 165.

161. Hsieh EA, Chai CM, Hellerstein MK. Effects of caloric restriction on cell proliferation in several tissues in mice: Role of intermittent feeding. *American Journal of Physiology Endocrinology and Metabolism*. 2005;288 (5): E965–972.

162. Druz A, Chu C, Majors B, Santuary R, Betenbaugh M, Shiloach J. A novel microRNA mmu-miR-466h affects apoptosis regulation in mammalian cells. *Biotechnology and Bioengineering*. 2011;108 (7): 1651–61.

163. Wang N, Tan H-Y, Feng Y-G, Zhang C, Chen F, Feng Y. microRNA-23a in Human Cancer: Its Roles, Mechanisms and Therapeutic Relevance. *Cancers*. 2018;11 (1): 7.

164. Li L, Zhang X, Ren H, Huang X, Shen T, Tang W, et al. miR-23a/b-3p promotes hepatic lipid accumulation by regulating Srebp-1c and Fas. *Journal of Molecular Endocrinology*. 2022;68 (1): 35–49.

165. Wang B, Hsu S-H, Frankel W, Ghoshal K, Jacob ST. Stat3-mediated activation of microRNA-23a suppresses gluconeogenesis in hepatocellular carcinoma by down-regulating Glucose-6-phosphatase and peroxisome proliferator-activated receptor gamma, coactivator 1 alpha. *Hepatology*. 2012;56 (1): 186–97.

166. De Craene J-O, Bertazzi D, Bär S, Friant S. Phosphoinositides, Major Actors in Membrane Trafficking and Lipid Signaling Pathways. *International Journal of Molecular Sciences*. 2017;18 (3): 634.

167. Kim HJ, Jung KJ, Yu BP, Cho CG, Chung HY. Influence of aging and calorie restriction on MAPKs activity in rat kidney. *Experimental Gerontology*. 2002;37 (8-9): 1041–53.

168. De Smet R, Marchal K. Advantages and limitations of current network inference methods. *Nature Reviews Microbiology*. 2010;8 (10): 717–29.

APPENDIX A: SIGNIFICANTLY EXPRESSED MICRORNAS

Table A.1 and Table A.2 show every significantly expressed miRNAs in both blood and MFP. LogFC: log fold change, adj.P.Val: adjusted p-value.

Table A.1. Significantly expressed miRNAs in blood.

miRNA	**logFC**	**adj.P.Val**	**diet**	**age**
miR-144-3p	2.081	0.001	AL	50
miR-23a-3p	4.818	0.031	AL	50
miR-19a-3p	1.514	0.034	AL	50
miR-144-5p	1.702	0.038	AL	50
miR-3073a-3p	-0.574	0.038	AL	50
miR-5626-5p	0.651	0.039	AL	50
miR-7216-3p	-0.638	0.039	AL	50
miR-494-3p	6.147	0.001	CCR	50
miR-3073a-3p	-0.617	0.032	CCR	50
miR-8114	2.815	0.005	ICR	50
miR-742-5p	-0.883	0.005	ICR	50
miR-6956-3p	-0.628	0.009	ICR	50
miR-6395	3.340	0.011	ICR	50
miR-1964-3p	2.505	0.011	ICR	50
miR-181a-5p	4.957	0.014	ICR	50
miR-365-1-5p	-2.300	0.037	ICR	50
miR-423-5p	4.109	0.038	ICR	50
miR-301b-5p	-0.585	0.041	ICR	50
miR-7044-5p	2.082	0.045	ICR	50
miR-6928-3p	-0.595	0.049	ICR	50

miR-875-3p	1.561	0.000	AL	81
miR-23a-3p	5.443	0.004	AL	81
miR-6939-5p	2.727	0.004	AL	81
miR-494-3p	5.377	0.004	AL	81
miR-376c-3p	1.111	0.006	AL	81
miR-6977-5p	3.095	0.011	AL	81
miR-3104-5p	4.187	0.025	AL	81
miR-491-5p	2.345	0.027	AL	81
miR-219c-5p	-0.686	0.027	AL	81
miR-351-5p	3.239	0.027	AL	81
miR-155-3p	0.982	0.027	AL	81
miR-23b-3p	4.285	0.027	AL	81
miR-8097	1.170	0.027	AL	81
miR-6239	5.088	0.027	AL	81
miR-7080-3p	-1.046	0.027	AL	81
miR-7216-3p	-0.617	0.027	AL	81
miR-384-5p	1.426	0.028	AL	81
miR-742-5p	-0.785	0.028	AL	81
miR-344c-3p	-0.923	0.028	AL	81
miR-671-5p	3.368	0.031	AL	81
miR-6991-5p	4.865	0.043	AL	81
miR-505-5p	4.128	0.044	AL	81
miR-7689-5p	1.020	0.044	AL	81
miR-181a-5p	4.719	0.045	AL	81
miR-31-5p	5.515	0.045	AL	81
miR-1962	2.149	0.045	AL	81
miR-328-5p	4.073	0.045	AL	81

miR-7083-5p	2.864	0.045	AL	81
miR-7045-5p	3.028	0.045	AL	81
miR-6928-3p	-0.636	0.045	AL	81
miR-742-5p	-1.102	0.002	CCR	81
miR-491-5p	2.937	0.003	CCR	81
miR-23a-3p	5.317	0.004	CCR	81
miR-494-3p	5.229	0.007	CCR	81
miR-31-5p	6.851	0.011	CCR	81
miR-6239	5.762	0.011	CCR	81
miR-331-3p	2.210	0.017	CCR	81
miR-181a-5p	5.546	0.017	CCR	81
miR-505-5p	4.692	0.021	CCR	81
miR-351-5p	3.263	0.022	CCR	81
miR-1981-5p	3.599	0.022	CCR	81
miR-700-5p	2.408	0.022	CCR	81
let-7e-5p	5.259	0.022	CCR	81
miR-1950	1.121	0.022	CCR	81
miR-7036-5p	4.056	0.024	CCR	81
miR-719	1.972	0.026	CCR	81
miR-532-3p	4.340	0.026	CCR	81
miR-466l-3p	-0.980	0.027	CCR	81
miR-423-5p	4.556	0.027	CCR	81
miR-18a-3p	2.592	0.027	CCR	81
miR-210-3p	4.376	0.027	CCR	81
miR-700-3p	4.094	0.030	CCR	81
miR-484	4.001	0.032	CCR	81
miR-25-5p	4.541	0.033	CCR	81

miR-324-3p	3.091	0.035	CCR	81
miR-335-5p	3.947	0.035	CCR	81
miR-181b-5p	3.362	0.038	CCR	81
miR-374c-3p	-0.537	0.038	CCR	81
miR-7083-5p	2.909	0.038	CCR	81
miR-5100	5.685	0.046	CCR	81
miR-7044-5p	2.177	0.048	CCR	81
miR-93-3p	4.374	0.050	CCR	81
miR-742-5p	-0.899	0.007	ICR	81

Table A.2. Significantly expressed miRNAs in MFP

miRNA	**logFC**	**adj.P.Val**	**diet**	**age**
miR-409-3p	-2.363086	0.000006	AL	50
miR-540-3p	-1.056049	0.013741	AL	50
miR-337-5p	-1.948767	0.013741	AL	50
miR-127-5p	-1.027562	0.015471	AL	50
miR-127-3p	-3.768188	0.016832	AL	50
miR-382-5p	-2.096003	0.048161	AL	50
miR-540-3p	-1.182345	0.004194	CCR	50
miR-29b-3p	2.819627	0.017527	CCR	50
miR-101b-3p	1.616446	0.018539	CCR	50
miR-466g	1.305594	0.018539	CCR	50
miR-466h-3p	1.480834	0.018539	CCR	50
miR-8103	0.931204	0.018539	CCR	50
miR-409-3p	-1.453885	0.018539	CCR	50
miR-7024-3p	0.967029	0.018539	CCR	50
miR-383-5p	1.453968	0.018539	CCR	50

miRNA	logFC	adj.P.Val	diet	age
miR-7062-3p	1.795309	0.022447	CCR	50
miR-7b-3p	1.482915	0.033658	CCR	50
miR-449c-3p	0.717305	0.036343	CCR	50
miR-127-3p	-3.296748	0.041996	CCR	50
miR-409-3p	-2.447536	0.000000	ICR	50
miR-540-3p	-0.989093	0.003834	ICR	50
miR-127-3p	-3.621276	0.003834	ICR	50
miR-337-5p	-1.788103	0.003834	ICR	50
miR-485-5p	-1.385200	0.007630	ICR	50
miR-434-3p	-1.451484	0.044302	ICR	50
miR-409-3p	-2.551006	0.000001	AL	81
miR-127-3p	-4.313000	0.003500	AL	81
miR-540-3p	-1.126412	0.003500	AL	81
miR-485-5p	-1.658284	0.005171	AL	81
miR-370-3p	-2.524145	0.011779	AL	81
miR-7056-5p	-2.845922	0.043518	AL	81
miR-1907	-1.914893	0.047177	AL	81
miR-143-5p	2.105882	0.000277	CCR	81
miR-409-3p	-1.883981	0.000726	CCR	81
miR-133a-5p	3.125742	0.000767	CCR	81
miR-129-2-3p	2.317683	0.003185	CCR	81
miR-129-5p	2.488704	0.003647	CCR	81
miR-370-3p	-2.436817	0.016954	CCR	81
miR-434-3p	-1.695184	0.032448	CCR	81
miR-10b-3p	0.788530	0.034997	CCR	81
miR-27a-5p	1.521033	0.035052	CCR	81

miRNA	**logFC**	**adj.P.Val**	**diet**	**age**
miR-485-5p	-1.350704	0.041425	CCR	81
miR-7036-3p	0.877366	0.041425	CCR	81
miR-7a-2-3p	1.296412	0.041425	CCR	81
miR-1a-3p	5.165919	0.048745	CCR	81
miR-540-3p	-0.852301	0.048745	CCR	81
miR-133b-3p	5.423821	0.048745	CCR	81
miR-409-3p	-1.989416	0.000013	ICR	81
miR-540-3p	-1.171590	0.000118	ICR	81
miR-127-3p	-4.033603	0.000629	ICR	81
miR-434-3p	-1.687801	0.006564	ICR	81
miR-668-3p	-1.341681	0.013400	ICR	81
miR-541-5p	-2.055872	0.019812	ICR	81
miR-127-5p	-0.843524	0.019812	ICR	81
miR-184-3p	-3.515289	0.019812	ICR	81
miR-6414	-1.369454	0.043451	ICR	81

APPENDIX B: TARGETS OF SIGNIFICANTLY EXPRESSED MIRNAS

Table B.1. shows subset of target genes of mentioned miRNAs in the main text. The full table is available at https://github.com/aaydenn/rewiring.

Table B.1. Selected miRNA-mRNA pairs

miRNA	**Entrez**	**Symbol**	**Type**
miR-144-3p	15251	Hif1a	predicted
miR-144-3p	76800	Usp42	predicted
miR-144-3p	93760	Arid1a	predicted
miR-144-3p	329628	Fat4	predicted
miR-144-3p	241311	Zbtb34	predicted
miR-144-3p	12014	Bach2	predicted
miR-144-3p	73677	Psma8	predicted
miR-144-3p	18472	Pafah1b1	predicted
miR-144-3p	70508	Bbx	predicted
miR-144-3p	77128	Crebrf	predicted
miR-144-3p	80892	Zfhx4	predicted
miR-144-3p	67381	Med4	predicted
miR-494-3p	140486	Igf2bp1	predicted
miR-494-3p	19017	Ppargc1a	predicted
miR-742-5p	214968	Sema6d	predicted
miR-742-5p	15182	Hdac2	predicted
miR-3104-5p	67150	Rnf141	predicted
miR-3104-5p	17476	Mpeg1	predicted
miR-3104-5p	21939	Cd40	predicted

miRNA	Entrez	Symbol	Type
miR-3104-5p	269881	Map3k10	predicted
miR-505-5p	105245	Txndc5	predicted
miR-505-5p	13205	Ddx3x	predicted
miR-505-5p	27381	Tcl1b2	predicted
miR-7045-5p	100019	Mdn1	predicted
miR-7045-5p	544963	Iqgap2	predicted
miR-374c-3p	70676	Gulp1	predicted
miR-374c-3p	24017	Rnf13	predicted
miR-374c-3p	64058	Perp	predicted
miR-374c-3p	68776	Taf11	predicted
miR-540-3p	70296	Tbc1d13	predicted
miR-540-3p	230088	Fam214b	predicted
miR-540-3p	19695	Reg3g	predicted
miR-127-3p	235072	Septin7	predicted
miR-29b-3p	16000	Igf1	predicted
miR-29b-3p	22031	Traf3	predicted
miR-29b-3p	245555	Nexmif	predicted
miR-29b-3p	69069	Tmem273	predicted
miR-29b-3p	14025	Bcl11a	predicted
miR-29b-3p	15482	Hspa1l	predicted
miR-29b-3p	54446	Nfat5	predicted
miR-29b-3p	53417	Hif3a	predicted

APPENDIX C: RELATIONSHIP BETWEEN CENTRALITY AND DEGREE

Figure C.1. shows the linear relationship between eigenvector centrality and degree of miRNAs in every co-expression network. Larger and darker points indicate low average neighbor degrees. First row represents the blood co-expression networks (AL, CCR, ICR). Second row represents the MFP co-expression networks (AL, CCR, ICR). The miRNAs with high degree tend to have high eigenvector centrality and low average neighbor degree.

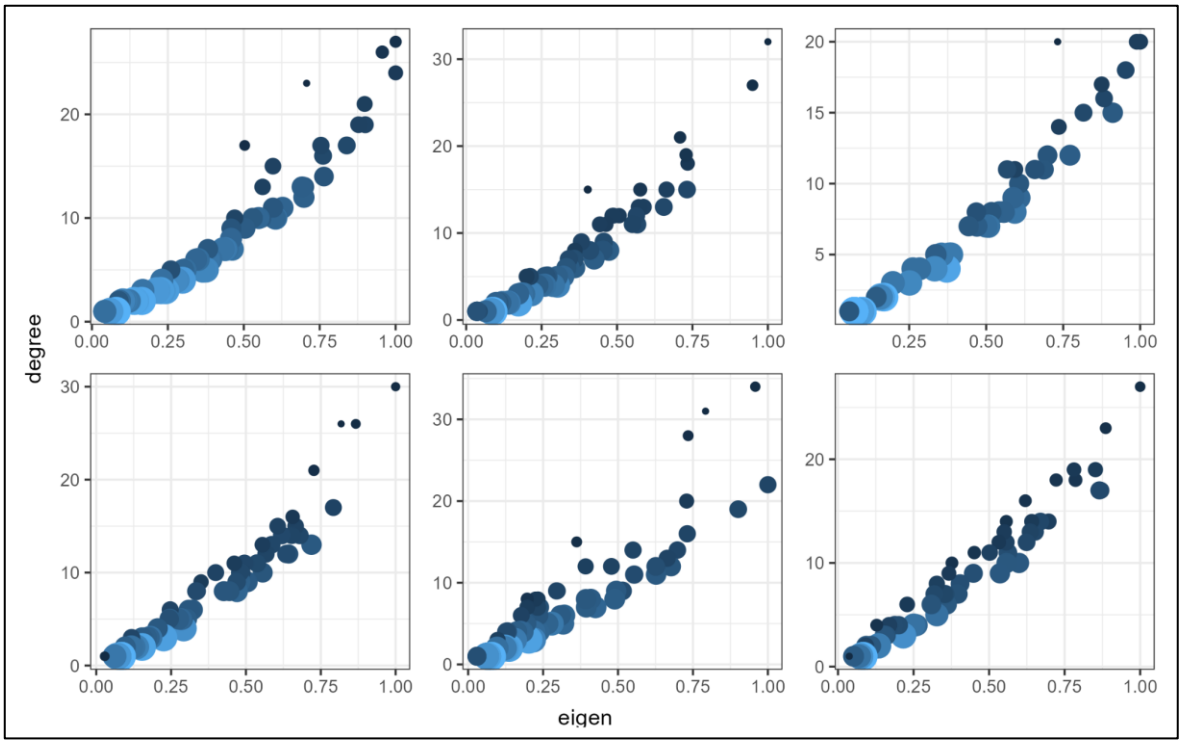

Figure C.1. Scatter plot of degree and eigenvector centrality indices

APPENDIX D: INFLUENCE SCORES FOR EACH KEGG PATHWAY

Table D.1. shows influence scores for top 200 KEGG pathways for each dietary condition in both blood and MFP.

Table D.1. Influence scores of KEGG pathways

	Blood			**MFP**		
Term	**AL**	**CCR**	**ICR**	**AL**	**CCR**	**ICR**
Phosphatidylinositol signaling system	21.0	17.8	15.0	15.0	15.8	14.2
Pathways in cancer	16.1	15.3	6.6	15.1	14.4	15.5
Inositol phosphate metabolism	15.4	12.2	10.5	11.9	12.5	11.4
Purine metabolism	12.5	11.1	10.5	11.1	11.1	11.1
Hepatocellular carcinoma	9.4	8.6	3.5	9.7	10.6	10.0
Focal adhesion	8.3	6.0	5.6	10.4	10.4	10.0
Metabolic pathways	5.9	5.9	5.1	7.0	8.1	8.0
Human papillomavirus infection	7.0	4.0	4.0	8.0	8.0	8.0
MAPK signaling pathway	8.1	6.8	8.3	7.5	7.7	7.9
Sphingolipid metabolism	5.8	4.2	4.2	6.6	7.7	7.6
Dilated cardiomyopathy	6.7	3.8	3.8	7.6	7.6	7.6
Glycerophospholipid metabolism	6.9	6.5	5.4	7.0	7.2	7.2
Glycerolipid metabolism	6.9	5.0	4.5	5.9	6.4	5.9
Hepatitis B	6.9	5.7	7.3	6.1	6.4	6.5
Herpes simplex virus 1 infection	6.9	5.8	7.2	6.0	6.3	6.9
Proteoglycans in cancer	7.5	6.4	6.5	6.7	6.1	6.5
Dopaminergic synapse	3.1	3.1	3.1	6.0	6.0	6.0
Fluid shear stress and atherosclerosis	2.0	4.0	1.0	6.0	6.0	6.0
Human T-cell leukemia virus 1 infection	7.3	5.3	7.1	5.7	6.0	6.0

	Blood			**MFP**		
Arachidonic acid metabolism	3.9	3.5	3.5	4.7	5.6	5.6
MicroRNAs in cancer	6.6	5.5	6.5	5.8	5.4	6.0
Kaposi sarcoma-associated herpesvirus infection	6.0	4.8	4.4	5.1	4.7	5.0
Ras signaling pathway	3.5	3.7	3.6	5.1	4.6	5.3
Small cell lung cancer	3.9	2.9	3.2	4.2	4.6	4.9
Breast cancer	5.4	6.8	7.0	5.3	4.5	5.4
Hippo signaling pathway	6.2	6.3	9.0	6.1	4.5	5.4
Epstein-Barr virus infection	5.1	4.3	5.2	4.6	4.4	5.2
mTOR signaling pathway	5.6	6.9	6.5	5.3	4.4	5.2
PI3K-Akt signaling pathway	6.0	6.0	4.0	4.4	4.4	4.4
Gastric cancer	5.8	7.4	7.0	5.6	4.4	5.2
cAMP signaling pathway	4.8	4.2	4.5	4.4	4.4	4.8
beta-Alanine metabolism	2.8	1.8	0.9	2.8	4.3	4.3
Human cytomegalovirus infection	6.2	5.4	7.1	5.1	4.2	4.7
Cytokine-cytokine receptor interaction	5.6	4.6	5.4	4.4	4.2	4.7
Rap1 signaling pathway	5.7	5.2	6.4	5.0	4.1	4.4
Cellular senescence	5.5	4.4	5.2	4.5	4.1	4.6
Signaling pathways regulating pluripotency of stem cells	4.0	3.7	4.0	4.4	4.1	4.5
Nicotinate and nicotinamide metabolism	4.1	3.2	2.4	4.0	4.0	4.0
Axon guidance	5.3	4.6	5.1	4.7	4.0	4.6
JAK-STAT signaling pathway	7.9	7.9	13.7	4.3	3.9	4.9
Fanconi anemia pathway	2.9	2.8	1.9	3.8	3.8	3.8
Growth hormone synthesis. secretion and action	4.2	3.2	4.6	3.5	3.8	3.5
Measles	3.9	3.5	4.3	3.5	3.7	4.1

	Blood			**MFP**		
Lipid and atherosclerosis	3.6	3.3	3.5	3.8	3.6	4.1
Glycosphingolipid biosynthesis - lacto and neolacto series	3.5	3.4	2.7	3.4	3.5	2.7
Fatty acid degradation	5.9	3.5	5.9	2.9	3.5	2.9
Glucagon signaling pathway	3.0	5.8	4.4	3.8	3.5	3.6
TGF-beta signaling pathway	4.5	3.9	4.6	3.7	3.5	3.8
Relaxin signaling pathway	3.1	2.4	3.0	3.9	3.5	4.0
Pyrimidine metabolism	2.8	3.0	1.7	3.2	3.4	3.2
HIF-1 signaling pathway	4.9	3.9	3.0	3.6	3.4	3.2
FoxO signaling pathway	4.3	3.2	3.4	3.5	3.4	3.9
Human immunodeficiency virus 1 infection	5.0	4.5	6.1	4.2	3.4	3.7
Valine. leucine and isoleucine degradation	3.6	3.3	3.4	2.3	3.3	2.3
Oocyte meiosis	1.4	1.4	1.1	1.5	3.3	2.5
NOD-like receptor signaling pathway	3.7	3.3	3.9	3.2	3.2	3.5
Ether lipid metabolism	3.2	3.2	1.9	3.2	3.2	3.2
Apelin signaling pathway	4.7	3.6	4.8	3.4	3.1	3.5
Prostate cancer	3.1	2.7	2.8	3.2	3.1	3.1
Tuberculosis	3.8	3.5	4.3	3.0	3.1	3.2
Hepatitis C	3.8	3.2	3.7	3.4	3.1	3.8
AMPK signaling pathway	3.2	2.3	2.5	2.8	3.1	3.2
NF-kappa B signaling pathway	3.4	3.0	3.3	3.1	3.0	3.2
Pentose phosphate pathway	2.4	2.5	1.2	1.8	3.0	3.0
Influenza A	3.3	3.0	3.6	3.0	3.0	3.5
Thyroid hormone signaling pathway	5.8	4.3	3.2	3.4	2.9	2.8
AGE-RAGE signaling pathway in diabetic complications	3.8	3.6	4.6	3.5	2.9	3.2

	Blood			**MFP**		
Apoptosis	2.9	2.3	3.3	2.6	2.9	2.9
Neurotrophin signaling pathway	3.4	2.9	3.5	2.8	2.9	2.8
cGMP-PKG signaling pathway	3.9	3.4	4.0	3.1	2.8	3.2
Longevity regulating pathway	2.4	1.9	2.1	2.6	2.8	3.0
Glutathione metabolism	2.8	2.1	2.1	2.8	2.8	2.8
Chemokine signaling pathway	4.5	3.9	5.0	3.3	2.8	3.0
EGFR tyrosine kinase inhibitor resistance	2.8	2.6	2.8	2.9	2.8	2.8
Wnt signaling pathway	3.4	3.2	3.8	3.6	2.8	3.3
Aldosterone synthesis and secretion	2.5	2.3	4.9	2.8	2.8	2.6
RIG-I-like receptor signaling pathway	2.9	2.2	2.5	2.3	2.7	2.7
Adrenergic signaling in cardiomyocytes	4.4	3.5	4.8	3.1	2.7	3.0
Necroptosis	3.1	2.5	3.5	2.3	2.7	2.8
Olfactory transduction	0.3	0.4	2.0	3.3	2.7	3.3
Glioma	2.7	2.3	2.3	2.7	2.6	2.9
Cushing syndrome	4.5	3.7	5.2	3.5	2.6	3.1
Renal cell carcinoma	3.6	2.6	2.1	2.7	2.6	2.3
Oxytocin signaling pathway	4.6	3.9	4.9	3.2	2.5	2.8
ECM-receptor interaction	1.7	1.2	1.8	2.4	2.5	3.0
Autophagy - animal	5.4	3.5	3.0	2.9	2.5	2.3
p53 signaling pathway	2.8	2.0	2.4	2.0	2.5	2.5
Diabetic cardiomyopathy	3.3	2.6	3.2	2.9	2.5	2.9
IL-17 signaling pathway	2.1	1.7	1.8	2.4	2.5	2.7
Calcium signaling pathway	5.7	4.8	5.9	3.3	2.5	2.8
Melanogenesis	3.7	3.1	4.3	3.3	2.5	2.6
GnRH signaling pathway	3.6	2.7	4.1	2.3	2.4	2.1
Insulin resistance	3.2	2.3	2.7	2.3	2.4	2.3

	Blood			**MFP**		
Chagas disease	4.3	3.2	4.1	2.5	2.3	2.5
Glycolysis / Gluconeogenesis	2.3	2.3	2.3	2.3	2.3	2.3
Toll-like receptor signaling pathway	2.5	2.2	2.3	2.4	2.3	2.8
Sphingolipid signaling pathway	4.6	3.7	4.6	2.7	2.3	2.2
Th17 cell differentiation	4.5	3.3	3.1	2.6	2.2	2.2
Endocrine resistance	2.5	2.2	2.8	2.4	2.2	2.5
Pancreatic cancer	2.7	2.2	2.8	2.4	2.2	2.6
Linoleic acid metabolism	1.3	1.3	1.3	2.2	2.2	2.2
Thermogenesis	2.6	2.0	2.7	2.1	2.2	2.2
Salmonella infection	3.9	3.9	2.2	2.2	2.2	2.2
Regulation of actin cytoskeleton	3.6	3.3	3.7	2.6	2.1	2.6
Melanoma	2.2	1.7	1.7	2.1	2.1	2.3
PD-1 checkpoint pathway in cancer	4.7	3.0	2.5	2.3	2.1	2.0
Gap junction	3.2	2.8	3.6	2.6	2.0	2.1
Pathways of neurodegeneration - multiple diseases	2.0	2.0	1.0	1.0	2.0	2.0
Alzheimer disease	2.0	2.0	1.0	1.0	2.0	2.0
Tight junction	2.0	1.0	1.0	2.0	2.0	2.0
Coronavirus disease - COVID-19	3.0	4.0	3.0	2.0	2.0	2.0
Alcoholism	2.0	3.0	2.0	2.0	2.0	2.0
Huntington disease	2.0	2.0	1.0	1.0	2.0	2.0
Amyotrophic lateral sclerosis	2.0	2.0	1.0	1.0	2.0	2.0
Parkinson disease	2.0	2.0	1.0	1.0	2.0	2.0
Prion disease	2.0	2.0	1.0	1.0	2.0	2.0
Spinocerebellar ataxia	2.0	2.0	1.0	1.0	2.0	2.0
Toxoplasmosis	3.1	2.6	3.3	1.9	2.0	2.1

	Blood			**MFP**		
Platinum drug resistance	1.6	1.5	2.1	1.5	2.0	1.7
Chronic myeloid leukemia	2.9	2.4	2.9	2.4	2.0	2.3
Parathyroid hormone synthesis. secretion and action	3.2	2.6	3.8	2.3	2.0	1.8
Yersinia infection	3.9	3.3	3.9	2.4	1.9	2.4
Estrogen signaling pathway	3.1	2.5	3.6	2.3	1.9	1.9
Colorectal cancer	2.3	2.1	2.5	2.3	1.9	2.1
Cholinergic synapse	3.4	3.0	4.0	2.6	1.9	1.9
Inflammatory mediator regulation of TRP channels	2.3	2.0	2.8	2.1	1.9	2.0
Platelet activation	3.3	2.6	3.5	2.2	1.9	2.2
Progesterone-mediated oocyte maturation	1.5	1.4	1.5	2.0	1.8	2.2
Insulin signaling pathway	2.0	1.7	2.2	1.7	1.8	1.8
Vascular smooth muscle contraction	3.3	2.9	3.9	2.2	1.8	1.9
Longevity regulating pathway - multiple species	1.2	0.9	1.1	1.7	1.8	1.9
Glycine. serine and threonine metabolism	1.8	0.9	0.9	1.8	1.8	1.8
Long-term depression	1.9	1.9	2.5	2.1	1.7	1.8
Apoptosis - multiple species	1.4	1.2	1.7	1.3	1.6	1.5
Leishmaniasis	2.6	2.4	3.0	1.7	1.6	1.7
Retinol metabolism	3.1	3.1	2.1	1.5	1.6	1.5
Endocytosis	1.3	1.2	1.1	2.0	1.6	1.9
Central carbon metabolism in cancer	3.7	2.1	1.4	1.6	1.6	1.2
Cell adhesion molecules	2.3	2.0	2.5	2.1	1.5	1.9
Circadian entrainment	2.7	2.3	3.3	2.1	1.5	1.6
Choline metabolism in cancer	3.3	2.2	1.5	1.9	1.5	1.4
Phospholipase D signaling pathway	2.5	2.1	2.4	1.9	1.5	1.7

	Blood			**MFP**		
Cysteine and methionine metabolism	0.4	0.2	0.1	1.5	1.5	1.7
Long-term potentiation	3.2	2.7	3.7	2.0	1.5	1.6
Adherens junction	1.7	1.5	1.5	2.0	1.5	1.9
Ovarian steroidogenesis	1.0	0.8	1.0	1.3	1.4	1.5
Natural killer cell mediated cytotoxicity	2.6	2.4	3.2	2.0	1.4	1.7
Inflammatory bowel disease	2.0	1.7	2.1	1.2	1.3	1.5
Amphetamine addiction	1.2	1.4	1.5	1.5	1.3	1.2
Non-alcoholic fatty liver disease	1.6	1.2	1.6	1.3	1.3	1.5
Adipocytokine signaling pathway	1.6	1.0	1.3	1.1	1.2	1.2
Glutamatergic synapse	3.2	2.6	3.6	2.0	1.2	1.4
Leukocyte transendothelial migration	1.9	2.1	2.2	1.6	1.2	1.3
Insulin secretion	2.1	1.6	2.6	1.4	1.2	1.1
Fc gamma R-mediated phagocytosis	1.8	1.9	2.1	2.0	1.2	1.7
Thyroid hormone synthesis	2.0	1.6	2.5	1.4	1.2	1.0
Salivary secretion	2.3	1.7	2.8	1.5	1.1	1.2
Gastric acid secretion	2.2	1.7	2.7	1.4	1.1	1.2
Renin secretion	1.7	1.3	1.9	1.3	1.1	1.2
Aldosterone-regulated sodium reabsorption	0.3	0.3	0.2	1.1	1.1	1.3
Non-small cell lung cancer	1.6	1.5	1.8	1.6	1.1	1.3
Th1 and Th2 cell differentiation	1.7	1.5	2.0	1.3	1.1	1.4
C-type lectin receptor signaling pathway	1.7	1.6	1.5	1.4	1.1	1.5
Retrograde endocannabinoid signaling	2.6	2.0	3.0	1.7	1.1	1.3
SNARE interactions in vesicular transport	1.0	0.6	0.7	1.3	1.0	1.2
Lysine degradation	1.9	1.7	2.2	1.6	1.0	1.5
Notch signaling pathway	1.6	0.9	1.1	1.0	1.0	1.1
Osteoclast differentiation	1.0	1.0	1.0	1.0	1.0	1.0

	Blood			**MFP**		
Prolactin signaling pathway	1.4	1.2	1.5	1.1	1.0	1.2
Phagosome	2.0	2.0	1.0	1.0	1.0	1.0
Cortisol synthesis and secretion	1.7	1.2	2.0	1.1	1.0	0.9
Cell cycle	1.0	0.9	0.9	1.0	1.0	1.0
Endometrial cancer	1.8	1.2	1.3	1.1	1.0	1.0
Basal cell carcinoma	1.1	0.9	1.0	1.2	1.0	1.1
T cell receptor signaling pathway	2.1	1.9	1.9	1.4	0.9	1.3
Mitophagy - animal	2.3	1.3	0.6	1.1	0.9	0.6
Circadian rhythm	1.2	0.8	1.2	0.7	0.9	0.7
Hedgehog signaling pathway	1.1	0.9	1.2	0.9	0.9	0.8
Cocaine addiction	0.4	0.5	0.4	0.9	0.9	0.9
TNF signaling pathway	0.8	0.7	0.8	0.9	0.8	0.8
ErbB signaling pathway	1.2	1.3	1.4	1.2	0.8	1.1
Pancreatic secretion	2.0	1.5	2.5	1.2	0.8	0.9
African trypanosomiasis	1.6	1.3	2.0	1.0	0.8	0.8
Carbon metabolism	0.7	0.6	0.7	0.7	0.8	1.0
Endocrine and other factor-regulated calcium reabsorption	1.9	1.5	2.0	1.1	0.8	0.9
Morphine addiction	1.7	1.5	2.3	1.4	0.8	1.0
Amoebiasis	2.1	1.6	2.6	1.2	0.8	0.8
GABAergic synapse	1.7	1.2	1.7	1.2	0.8	1.0
Antigen processing and presentation	1.0	0.8	1.2	0.9	0.8	0.7
Alanine. aspartate and glutamate metabolism	1.7	2.4	1.7	0.9	0.7	0.8
One carbon pool by folate	0.7	0.0	0.0	0.7	0.7	0.7
B cell receptor signaling pathway	1.3	1.4	1.6	1.2	0.7	0.9
Serotonergic synapse	1.8	1.7	2.4	1.3	0.7	0.8

	Blood			**MFP**		
GnRH secretion	1.4	1.3	2.0	1.1	0.7	0.7
Graft-versus-host disease	0.8	0.7	1.0	0.7	0.6	0.7
Drug metabolism - cytochrome P450	0.6	0.6	0.6	0.6	0.6	0.6
Vasopressin-regulated water reabsorption	0.3	0.3	0.4	0.6	0.6	0.5
Protein processing in endoplasmic reticulum	0.8	0.8	1.0	0.6	0.6	0.5

APPENDIX E: HUB MIRNAS FOR EACH DIETARY GROUP

Table E.1. shows if a miRNA is a hub in each dietary group. The number one indicates that miRNA is hub. The number zero indicates that miRNA is not hub. Blank cells indicate that miRNA has zero degree.

Table E.1. Hubness of each miRNA in every dietary groups

	Blood			**MFP**		
miRNA	**AL**	**CCR**	**ICR**	**AL**	**CCR**	**ICR**
miR-3104-5p	1	0	0	1	1	1
miR-93-3p	0	1	1	1	1	1
miR-23b-3p	0	0	0	1	1	1
miR-127-3p	0	0	0	1	1	1
miR-1a-3p	0	0	0	1	1	1
miR-133b-3p	0	0	0	1	1	1
miR-181a-5p	1	1	1	0	0	0
let-7e-5p	1	1	1	0	0	0
miR-484	1	1	1	0	0	0
miR-505-5p	1	1	1	0	0	0
miR-423-5p	1	1	1	0	0	0
miR-370-3p	0	0	0	1	1	1
miR-532-3p	1	1	0	0	0	0
miR-31-5p	1	1	1	1	0	1
miR-5100	1	1	1	1	0	1
miR-328-5p	0	1	1	0	0	0
miR-6395	0	0	1	0	0	0
miR-23a-3p	1	1	1	0	1	1

miR-494-3p	1	1	0	0	1	1
miR-184-3p	0	0	0	1	0	1
miR-6991-5p	1	1	1	0	0	1
miR-6239	1	1	1	0	0	1
miR-210-3p	1	1	1	1	0	0
miR-7036-5p	0	0	0	0	0	1
miR-700-3p	0	0	0	0	0	1
miR-671-5p	0	0	0	1	0	0
miR-7045-5p	0	0	0	0	1	0
miR-7083-5p	0	0	0	0	0	1
miR-335-5p	0	0	0	0	1	0
miR-382-5p	0	0	0	1	0	0
miR-29b-3p	0	0	0	0	1	0
miR-25-5p	0	0	0	0	0	0
miR-365-1-5p	0	0	0	0	0	0
miR-6977-5p	0	0	0	0	0	0
miR-1981-5p	0	0	0	0	0	0
miR-351-5p	0	0	0	0	0	0
miR-6939-5p	0	0	0	0	0	0
miR-18a-3p	0	0	0	0		
miR-491-5p	0	0	0	0	0	0
miR-700-5p	0	0	0			0
miR-1962	0	0	0	0	0	0
miR-324-3p	0	0	0	0	0	0
miR-376c-3p	0	0	0		0	
miR-7044-5p	0	0	0	0	0	0
miR-8114	0	0	0			

miR-344c-3p	0	0	0			
miR-8097	0	0	0			
miR-331-3p	0	0	0	0	0	0
miR-181b-5p	0	0	0	0	0	0
miR-384-5p	0	0	0			
miR-1964-3p	0	0	0	0	0	0
miR-144-5p	0	0	0			
miR-434-3p	0	0	0	0	0	0
miR-742-5p	0	0	0			
miR-219c-5p	0	0	0			
miR-719	0	0	0	0	0	
miR-6956-3p	0	0	0		0	
miR-7080-3p	0	0	0			
miR-10b-3p	0	0	0		0	
miR-668-3p	0	0	0	0	0	0
miR-374c-3p	0	0	0			
miR-144-3p	0	0				
miR-875-3p	0	0				
miR-466l-3p	0	0				
miR-101b-3p	0	0		0	0	
miR-337-5p	0	0		0	0	0
miR-3073a-3p	0	0				
miR-7216-3p	0	0				
miR-541-5p	0	0		0	0	0
miR-6414	0	0		0	0	0
miR-6928-3p	0	0				
miR-19a-3p	0		0			

miR-155-3p	0		0			
miR-7689-5p	0			0		0
miR-129-5p	0			0	0	0
miR-409-3p	0			0	0	0
miR-133a-5p	0				0	0
miR-7a-2-3p		0	0	0	0	
miR-1950		0	0			
miR-7062-3p		0		0	0	0
miR-383-5p			0	0	0	0
miR-485-5p			0	0	0	0
miR-466h-3p			0	0	0	0
miR-127-5p				0	0	0
miR-143-5p				0	0	0
miR-27a-5p				0	0	0
miR-129-2-3p					0	0
miR-7b-3p				0	0	0
miR-540-3p				0	0	0
miR-449c-3p				0	0	
miR-466g					0	0
miR-1907				0	0	0
miR-7024-3p				0	0	
miR-7036-3p				0	0	0
miR-7056-5p				0	0	0
miR-8103					0	0